Supporting Information

Fluorophore Promoted Facile Deprotonation and Exocyclic Five-Membered Ring Cyclization for Selective and Dynamic Tracking Labile Glyoxals

Huan Xu,[#a] Qianqian Liu,[#a] Xiaodong Song,[#b] Chao Wang,[c] Xinru Wang,[d] Shengnan Ma,[a] Xiaolei Wang,[a] Yan Feng,[d] Xiangming Meng,[d] Xiaogang Liu,*[c] Wei Wang,*[a,e] and Kaiyan Lou*[a]

[a] *State Key Laboratory of Bioreactor Engineering, Shanghai Key Laboratory of New Drug Design, and Shanghai Key Laboratory of Chemical Biology, School of Pharmacy, East China University of Science & Technology, 130 Meilong Road, Shanghai 200237, China*

[b] *Medical Laboratory Department, Huashan Hospital North, Fudan University, 108 Luxiang Road, Shanghai 201907, China*

[c] *Fluorescence Research Group, Singapore University of Technology and Design, 8 Somapah Road, Singapore 487372*

[d] *School of Chemistry and Chemical Engineering, Anhui University, 111 Jiulong Road, Hefei, Anhui 230601, China*

[e] *Department of Pharmacology and Toxicology and BIO5 Institute, University of Arizona, Tucson, AZ 85721-0207, USA*

Table of Contents

General Information

Commercial reagents were purchased from commercial suppliers and used as received, unless otherwise stated. 1H and 13C NMR spectra were recorded on Bruke DRX 400 (400 MHz). Mass Spectra were obtained from East China University of Science and Technology LC-Mass spectral facility. UV-Vis spectra were collected on a Shimadzu UV-1800 spectrophotometer. Fluorescence spectra were collected on a FluoroMax-4 (Horiba Scientific) fluorescence spectrophotometer with slit widths were set at 4 nm both for excitation and emission unless otherwise stated. All fluorescence and absorption spectroscopic measurements were performed in 10 mM phosphate buffer (pH 7.4) at 25 ºC using 1 cm×1 cm quartz cuvettes (3.5 mL) unless otherwise stated. The pH measurements were carried out with a FE20 plus (Mettler Toledo) pH meter. UPLC-MS analysis was performed on Thermo Scientific UltiMate 3000 with Q-ExactiveTM plus MS/MS Mass Spectrometry equipped with Hypersil Gold C18 (Thermo Scientific) 3 μm, 100 mm×2.1 mm column.

Part I: Probe Design

1.1 Comparison of different recognition groups for design of fluorescent probes for reactive dicarbonyl species.

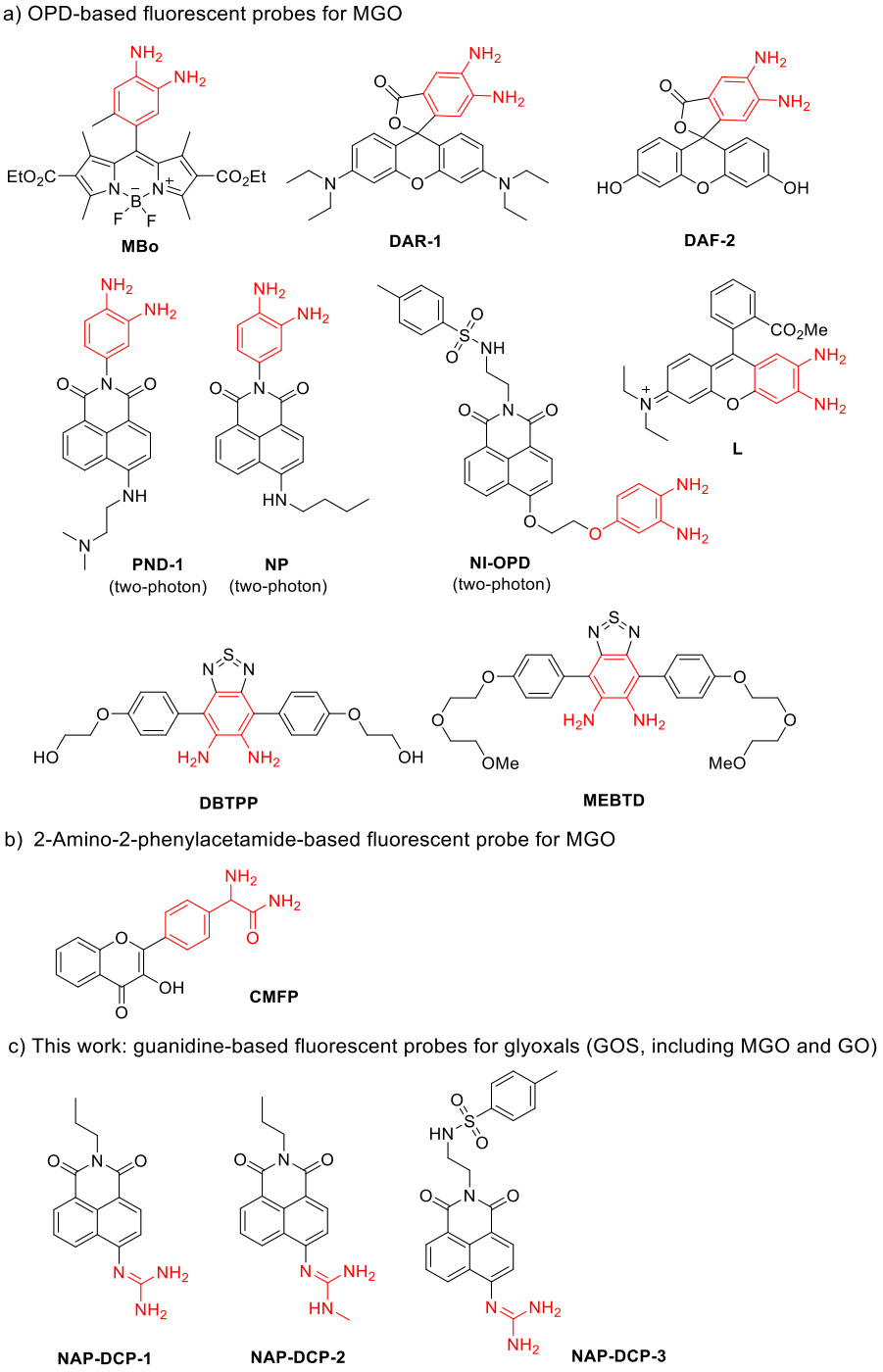

Figure S1 Structures of fluorescent probes for GOS: a) OPD-based fluorescent probes for MGO; b) 2-Amino-2-phenylacetamide based fluorescent probe for MGO; c) Guanidine-based fluorescent probes for GOS.

Table S1 Comparison of literature reported fluorescent probes for GOS.
(See Page S4, N. A. means the information "not available" from the literature)

Probe	Ex nm	Em nm	LOD for MGO μM	Optimized condition for MGO detection	Selectivity at the optimized condition (GO/NO/FA)	Ref.
CMFP	350	525↓440↑ (ratiometric)	0.24	10 μM probe + 500 μM MGO 90 min at 37°C in DMSO/PBS (1/9, v/v, 100 mM, pH 7.4).	good selectivity of MGO over GO/NO/FA	[1]
NI-OPD	380 780 (TP)	460↑ (turn-on)	0.56 nM	10 μM probe + 30 μM MGO 2h at 37°C in DMF/PBS (1/9, v/v, 10 mM, pH 7.4)	MGO over GO/NO/FA	[2]
NP	440 760 (TP)	550↑ (turn-on)	1.47	5 μM probe + 150 μM MGO 1 h in DMSO/PBS (1/19, v/v, pH 7.4)	MGO over NO/FA GO: N. A.	[3]
PND-1	440 880 (TP)	528↑ (turn-on)	77 nM	5 μM probe + 50 μM MGO 12 h at 37°C in DMSO/PBS (1/9, v/v, 10 mM, pH 7.4)	MGO over GO Significant interference from NO FA: N. A.	[4]
MBo	480	532↑ (turn-on)	50-100 nM	10 μM probe + 50 μM MGO 1 h at 37 °C in PBS (pH 7.4) slit =1/10 nm	MGO over NO GO: N. A. FA: N. A.	[5]
L	520	642↓ (turn-off)	N. A.	5 μM probe EtOH/tris-HCl buffer (3/7, v/v, 10 mM, pH 7.4) slit = 5/10 nm	FA: turn-on GO: slightly turn-off MGO: turn-off	[6]
DAF-2	435	510↑ (turn-on)	0.7	10 μM probe + 50 μM MGO 30 min at 37 °C in PBS (100 mM, pH 7.4)	Cross-reactivity with NO FA: N. A.	[7]
DAR-1	545	570↑ (turn-on)	N. A.	10 μM probe + 50 μM MGO 30 min at 37 °C in PBS (100 mM, pH 7.4)	Cross-reactivity with NO FA: N. A.	[7]
MEBTD	496	650↑ (turn-on)	18 nM	50 μM probe + 50 μM MGO DMAC/PBS (2/3, v/v, 10 mM, pH 7.4)	MGO over FA/NO	[8]
DBTPP	500	650↑ (turn-on)	262 nM	25 μM probe + 60 μM MGO DMAC/PBS (2/3, v/v, 10 mM, pH 7.4)	MGO over FA; Cross-reactivity with NO under acidic condition	[9]
NAP-DCP-1	425	564↑ (turn-on)	0.72 (MGO), 0.58 (GO)	2 μM probe + 200 μM MGO 30 min at r. t. in PBS (10 mM, pH 7.4)	Excellent selectivity of MGO and GO over NO/FA	This work
NAP-DCP-3	425	564↑ (turn-on)	0.13 (MGO), 0.16 (GO)	2 μM probe + 200 μM MGO 30 min at r. t. in PBS (10 mM, pH 7.4)	Excellent selectivity of MGO and GO over NO/FA	This work

Table S2 Comparison of literature reported fluorescent probes for MGO detection inside cell studies.

Probe	Cell Line	Condition (37 °C)	Ref.
CMFP	HeLa cells	100 μM MGO for 1 h and 10 μM probe for 40 min	[1]
NI-OPD	HeLa cells	10 μM probe for 1 h and 15 μM MGO for 2 h	[2]
NP	HeLa cells	5 μM probe for 1 h and 100 μM MGO for 1 h	[3]
PND-1	HeLa cells	5 μM probe for 10 h and 100 μM MGO for 10 h	[4]
MBo	HeLa cells	10 μM probe for 1 h and 5 μM MGO for 1 h	[5]
DAF-2	A549 cells	10 μM DAF-2DA for 30 min and 100 μM MGO for 1 h	[7]
DBTPP	SH-SY5Y cells	6 μM probe for 1.5 h and 2 μM MGO for 1.5 h	[8]
MEBTD	4T1 cells	10 μM probe for 1 h and 5 μM MGO for 1 h	[9]
NAP-DCP-1 (reversible)	HeLa cells	5 μM probe for 30 min and 5 μM MGO for 20 min (upregulated), and 5 mM NAC for 20 min (downregulated) 5 μM probe for 30 min and 5 μM GO for 25 min (upregulated), and 5 mM NAC for 20 min (downregulated) >70% fluorescence reduction for both GOS within the first 10 min upon addition of 5 mM NAC	This work (plate-reader based fluorescence readout)

1.2 Examples of OPD-based fluorescent probes for other reactive species.

Nitric Oxide (NO):

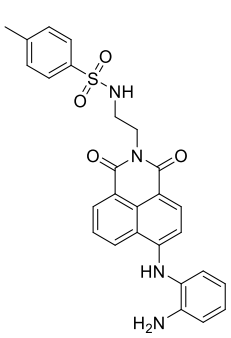

ER-Nap-NO[10]

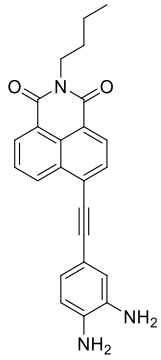

NPA[11]

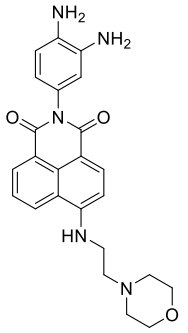

Lyso-NINO[12]

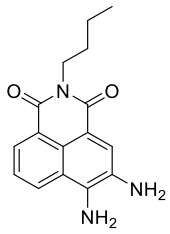

DAN[13]

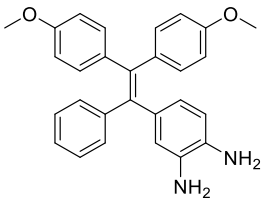

TPE-2NH2[14]

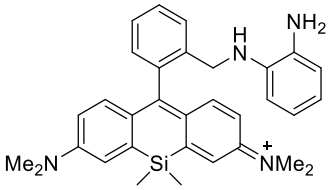

deOxy-DASiR[15]

Formaldehyde (FA):

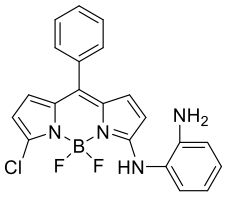

Bodipy-OPDA[16]

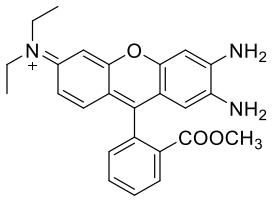

L[6]

Dihydroascorbic acid (DHA):

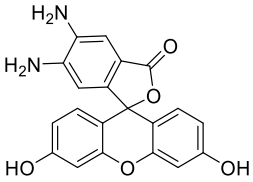

DFA-2[17]

Phosgene:

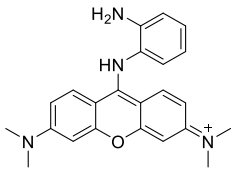

PY-OPD[18]

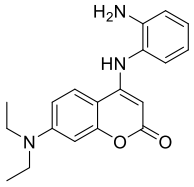

o-Pac[19]

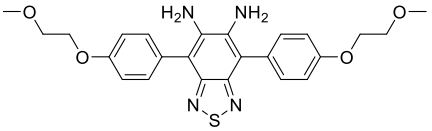

BTA[20]

Figure S2 Examples of OPD-based fluorescent probes for other reactive species.

1.3 Proposed Reaction and Fluorescence Sensing Mechanism of the probe NAP-DCP-1 for GOS

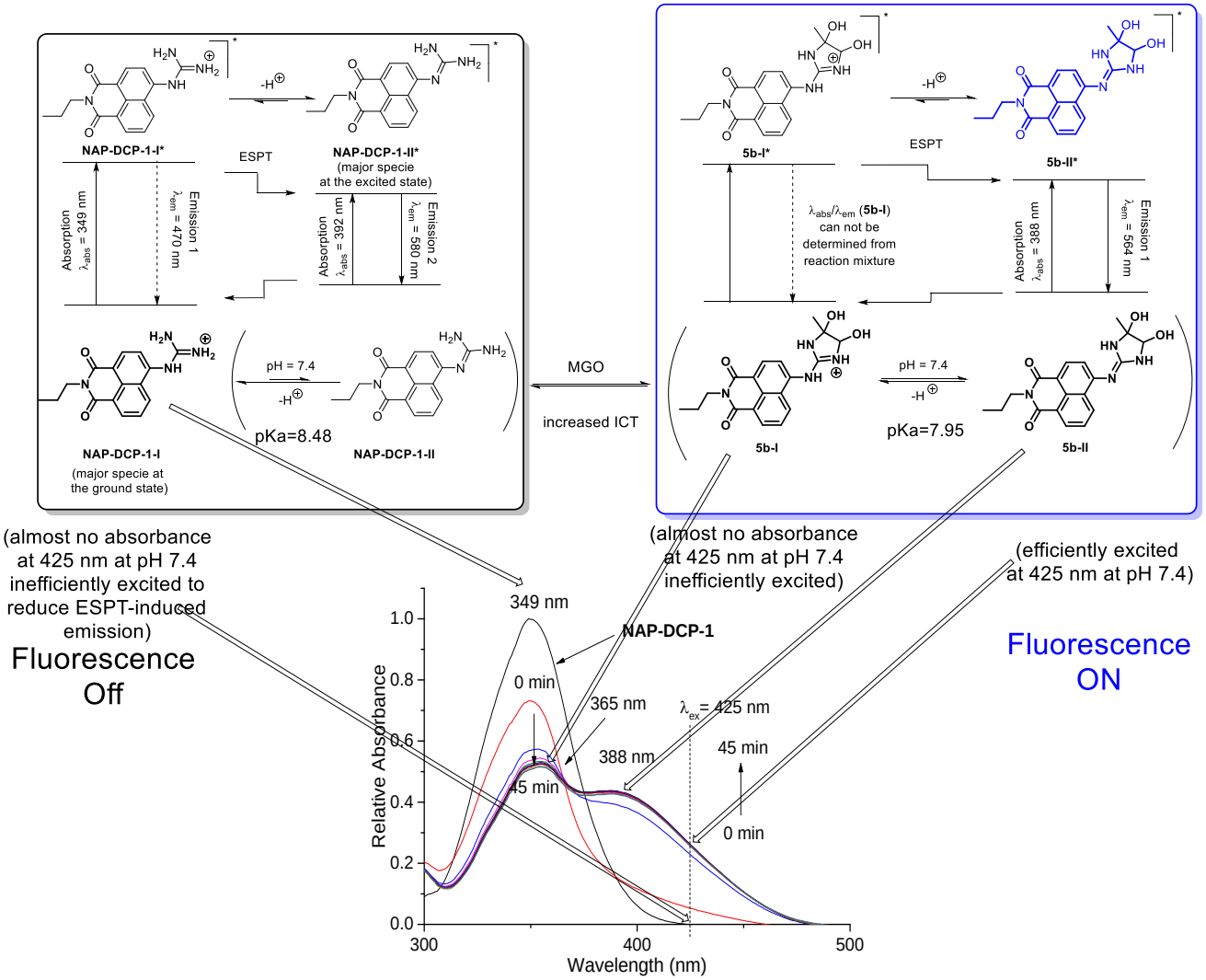

Figure S3 Proposed reaction and fluorescence sensing mechanism of the probe **NAP-DCP-1** for GOS as illustrated with MGO. (The major equilibrium species at the ground states are highlighted with darken structures, the major fluorescence specie at the excited state is highlighted in blue; the dashed local emissions are suppressed due to efficient excited state proton transfer (ESPT) to form deprotonated excited states)

Part II Synthetic Procedures and Structural Characterizations:

2.1 Synthesis of NAP-DCP-1 and its acetylated derivatives.

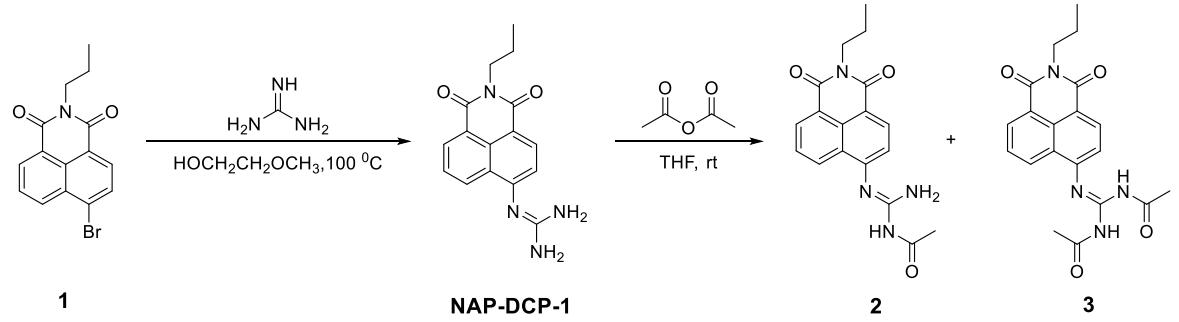

Scheme S1 Synthesis of the probe **NAP-DCP-1** and its acetylated derivatives

2-(*N*-propyl-1,8-naphthalimide-4-yl)guanidine (NAP-DCP-1)

To a suspended solution of *N*-propyl-4-bromo-1,8-naphthalimide (**1**)[21] (382 mg, 1.2 mmol) in 5 mL 2-methoxyethanol at r. t., was added dropwise a solution of guanidine (355 mg, 6.0 mmol) in 3 mL 2-methoxyethanol. The reaction mixture was then heated to 100 °C overnight. After cooled to r. t., the reaction mixture was diluted with water (100 mL) and then extracted with ethyl acetate (50 mL × 3). The combined organic layer was washed with saturated sodium chloride (100 mL) and dried over anhydrous sodium sulfate, filtered and concentrated under vacuum by a rotavapor. The residue was applied to flash column chromatography (silica gel) using DCM:MeOH =10:1 (V/V) as eluent to afford the probe **NAP-DCP-1** (138 mg, 39% yield) as an orange red solid. ^{1}H NMR (400 MHz, DMSO-d_6) δ 8.56 (dd, J = 8.2, 1.1 Hz, 1H), 8.44 (dd, J = 7.4, 1.1 Hz, 1H), 8.32 (d, J = 8.2 Hz, 1H), 7.72 (dd, J = 8.2, 7.4 Hz, 1H), 7.33 (d, J = 8.2 Hz, 1H), 6.70 (bs, 4H), 4.00 (m, 2H), 1.63 (h, J = 7.4 Hz, 2H), 0.90 (t, J = 7.4 Hz, 3H); ^{13}C NMR (100 MHz, DMSO-d_6) δ 163.7, 163.1, 156.2, 150.5, 132.6, 130.8, 130.6, 129.3, 127.4, 125.3, 121.8, 118.8, 113.4, 40.9, 21.0, 11.4. ESI-HRMS: m/z $[M+H]^+$ calcd for $[C_{16}H_{17}N_4O_2]^+$ 297.1346, found 297.1353.

1-acetyl-2-(*N*-propyl-1,8-naphthalimide-4-yl)guanidine (2)

1,3-diacetyl-2-(*N*-propyl-1,8-naphthalimide-4-yl)guanidine (3)

To a solution of **NAP-DCP-1** (100 mg, 0.338 mmol) in 3 mL THF, was added dropwise a solution of acetic anhydride (190 μL, 2.03 mmol) in 1 mL THF. The reaction mixture was stirred at r. t. for 3 h, diluted with saturated sodium carbonate solution (50 mL), and then extracted with methylene chloride (50 mL × 3). The organic layer was washed with saturated sodium chloride (100 mL), and dried over anhydrous sodium sulfate, filtered and concentrated under vacuum by a rotavapor. The residue was applied to flash column chromatography (silica gel) using DCM:EAc=8:1 (V/V) as eluent to afford the acetamide **2** (59 mg, 51% yield) and the diacetamide **3** (32 mg, 25% yield), both as yellow solid.

For compound **2**: ^{1}H NMR (400 MHz, DMSO-d_6) δ 10.76 (s, 1H), 8.46 (d, J = 7.5 Hz, 1H), 8.43 (d, J = 8.2 Hz, 1H) 8.38 (d, J = 8.0 Hz, 1H), 7.74 (dd, J = 8.2, 7.5 Hz, 1H), 7.36 (bs, 2H), 7.25 (d, J = 8.0 Hz, 1H), 4.00 (t, J = 7.4 Hz, 2H), 2.12 (s, 3H), 1.63 (h, J = 7.4 Hz, 2H), 0.90 (t, J = 7.4 Hz, 3H); ^{13}C NMR (100 MHz, DMSO-d_6) δ 172.8, 163.7, 163.3, 153.1, 148.9, 132.7, 130.8, 130.7, 129.1, 126.7, 125.7, 122.0, 118.3, 114.6, 40.9, 23.9, 21.0, 11.4. ESI-HRMS: m/z $[M+H]^+$ calcd for $[C_{18}H_{19}N_4O_3]^+$ 339.1452, found 339.1458.

For compound **3**: ^{1}H NMR (400 MHz, $CDCl_3$) δ 13.31 (s, 1H), 12.02 (s, 1H), 8.79 (d, J = 8.2 Hz, 1H), 8.64 (d, J = 7.5 Hz, 1 H), 8.62 (d, J = 8.2 Hz, 1H), 8.38 (d, J = 8.4 Hz, 1H), 7.82 (dd, J = 8.4, 7.5

Hz, 1H), 4.14 (m, 2H), 2.37 (s, 3H), 2.26 (s, 3H), 1.77 (h, J = 7.4 Hz, 2H), 1.02 (t, J = 7.4 Hz, 3H); ^{13}C NMR (100 MHz, $CDCl_3$) δ 187.3, 173.7, 164.2, 163.7, 152.8, 138.0, 132.0, 131.4, 128.9, 127.5, 126.8, 124.5, 123.5, 121.1, 119.2, 42.1, 29.1, 25.4, 21.5, 11.7. ESI-HRMS: m/z $[M+H]^+$ calcd for $[C_{20}H_{21}N_4O_4]^+$ 381.1557, found 381.1564.

2.2 Synthesis of NAP-DCP-2

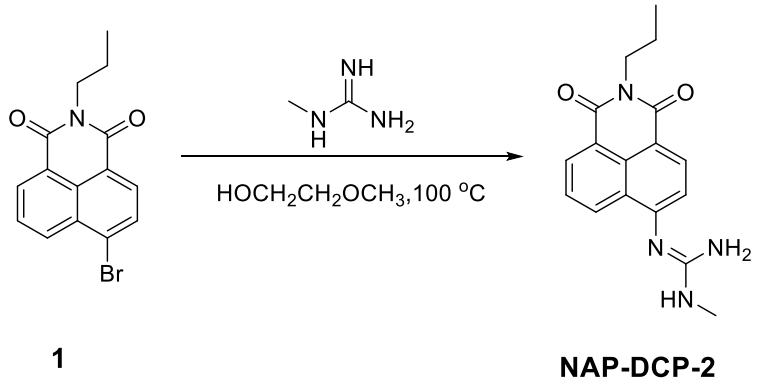

1 **NAP-DCP-2**

Scheme S2 Synthesis of **NAP-DCP-2**.

2-(*N*-propyl-1,8-naphthalimide-4-yl)-3-methylguanidine (NAP-DCP-2)

To a suspended solution of *N*-propyl-4-bromo-1,8-naphthalimide (**1**)[21] (100 mg, 0.314 mmol) in 1 mL 2-methoxyethanol at r. t., was added dropwise a solution of *N*-methylguanidine (115 mg, 1.57 mmol) in 1 mL 2-methoxyethanol. The reaction mixture was then heated to 100 °C overnight. After cooled to r. t., the reaction mixture was diluted with water (50 mL) and then extracted with ethyl acetate (50 mL × 3). The combined organic layer was washed with saturated sodium chloride (100 mL) and dried over anhydrous sodium sulfate, filtered and concentrated under vacuum by a rotavapor. The residue was applied to flash column chromatography (silica gel) using DCM:MeOH =10:1 (V/V) as eluent to afford the probe **NAP-DCP-2** (27 mg, 28% yield) as an orange red solid. ^{1}H NMR (400 MHz, DMSO-d_6) δ 8.63 (dd, J = 8.2, 1.2 Hz, 1H), 8.40 (dd, J = 7.4, 1.2 Hz, 1H), 8.24 (d, J = 8.3 Hz, 1H), 7.62 (dd, J = 8.2, 7.4 Hz, 1H), 7.08 (d, J = 8.3 Hz, 1H), 6.41 (bs, 1H), 6.07 (bs, 2H), 3.99 (m, 2H), 2.82 (s, 3H), 1.62 (h, J = 7.4 Hz, 2H), 0.90 (t, J = 7.4 Hz, 3H); ^{13}C NMR (100 MHz, DMSO-d_6) δ 164.1(2C), 163.3, 156.5, 133.2, 131.5, 130.7, 129.7, 127.5, 124.4, 121.5, 115.9, 110.2, 40.8, 28.1, 21.1, 11.4. ESI-HRMS: m/z $[M+H]^+$ calcd for $[C_{17}H_{19}N_4O_2]^+$ 311.1503, found 311.1510.

2.3 Synthesis of NAP-DCP-3

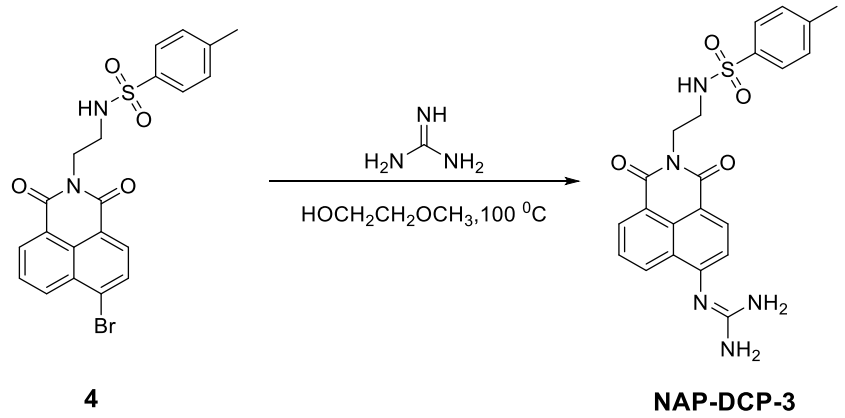

4 NAP-DCP-3

Scheme S3 Synthesis of **NAP-DCP-3**.

1-(*N*-(2-((4-methylphenyl)sulfonamido)ethyl)-1,8-naphthalimide-4-yl)guanidine (NAP-DCP-3)
To a suspended solution of *N*-(2-((4-methylphenyl)sulfonamide)ethyl)-4-bromo-1,8-naphthalimide (**4**)[10] (947 mg, 2.0 mmol) in 15 mL 2-methoxyethanol at r. t., was added dropwise a solution of guanidine (591 mg, 10 mmol) in 3 mL 2-methoxyethanol. The reaction mixture was then heated to 100 ^{o}C overnight. After cooled to r. t., the reaction mixture was diluted with water (150 mL) and then extracted with ethyl acetate (50 mL × 3). The combined organic layer was washed with saturated sodium chloride (100 mL) and dried over anhydrous sodium sulfate, filtered and concentrated under vacuum by a rotavapor. The residue was applied to flash column chromatography (silica gel) using DCM:MeOH:Et_3N =200:20:1 (V/V/V) as eluent to afford the probe **NAP-DCP-3** (160 mg, 18% yield) as an orange red solid. ^{1}H NMR (400 MHz, DMSO-d_6) δ 8.61 (dd, J = 8.3, 1.2 Hz, 1H), 8.36 (dd, J = 7.3, 1.2 Hz, 1H), 8.22 (d, J = 8.3 Hz, 1H), 7.72 (bs, 1H), 7.64 – 7.59 (m, 3H), 7.26 (d, J = 8.1 Hz, 2H), 7.12 (d, J = 8.3 Hz, 1H), 6.17 (bs, 4H), 4.09 (t, J = 6.7 Hz, 2H), 3.03 (bs, 2H), 2.28 (s, 3H); ^{13}C NMR (100 MHz, DMSO-d_6) δ 163.9, 163.1, 156.2, 142.5, 137.6, 132.7, 130.8, 130.7, 129.5(2C), 129.5, 127.3, 126.4(2C), 125.0, 121.7, 117.9, 112.6, 40.2, 38.9, 20.9. ESI-HRMS: m/z[M+H]$^+$ calcd for [$C_{22}H_{22}N_5O_4S$]$^+$ 452.1387, found 452.1393.

2.4 Separation and identification of hydroimidazolone 6b from NAP-DCP-1 and MGO.

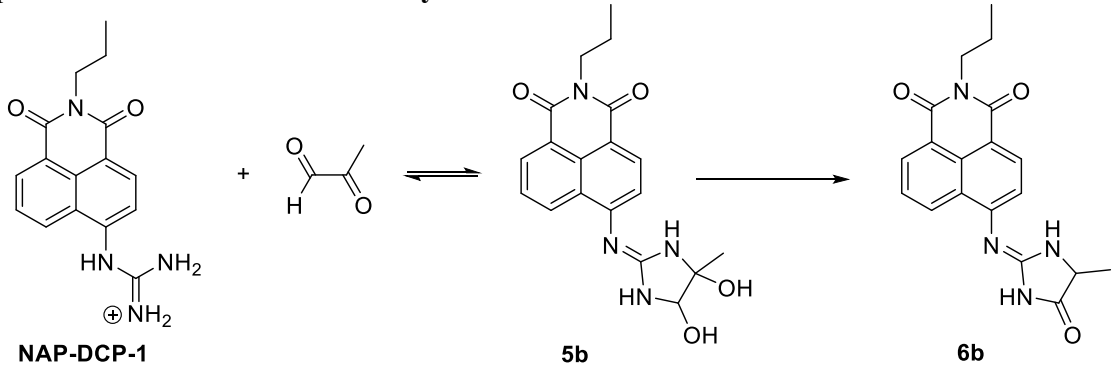

NAP-DCP-1 5b 6b

Scheme S4 Synthesis of hydroimidazolone **6b**.

To a suspended solution of the probe **NAP-DCP-1** (40 mg, 0.13 mmol) in 4 mL PBS buffer (10 mM, pH = 7.4) at r. t., was added dropwise a 40 % MGO in H_2O (4.08 mL, 26.5 mmol). The reaction

suspension became clear immediately (indicating formation of **5b**, also see SI part 4.3 UPLC-MS analysis of reaction mixture), and was stirred at room temperature for additional 3 h. The reaction mixture was diluted with 40 mL water and extracted with ethyl acetate (50 mL × 2). The organic layer was combined and washed with saturated sodium chloride (100 mL) and dried over anhydrous sodium sulfate, filtered and concentrated under vacuum by a rotavapor. The residue was applied to flash column chromatography (silica gel) using DCM:MeOH = 30:1 (V/V) as eluent to afford hydroimidazolone **6b** (10 mg, 21 % yield) both as yellow solid, which was likely formed during workup as no peak of **6b** was seen in the UPLC-MS analysis of the reaction mixture.

5-methyl-2-((*N*-propyl-1,8-naphthalimide-4-yl) amino)imidazolidin-4-one (6b)

^{1}H NMR (400 MHz, DMSO-d_6) δ 11.15 (bs, 1H), 8.51 (dd, J = 8.4, 1.1 Hz, 1H), 8.48 (dd, J = 7.3, 1.1 Hz, 1H), 8.40 (d, J = 8.0 Hz, 1H), 7.83 (bs, 1H), 7.77 (dd, J = 8.4, 7.3 Hz, 1H), 7.35 (d, J = 8.0 Hz, 1H), 4.11 (q, J = 6.9 Hz, 1 H), 4.02 (m, 2H), 1.62 (h, J = 7.4 Hz, 2H), 1.25 (d, J = 6.9 Hz, 3H), 0.91 (t, J = 7.4 Hz, 3H); ^{13}C NMR (though tried several times, satisfactory spectrum could not be obtained due to its low solubility); ESI-HRMS: m/z [M-H]$^-$ calcd for $[C_{19}H_{17}N_4O_3]^-$ 349.1306, found 349.1302.

2.5 Time-dependent ^{1}H-NMR study of formation of dihydroxyimidazolidine adducts 5b from NAP-DCP-1 and MGO in deuterated DMSO.

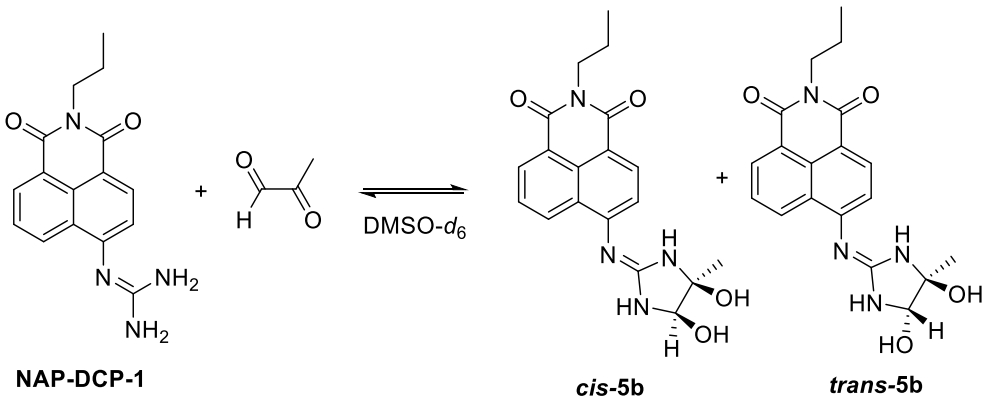

Scheme S5 Reversible formation of dihydroxyimidazolidines

To a solution of 6.0 mg (0.02 mmol) of the probe **NAP-DCP-1** in 1 mL DMSO-d_6 in NMR tube, was added 31 μL 40 % MGO (0.20 mmol) in water. The NMR tube was then flipped upside down several times for the reaction mixture to be well-mixed. ^{1}HNMR was taken thereafter at the time-points of 10, 20, and 30 min. The assignment of ^{1}H NMR data of ***cis*-5b** and ***trans*-5b** were based on the existence of two sets of product peaks in time-dependent ^{1}H NMR spectra of the reaction mixture and experimental evidences supporting that ***cis*-5b** being the major adduct.

***cis*-5b:** ^{1}H NMR (400 MHz, DMSO-d_6) δ 8.61 (d, J = 8.4 Hz, 1H, 5-H), 8.42 (d, J = 7.2 Hz, 1H, 7-H), 8.28 (d, J = 8.2 Hz, 1H, 2-H), 7.66 (t, J (average) = 7.8 Hz, 1H, 6-H), 7.21 (d, J = 8.2 Hz, 1H, 3-H), 4.74 (s, 1H, CH), 4.01 (m, 2H), 1.64 (h, J = 7.4 Hz, 2H, CH_2), 1.38 (s, 3H, Me), 0.92 (t, J = 7.4 Hz, 3H, Me).

***trans*-5b:** ^{1}H NMR (400 MHz, DMSO-d_6) δ 8.65 (d, J = 8.5 Hz, 1H, 5-H), 8.42 (d, J = 7.2 Hz, 1H, 7-H), 8.28 (d, J = 8.2 Hz, 1H, 2-H), 7.66 (t, J (average) = 7.8 Hz, 1H, 6-H), 7.25 (d, J = 8.2 Hz, 1H, 3-H), 4.80 (s, 1H, CH), 4.01 (m, 2H), 1.64 (h, J = 7.4 Hz, 2H, CH_2), 1.35 (s, 3H, Me), 0.92 (t, J = 7.4 Hz, 3H, Me).

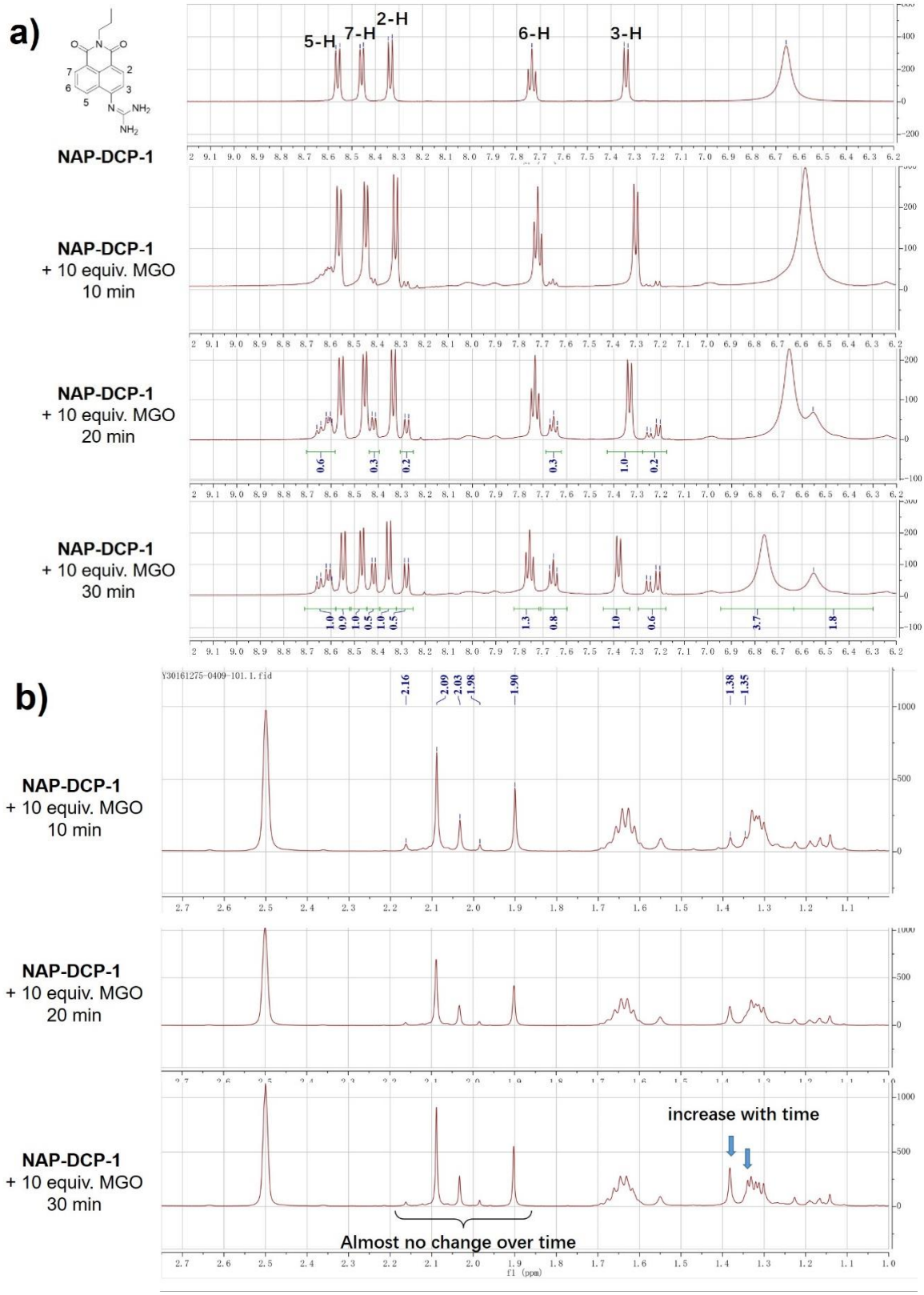

Figure S4 Time-dependent ^{1}HNMR study of **NAP-DCP-1** with 10 equiv. MGO in DMSO-d_6. Two dihydroxyimidazolidine adducts were formed (**Scheme S5**): a) Chemical shift region from δ 9.2 to 6.2; b) Chemical shift region from δ 2.5 to 1.0 (also see **Figure S53**).

Part III: Fluorescence and Absorption Spectroscopy Studies

3.1 Spectroscopic materials

All aqueous solutions were prepared using double distilled water. Probe stock solution (1 mM in dry DMSO) was prepared and stored at -20 °C. All fluorescence and absorption spectroscopic measurements were performed in 10 mM phosphate buffer (pH 7.4) at 25 °C unless otherwise stated. Samples for absorption and fluorescence measurements were contained in 1 cm×1 cm quartz cuvettes (3.5 mL volume).

3.2 Time-dependent absorption spectra of NAP-DCP-1 or NAP-DCP-2 upon addition of 200 equiv. reactive dicarbonyls (MGO or GO) at pH 7.4.

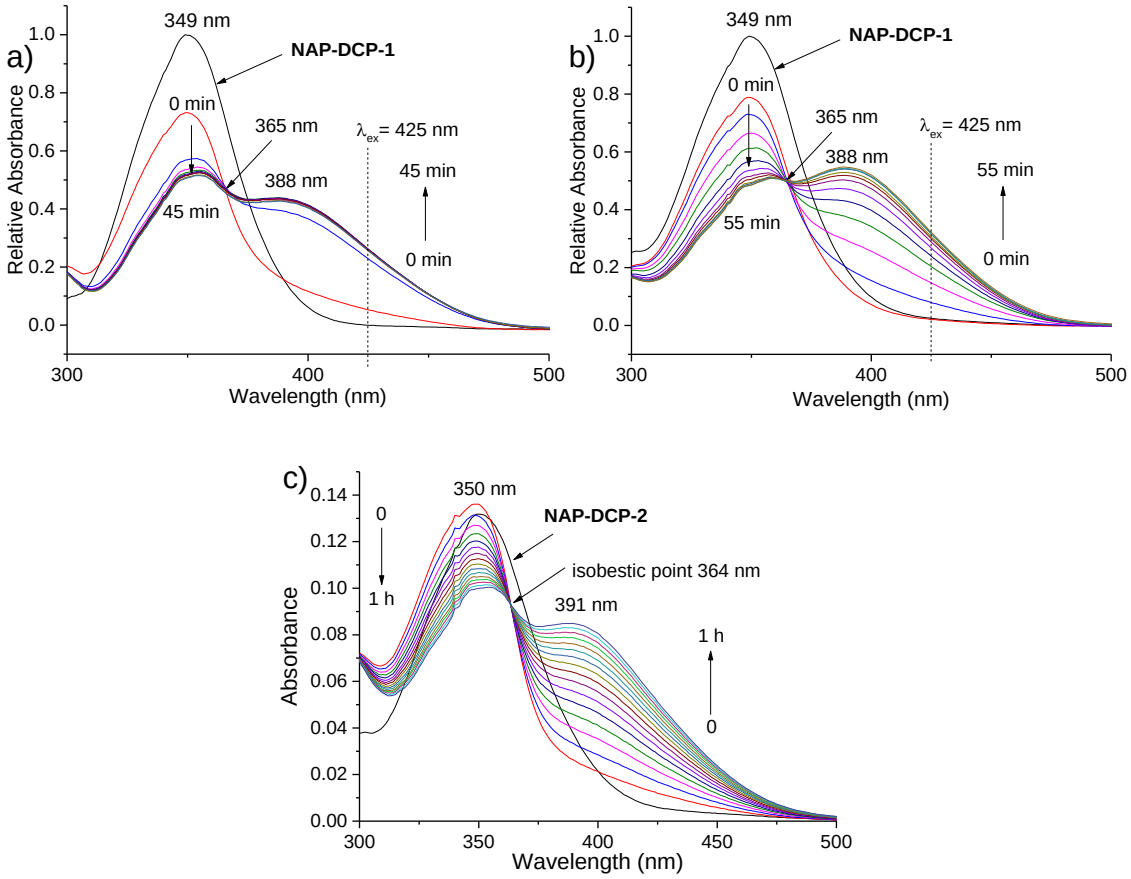

Figure S5 a-b) Time-dependent relative absorption spectra of **NAP-DCP-1** (10 μM) upon addition of 200 equiv. MGO (a) or GO (b) (The maximum absorbance of **NAP-DCP-1** (10 μM) at 349 nm was set as 1; c) Time-dependent relative absorption spectra of **NAP-DCP-2** (10 μM) upon addition of 200 equiv. MGO. (Data were taken every 5 min until reaching equilibrium in 10 mM PBS buffer solution at pH 7.4).

3.3 Normalized fluorescence excitation and emission spectra of NAP-DCP-1, reaction equilibrium mixture of NAP-DCP-1 with MGO or GO), and hydroimidazolone 6b.

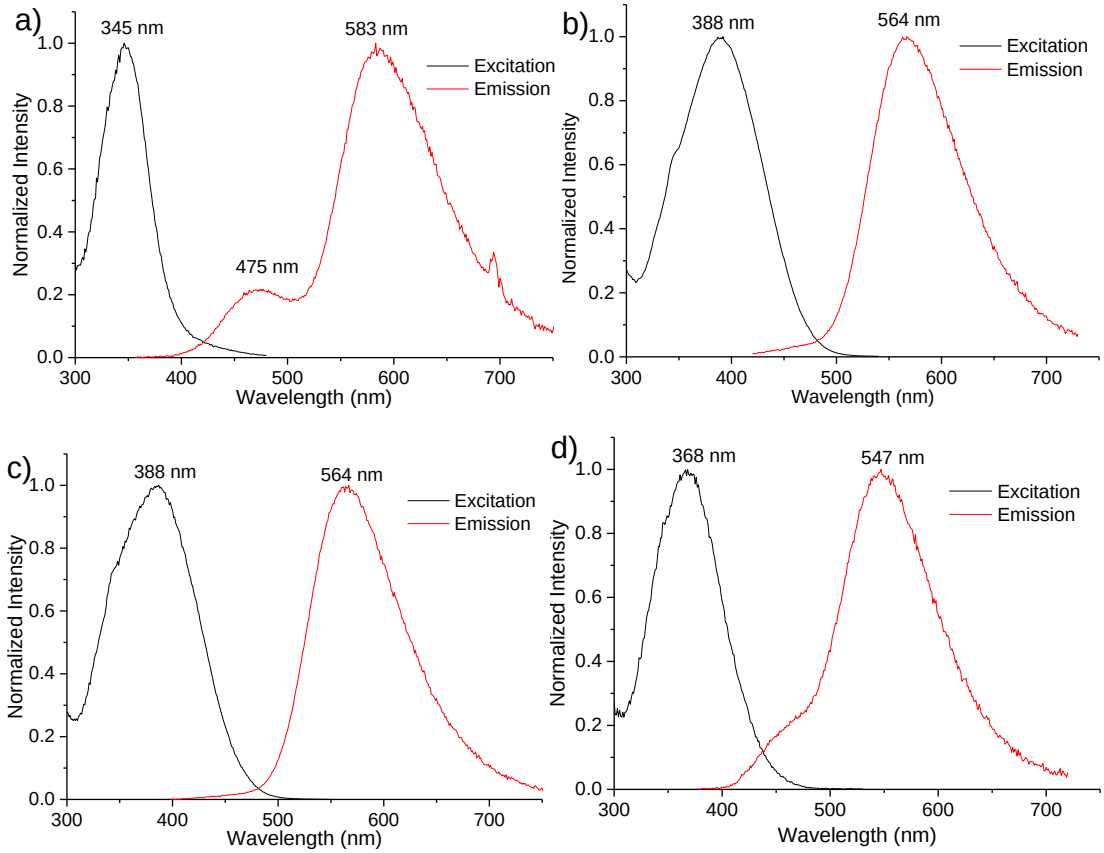

Figure S6 a) Normalized fluorescence excitation (λ_{em}=583 nm) and emission spectra (λ_{ex}= 345 nm) of the probe **NAP-DCP-1** (2 μM); b) Normalized fluorescence excitation (λ_{em}=564 nm) and emission spectra (λ_{ex}= 388 nm) of the probe **NAP-DCP-1** (2 μM) after incubation with MGO (200 μM) for 30 min; c) Normalized fluorescence excitation (λ_{em}=564 nm) and emission spectra (λ_{ex}= 388 nm) of the probe **NAP-DCP-1** (2 μM) after incubation with GO (200 μM) for 30 min; d) Normalized fluorescence excitation (λ_{em}=547 nm) and emission spectra (λ_{ex}= 368 nm) of the hydroimidazolone **6b** (2 μM). (All measurements were performed in PBS buffer (10 mM, pH 7.4) with slit =4/4 nm).

3.4 Excitation-wavelength-dependent fluorescence turn-on response studies of NAP-DCP-1 upon addition of 100 equiv. GOS (MGO or GO).

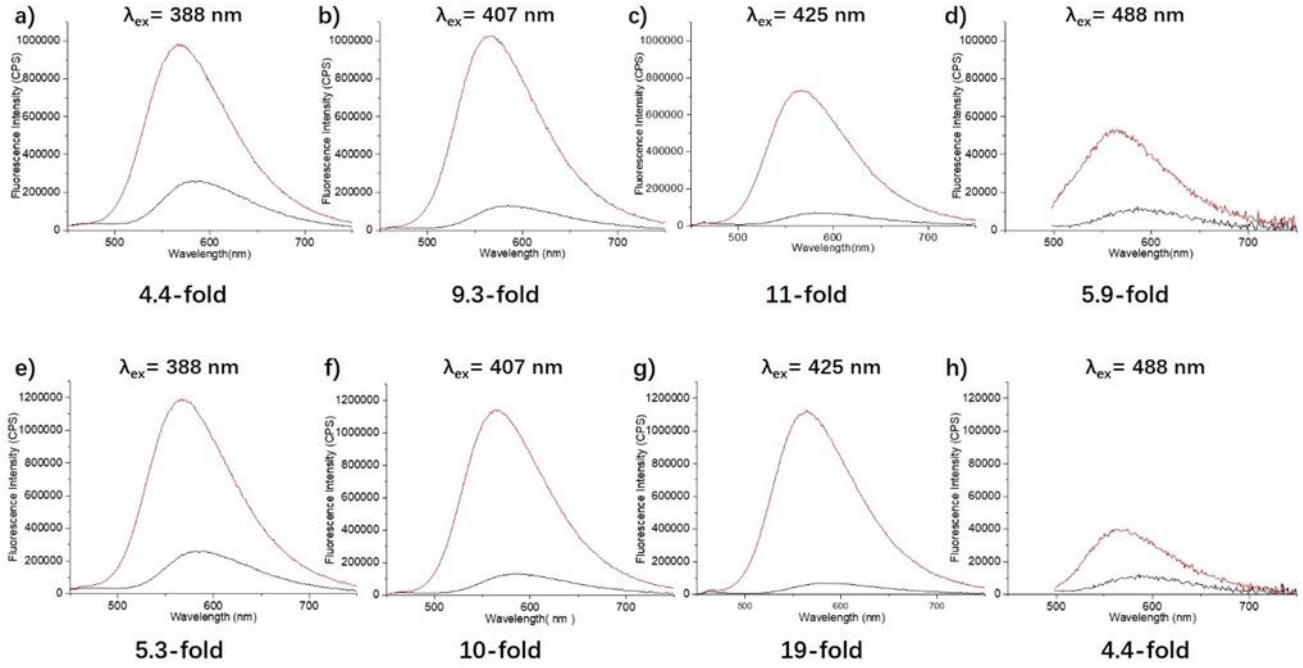

Figure S7 a-d) Fluorescence emission spectra of the probe **NAP-DCP-1** (2 μM) and the probe **NAP-DCP-1** (2 μM) after incubation with 200 μM MGO for 30 min in 10 mM PBS buffer solution at pH 7.4; e-h) Fluorescence emission spectra of the probe **NAP-DCP-1** (2 μM) and the probe **NAP-DCP-1** (2 μM) after incubation with 200 μM GO for 30 min in 10 mM PBS buffer solution at pH 7.4. (The corresponding excitation wavelength and fluorescence turn-on ratio at 564 nm were given for comparison.)

3.5 More reversibility studies of the turn-on response of the probe NAP-DCP-1 for reactive dicarbonyls (MGO and GO)

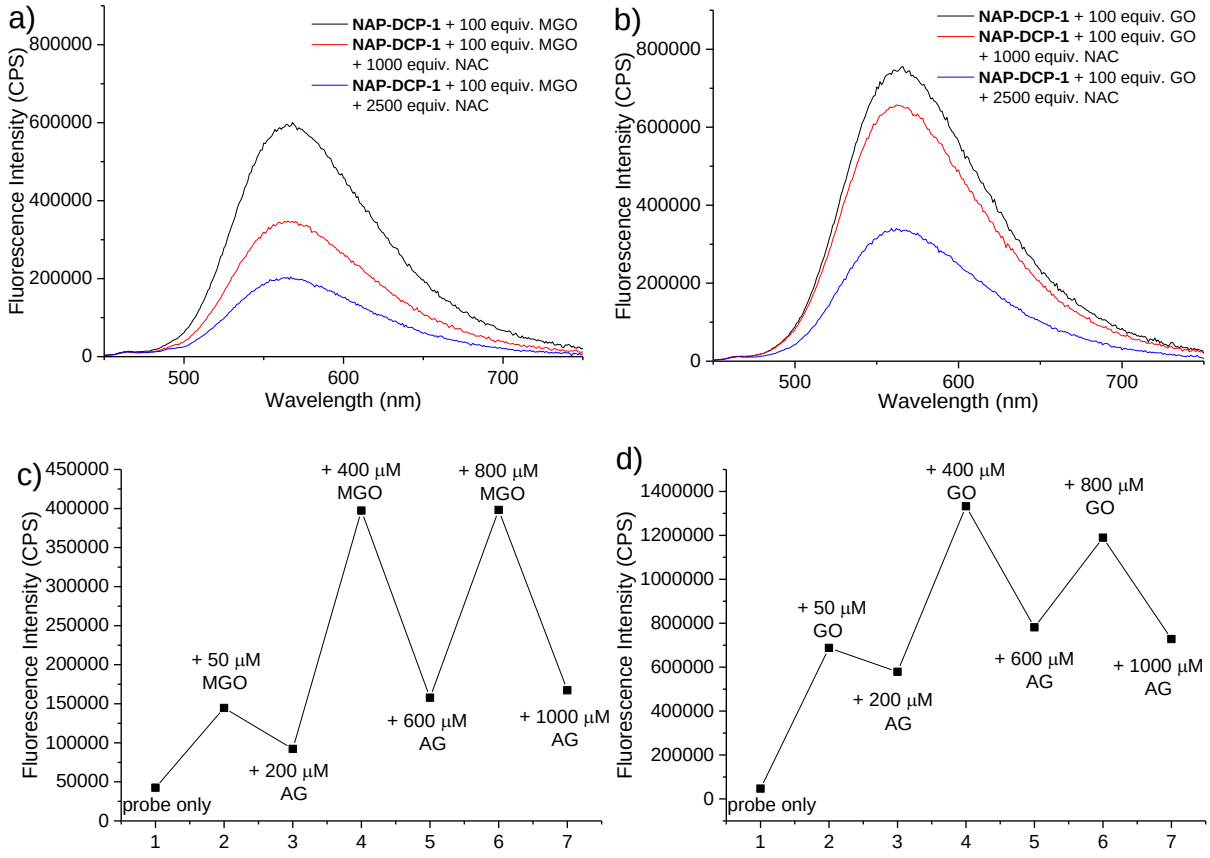

Figure S8 a-b) Concentration-dependent fluorescence emission spectra (λ_{ex} = 425 nm, slit = 4/4 nm) of the probe **NAP-DCP-1** (2 μM) preincubated with 200 μM MGO (a) or GO (b in PBS buffer (10 mM, pH = 7.4) for 30 min and then incubated with two different amount of *N*-acetyl cysteine (NAC) hydrochloride (2000 and 5000 μM) for 30 min; c) Fluorescence intensity at 564 nm (λ_{ex} = 425 nm, slit = 4/4 nm) of **NAP-DCP-1** (2 μM) in DMEM media with 10% FBS at 37 ºC after treatments with MGO and AG in turns: 1, probe only; 2, probe + 50 μM MGO for 30 min; 3, further+200 μM AG for 30 min; 4, further + 400 μM MGO for 30 min; 5, further + 600 μM AG for 30 min; 6, further + 800 μM MGO for 30 min; 7, further +1000 mM AG for 30 min; d) Fluorescence intensity at 564 nm (λ_{ex} = 425 nm, slit = 4/4 nm) of **NAP-DCP-1** (2 μM) in DMEM media with 10% FBS at 37 ºC after treatments with GO and AG in turns: 1, probe only; 2, probe + 50 μM GO for 90 min; 3, further+200 μM AG for 60 min; 4, further + 400 μM MGO for 60 min; 5, further + 600 μM AG for 60 min; 6, further + 800 μM MGO for 60 min; 7, further +1000 mM AG for 60 min.

3.6 Determination of detection limit of the NAP-DCP-1 for MGO and GO.

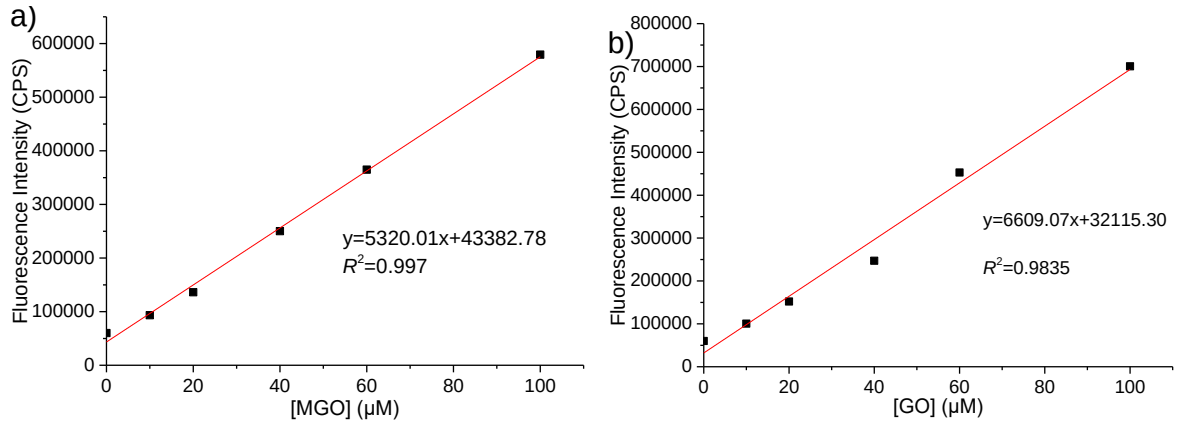

Figure S9 a) Linear regression of concentration-dependent fluorescence emission intensity at 564 nm (λ_{ex} = 425 nm, slit = 4/4 nm) of the probe **NAP-DCP-1** (2 μM) incubated with 0, 10, 20, 40, 60, and 100 μM GO in PBS buffer (10 mM, pH = 7.4) for 30 min. The limit of detection of the probe for MGO was determined to be 0.72 μM. b) Linear regression of concentration-dependent fluorescence emission intensity at 564 nm (λ_{ex} = 425 nm, slit = 4/4 nm) of the probe **NAP-DCP-1** (2 μM) incubated with 0, 10, 20, 40, 60, and 100 μM GO in PBS buffer (10 mM, pH = 7.4) for 30 min. The limit of detection of the probe for GO was determined to be 0.58 μM.

3.7 Selectivity studies of turn-on fluorescence response of NAP-DCP-1 towards MGO and GO.

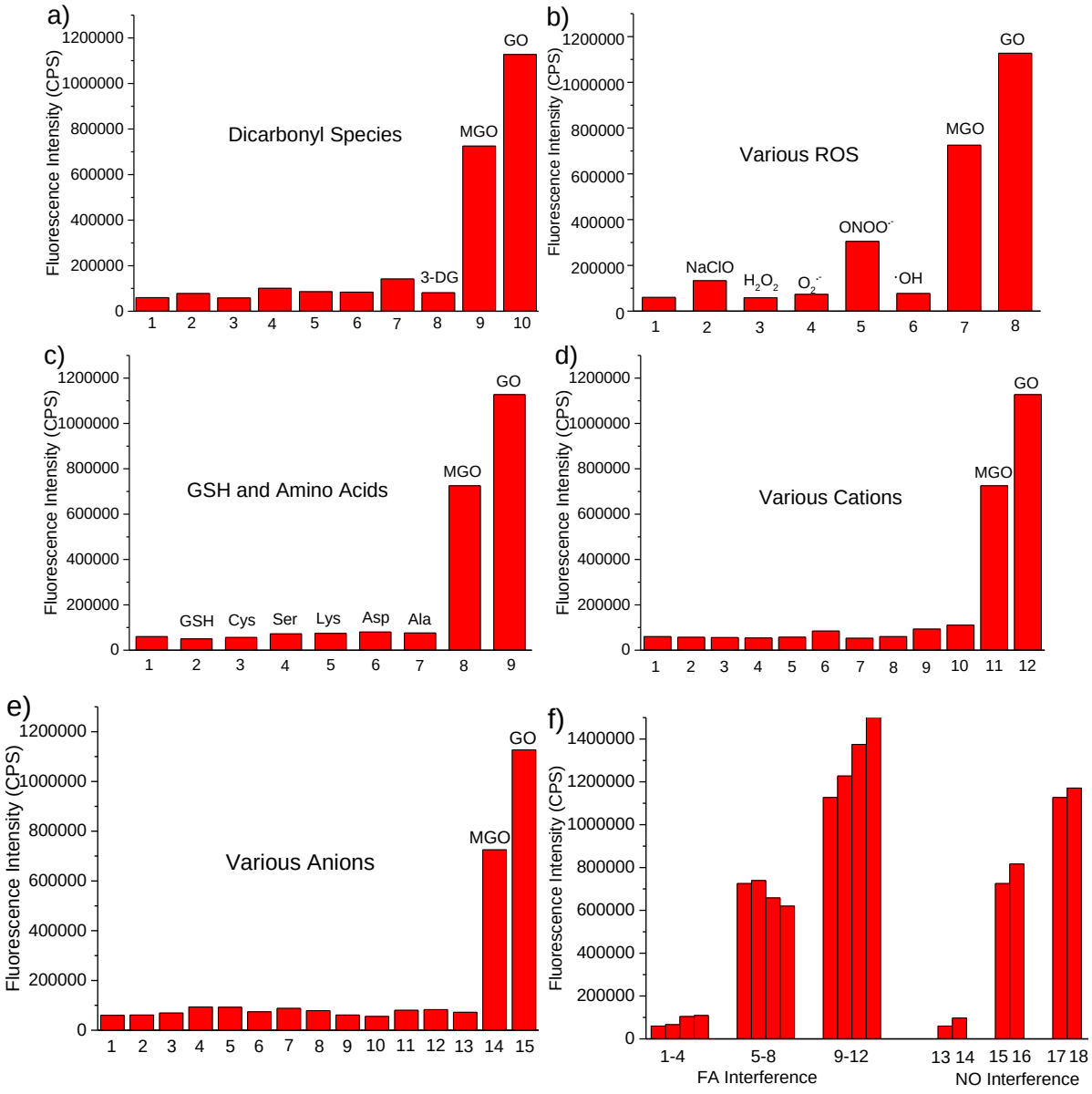

Figure S10 a) Fluorescence intensity at 564 nm of the probe **NAP-DCP-1** (2 μM) upon incubation with 100 equiv. of various dicarbonyl species, 1: probe only; 2: glyoxylic acid; 3: *o*-phthalaldehyde; 4: ethyl pyruvate; 5: pyruvic acid; 6: glutaraldehyde; 7: diacetyl; 8: 3-deoxyglucosome (3-DG); 9: MGO; 10: GO. b) Fluorescence intensity at 564 nm of the probe **NAP-DCP-1** (2 μM) upon incubation with 100 equiv. of various reactive oxygen species, 1: probe only; 2: NaClO; 3: H_2O_2; 4: $O_2^{\cdot-}$; 5: $ONOO^-$; 6: $OH^{\cdot}$; 7: MGO; 8: GO. c) Fluorescence intensity at 564 nm of the probe **NAP-DCP-1** (2 μM) upon incubation with 100 equiv. of various amino acids, 1: probe only; 2: GSH; 3: Cys; 4: Ser; 5: Lys; 6: Asp; 7: Ala; 8: MGO; 9: GO. d) Fluorescence intensity at 564 nm of the probe **NAP-DCP-1** (2 μM) upon incubation with 100 equiv. of various cations, 1: probe only; 2: Na^+; 3: K^+; 4: Zn^{2+}; 5: Ca^{2+}; 6: Mg^{2+}; 7: Al^{3+}; 8: Cu^{2+}; 9: Fe^{2+}; 10: Fe^{3+}; 11: MGO; 12: GO. e) Fluorescence intensity at 564 nm of the probe **NAP-DCP-1** (2 μM) upon incubation with 100 equiv. of various anions, 1: probe only; 2: F^-; 3: Cl^-; 4: Br^-; 5: I^-; 6: S^{2-}; 7: HSO_3^-; 8: SO_4^{2-}; 9: NO_2^-; 10: NO_3^-; 11: HCO_3^-; 12: CO_3^{2-}; 13: OAc^-; 14: MGO; 15 GO. f) Comparison of fluorescence intensity at 564 nm of the probe **NAP-DCP-1** (2 μM)

towards FA or NOC-18 (an NO-donor), MGO or GO without or in the presence of formaldehyde (FA) or NOC-18. 1: probe only; 2: FA (1 mM); 3: FA (2 mM); 4: FA (3 mM); 5: MGO (200 μM); 6: MGO (200 μM) + FA (1 mM); 7: MGO (200 μM) + FA (2 mM); 8: MGO (200 μM) + FA (3 mM); 9: GO (200 μM); 10: GO (200 μM) + FA (1 mM); 11: GO (200 μM) + FA (2 mM); 12: GO (200 μM) + FA (3 mM); 13: probe only; 14: NOC-18 (1 mM); 15: MGO (200 μM); 16: MGO (200 μM) + NOC-18 (1 mM); 17: GO (200 μM); 18: GO (200 μM) + NOC-18 (1 mM). (All measurements were performed in PBS buffer (10 mM, pH 7.4) with λ_{ex} = 425 nm and slit=4/4 nm, incubation time = 30 min)

3.8 pH-Dependent fluorescence response of the NAP-DCP-1 for MGO and GO.

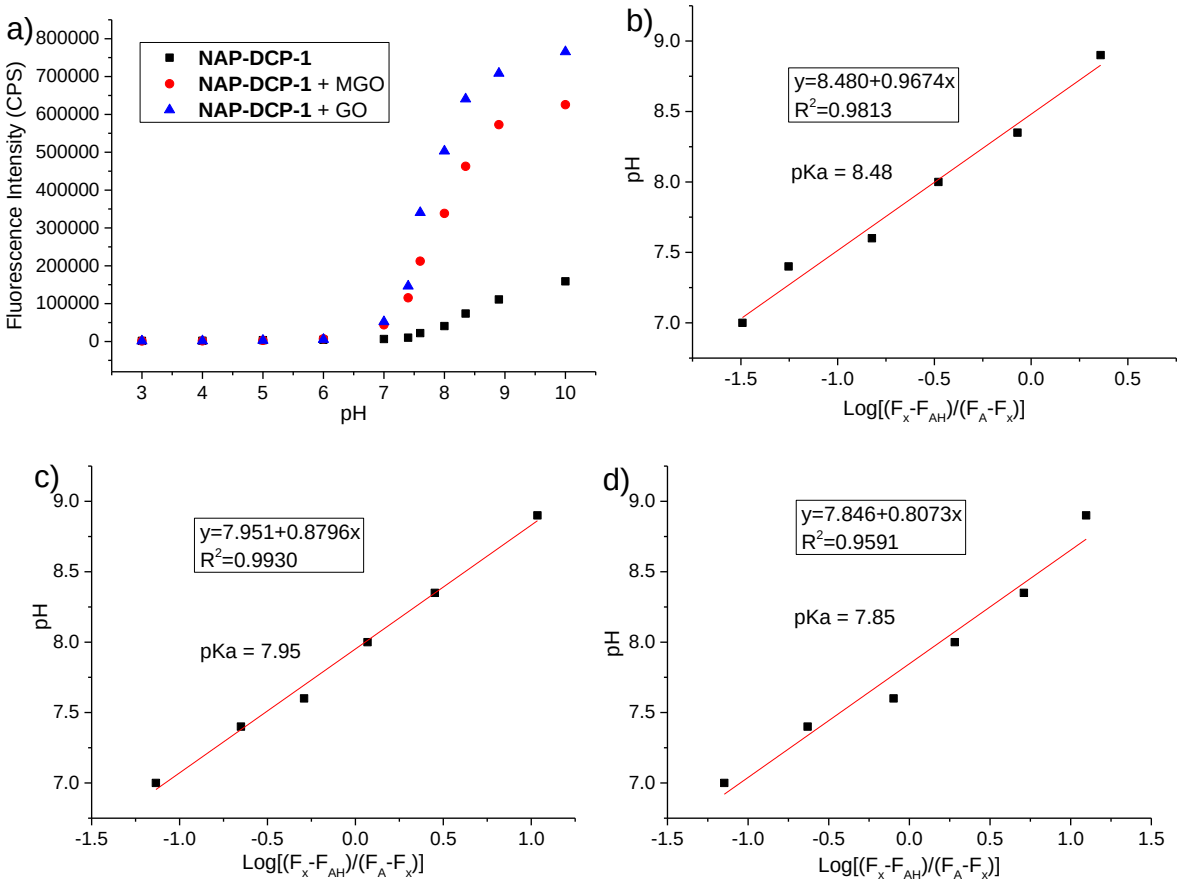

Figure S11 a) pH-dependent (pH from 3 to 10) fluorescence emission intensity at 564 nm (λ_{ex} = 425 nm, slit = 3/3 nm) of the probe **NAP-DCP-1** (2 μM) after incubation with 100 equiv. MGO or GO in PBS solution (10 mM) for 30 min; b-d) Linear regression for pKa calculations from data shown in **NAP-DCP-1** (b); **NAP-DCP-1** and MGO adducts (c): **NAP-DCP-1** and GO adducts (d).

3.9 Absorption spectra of the NAP-DCP-1 before and after addition of FA and NO

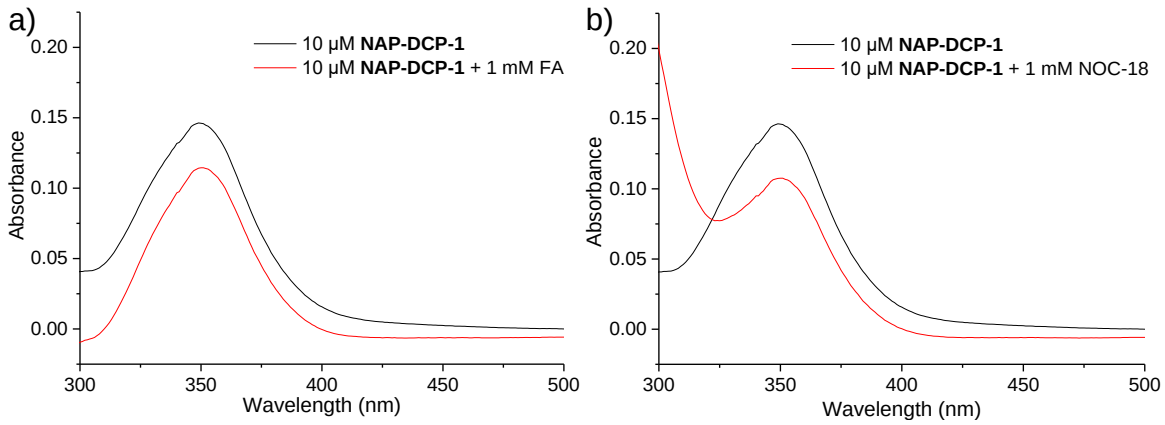

Figure S12 Absorption spectra of **NAP-DCP-1** (10 μM) before and after addition of 100 equiv. of (a) FA or (b) NOC-18.

3.10 Fluorescence emission spectra of the NAP-DCP-1 with its acetylated derivatives.

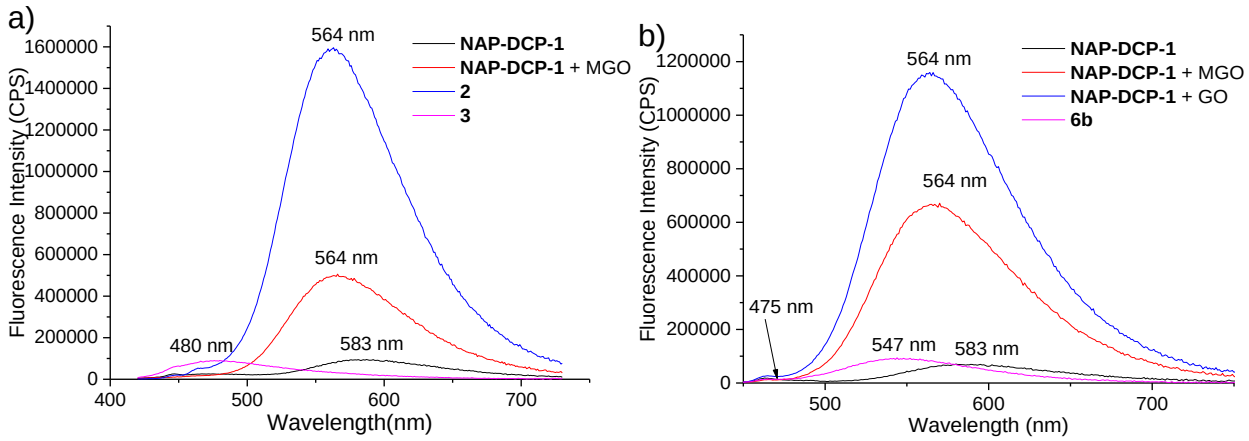

Figure S13 a) Fluorescence emission spectra of **NAP-DCP-1** (2 μM), reaction equilibrium mixture of **NAP-DCP-1** (2 μM) and 200 equiv. MGO, mono-acetylated derivative **2** (2 μM) and di-acetylated derivative **3** (2 μM); b) Fluorescence emission spectra of **NAP-DCP-1** (2 μM), reaction equilibrium mixture of **NAP-DCP-1** (2 μM) and 100 equiv. MGO or GO, and the hydroimidazolone **6b** (2 μM).

3.11 Absorption spectra of the mono- and di-acetylated derivatives versus deprotonated probe NAP-DCP-1 at pH 11.0.

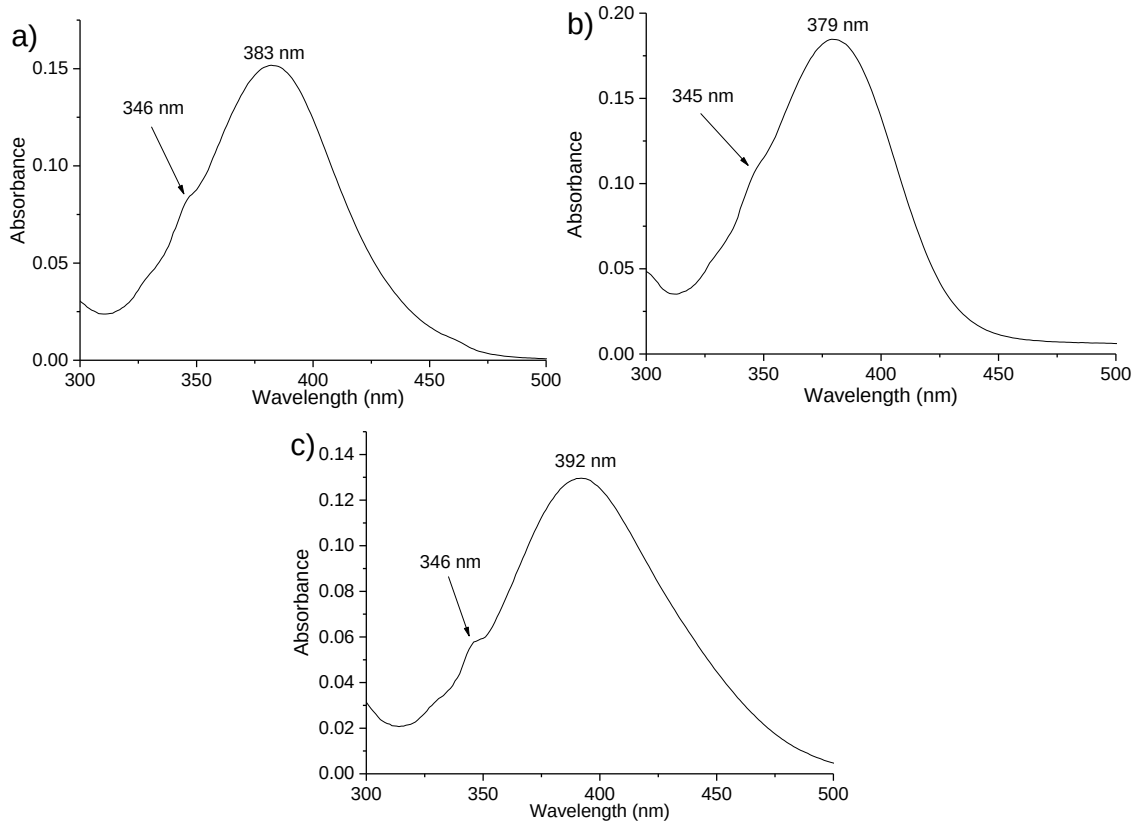

Figure S14 a) Absorption spectrum of the mono-acetylated derivative **2** (10 μM) in PBS buffer (10 mM, pH 7.4) ; b) Absorption spectrum of the di-acetylated derivative **3** (10 μM) in PBS buffer (10 mM, pH 7.4); c) Absorption spectrum of **NAP-DCP-1** at pH 11.0 PBS solution. (The should peak is from their corresponding protonated form)

3.12 Time-dependent absorption spectra of NAP-DCP-3 in detection of MGO and GO

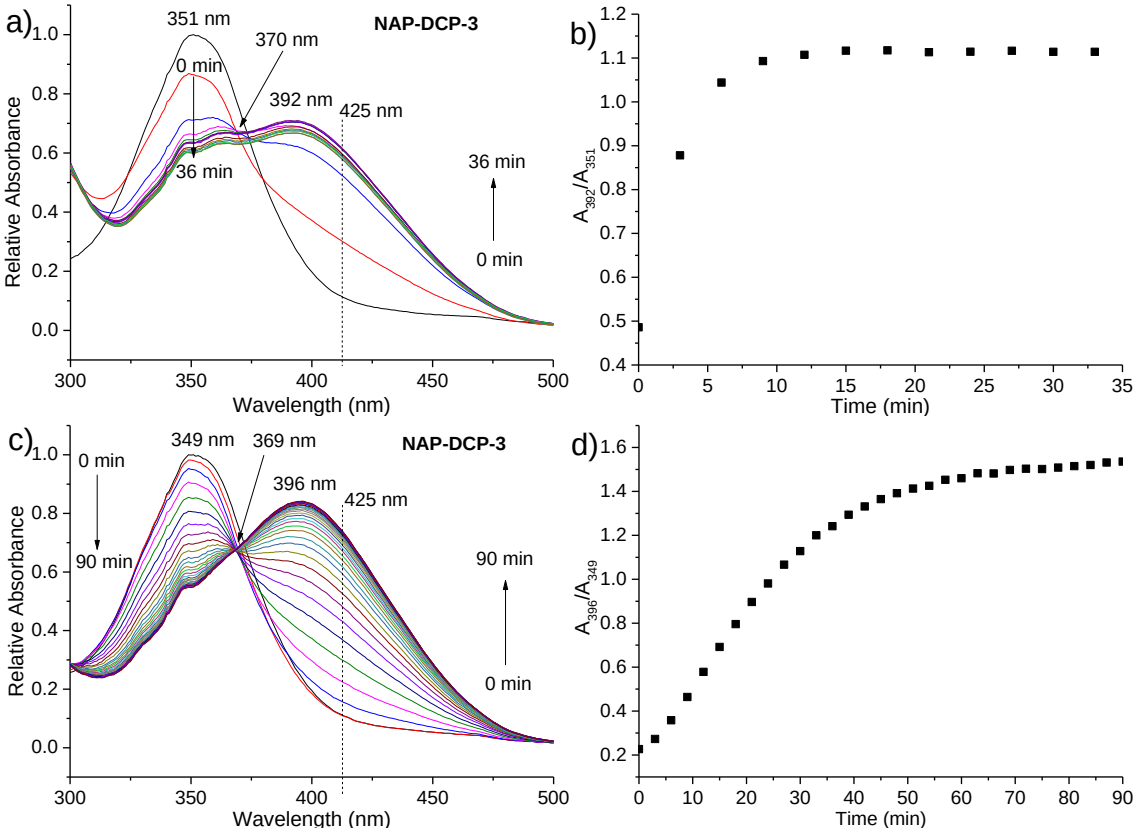

Figure S15 a) Time-dependent relative absorption spectra of **NAP-DCP-3** (10 μM) upon addition of 2 mM MGO; b) Time-dependent ratio of A_{392}/A_{351} of **NAP-DCP-3** (10 μM) upon addition of 2 mM MGO; c) Time-dependent relative absorption spectra of **NAP-DCP-3** (10 μM) upon addition of 2 mM GO; d) Time-dependent ratio of A_{392}/A_{351} of **NAP-DCP-3** (10 μM) upon addition of 2 mM GO.

3.13 Time-dependent fluorescence emission spectra of NAP-DCP-3 in detection of MGO and GO

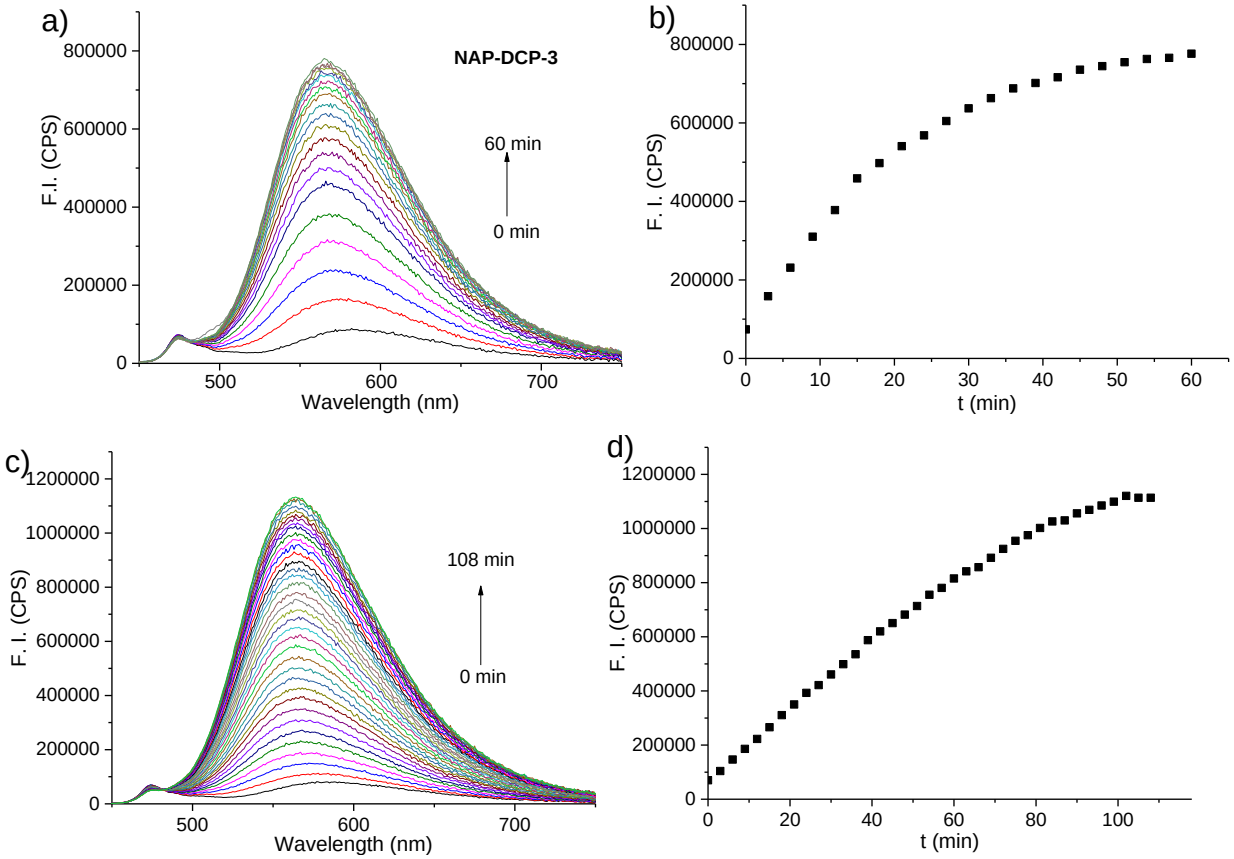

Figure S16 a) Time-dependent fluorescence emission spectra of **NAP-DCP-3** (2 μM) upon addition of 200 μM MGO; b) Time-dependent fluorescence intensity at 564 nm of **NAP-DCP-3** (2 μM) upon addition of 200 μM MGO; c) Time-dependent fluorescence emission spectra of **NAP-DCP-3** (2 μM) upon addition of 200 μM GO; d) Time-dependent fluorescence intensity at 564 nm of **NAP-DCP-3** (2 μM) upon addition of 200 μM GO.

3.14 Concentration-dependent fluorescence emission spectra of NAP-DCP-3 in detection of MGO and GO

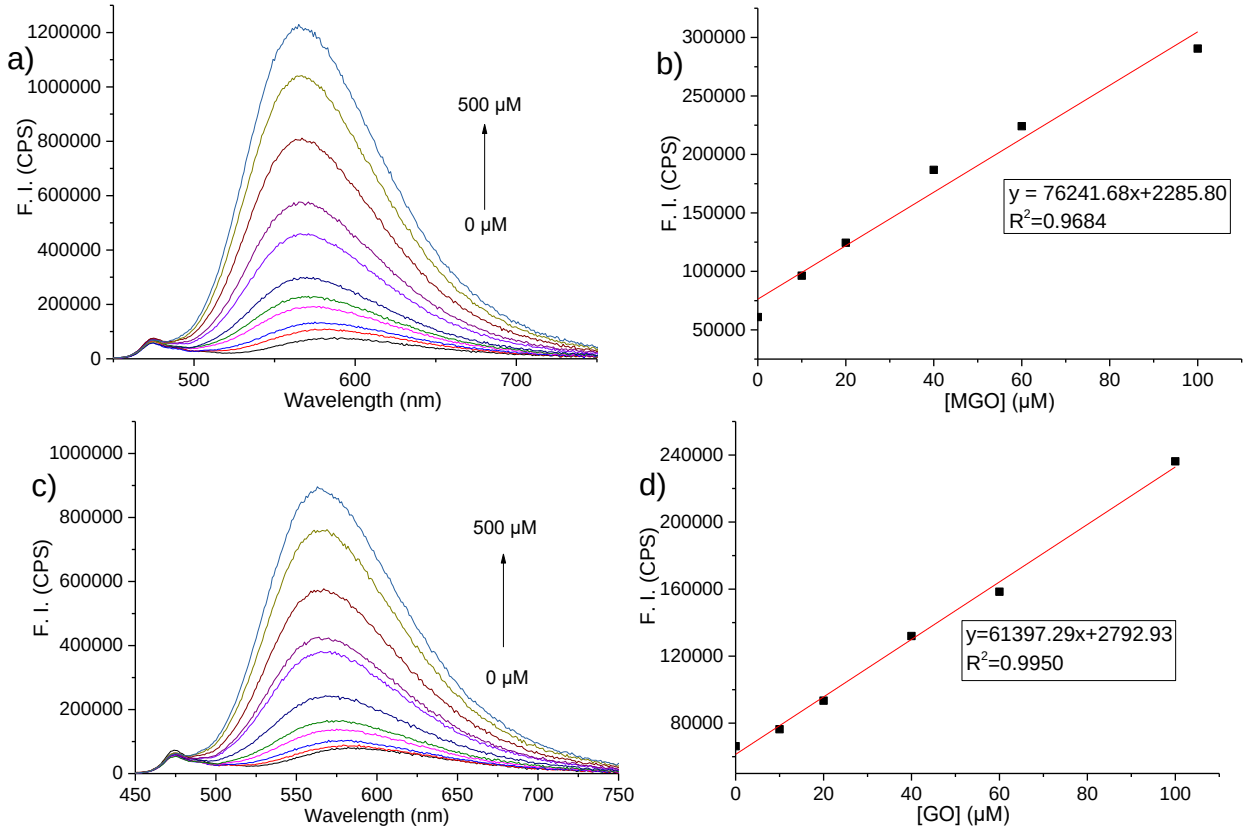

Figure S17 a) Concentration-dependent fluorescence emission spectra (λ_{ex} = 425 nm, slit = 4/4 nm) of **NAP-DCP-3** (2 μM) upon addition of various concentrations of MGO (0 to 500 μM) ; b) Linear regression of concentration-dependent fluorescence intensity at 564 nm (λ_{ex} = 425 nm, slit = 4/4 nm) of **NAP-DCP-3** (2 μM) upon addition of various concentrations of MGO (0, 10, 20, 40, 60, and 100 μM) for 30 min. The limit of detection of the probe **NAP-DCP-3** for MGO was determined to be 0.13 μM; a) Concentration-dependent fluorescence emission spectra (λ_{ex} = 425 nm, slit = 4/4 nm) of **NAP-DCP-3** (2 μM) upon addition of various concentrations of GO (0 to 500 μM) ; b) Linear regression of concentration-dependent fluorescence intensity at 564 nm (λ_{ex} = 425 nm, slit = 4/4 nm) of **NAP-DCP-3** (2 μM) upon addition of various concentrations of GO (0, 10, 20, 40, 60, and 100 μM) for 30 min. The limit of detection of the probe **NAP-DCP-3** for MGO was determined to be 0.16 μM.

3.15 Fluorescence response of the NAP-DCP-3 toward MGO and GO.

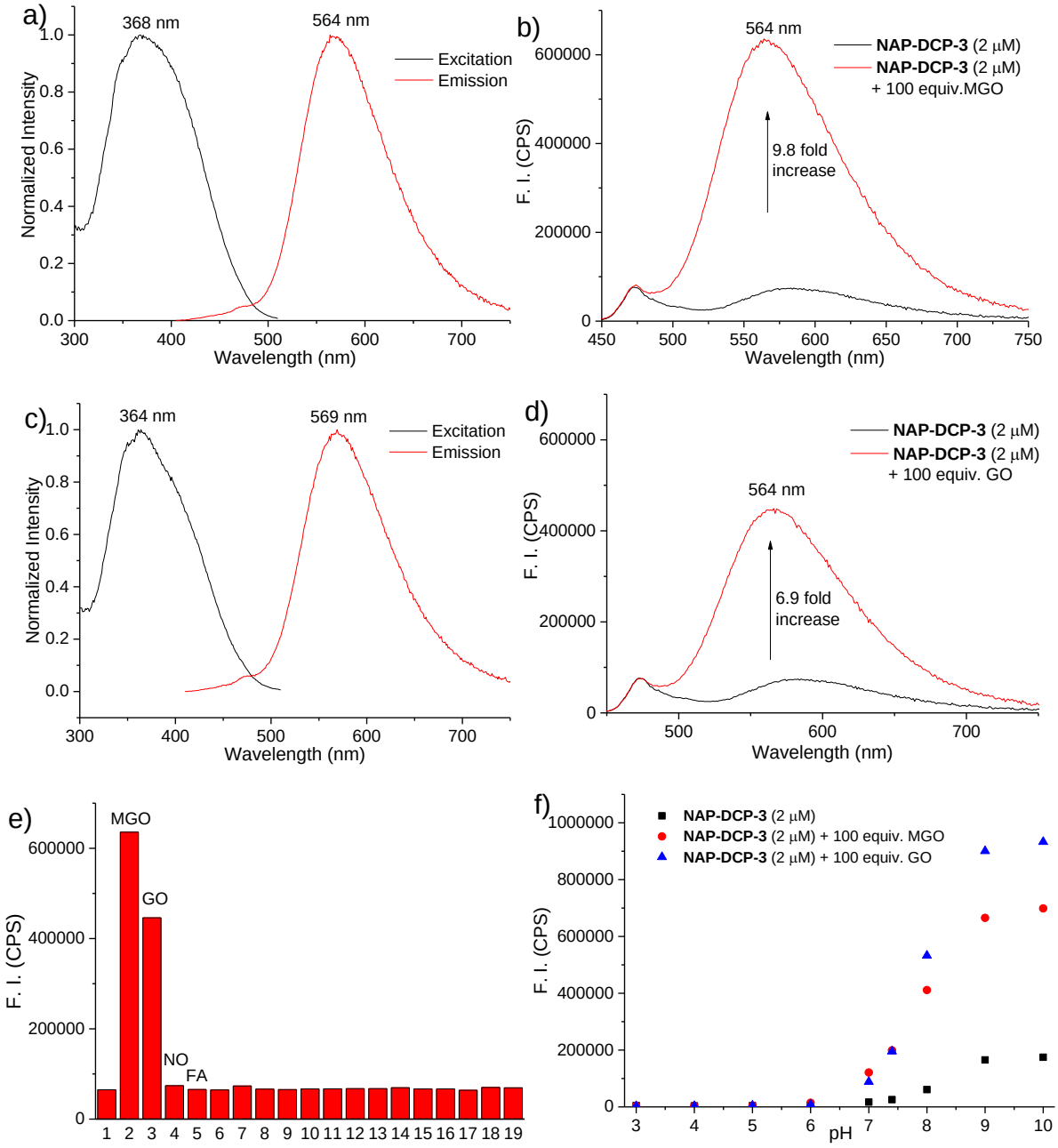

Figure S18 a) Normalized fluorescence excitation (λ_{em} = 564 nm) and emission (λ_{ex} = 392 nm) spectra of probe **NAP-DCP-3** (2 μM) in the presence of MGO (200 μM) in PBS buffer (pH 7.4); b) Fluorescence emission spectra of probe **NAP-DCP-3** (2 μM) in the absence and presence of 200 μM MGO in PBS buffer (λ_{ex} = 425 nm, slit = 4/4 nm); c) Normalized fluorescence excitation (λ_{em} = 564 nm) and emission (λ_{ex} = 396 nm) spectra of probe **NAP-DCP-3** (2 μM) in the presence of GO (200 μM) in PBS buffer (pH 7.4); d) Fluorescence emission spectra of probe **NAP-DCP-3** (2 μM) in the absence and presence of 200 μM GO in PBS buffer (λ_{ex} = 425 nm, slit =4/4 nm); e) Fluorescence intensity of **NAP-DCP-3** (2 μM) at 564 nm upon addition of various species (200 μM) including: (1) blank; (2) MGO; (3) GO; (4) NO (NOC-18) (5) FA; (6) *o*-phthalaldehyde; (7) glyoxylic acid; (8) benzaldehyde; (9) glutathione; (10) glucose; (11) cysteine; (12) acetaldehyde; (13) K^+; (14) Na^+; (15) Cu^{2+}; (16) Zn^{2+}; (17) Al^{3+}; (18) Ca^{2+}, (19) H_2O_2; f) pH-dependment fluorescence intensity at 564 nm (λ_{ex} = 425 nm) for probe **NAP-DCP-3** (2 μM) after incubation with 100 equiv. of MGO or GO. (All

measurements were performed in 10 mM PBS buffer with incubation time of 30 min.)

3.16 Fluorescence response of the NAP-DCP-3 toward MGO upon addition of increased amount of AG.

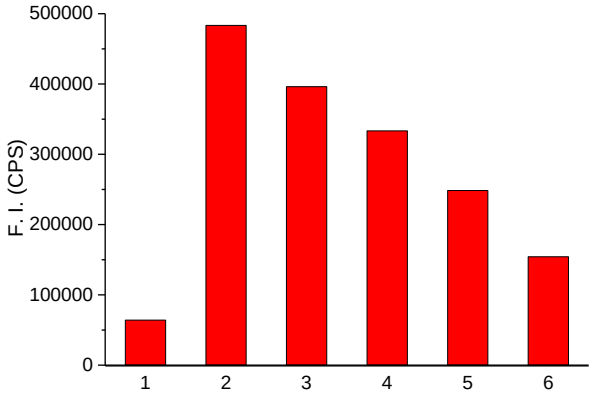

Figure S19 Fluorescence intensity at 564 nm (λ_{ex}= 425 nm, slit = 3/3 nm) of **NAP-DCP-3** (2 μM) preincubated with 200 μM MGO for 30 min and then incubated with various concentrations of AG for 4 h: 1) **NAP-DCP-3** (2 μM); 2) **NAP-DCP-3** (2 μM) + MGO (200 μM) for 30 min; 3) **NAP-DCP-3** (2 μM) + MGO (200 μM) for 30 min, and then + AG (150 μM) for 4 h); 4) **NAP-DCP-3** (2 μM) + MGO (200 μM) for 30 min, and then + AG (200 μM) for 4 h); 5) **NAP-DCP-3** (2 μM) + MGO (200 μM) for 30 min, and then + AG (400 μM) for 4 h); 6) **NAP-DCP-3** (2 μM) + MGO (200 μM) for 30 min, and then + AG (1 mM) for 4 h).

3.17 Fluorescence response of the NAP-DCP-3 toward FA or MGO/GO in the presence of FA

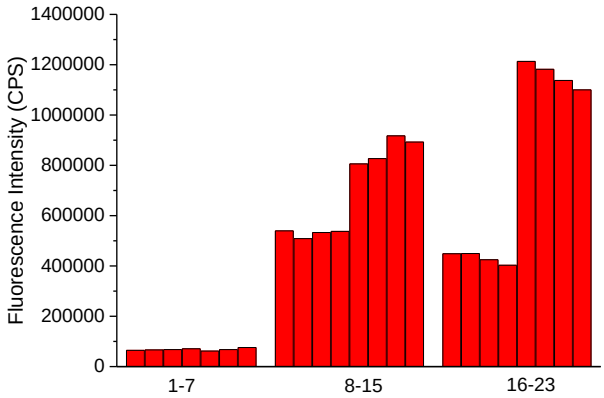

Figure S20 Comparison of fluorescence intensity at 564 nm of the probe **NAP-DCP-3** (2 μM) towards FA, MGO or GO without or in the presence of formaldehyde (FA). 1: probe only; 2: FA (1 mM, 30 min); 3: FA (2 mM, 30 min); 4: FA (3 mM, 30 min); 5: FA (1 mM, 2 h); 6:FA (2 mM, 2 h); 7: FA (3 mM, 2 h); 8: MGO (200 μM, 30 min); 9: MGO (200 μM) + FA (1 mM), 30 min; 10: MGO (200 μM) + FA (2 mM), 30 min; 11: MGO (200 μM) + FA (3 mM), 30 min; 12:MGO (200 μM, 2 h); 13: MGO (200 μM) + FA (1 mM), 2 h; 14:MGO (200 μM) + FA (2 mM), 2 h; 15: MGO (200 μM) + FA (3 mM), 2 h; 16: GO (200 μM, 30 min); 17: GO (200 μM) + FA (1 mM), 30 min; 18: GO (200 μM) + FA (2 mM), 30 min; 19: GO (200 μM) + FA (3 mM), 30 min; 20: GO (200 μM, 30 min); 21: GO (200 μM) + FA (1 mM), 2 h; 22: GO (200 μM) + FA(2 mM), 2 h; 23: GO (200 μM) + FA (3 mM), 2 h. (All measurements were performed in PBS buffer (10 mM, pH 7.4) with λ_{ex} = 425 nm and slit=4/4 nm)

3.18 Fluorescence quantum yield studies of the NAP-DCP-1 and NAP-DCP-3

The quantum yield of **NAP-DCP-1** and **NAP-DCP-3** were determined according to the literature.[22] Quinine sulfate with 0.1 M H_2SO_4 was chosen as standard (ϕ = 0.557, λ_{ex}= 350 nm). The quantum yields of **NAP-DCP-1** were measured in PBS buffer (10 mM, pH=7.4, λ_{ex}= 350 nm). Fluorescence quantum yields were obtained with the following equation: $\phi_s = \phi_b I_s A_b \eta_s / I_b A_s \eta_b$. Where ϕ is quantum yield; I is integrated area under the corrected emission spectra; A is absorbance at the excitation wavelength; η is the refractive index of the solution; the subscripts s and b refer to the sample and the standard, respectively. Generally, in diluted solution, $\eta_s \approx \eta_b$ then fluorescence quantum yields were obtained with the following equation $\phi_s = \phi_b I_s A_b / I_b A_s$.

As the products were not able to be separated as pure compounds, we measured the apparent quantum yields of the equilibrium mixture of the probe (90 μM) with 6 equiv. of MGO or GO.

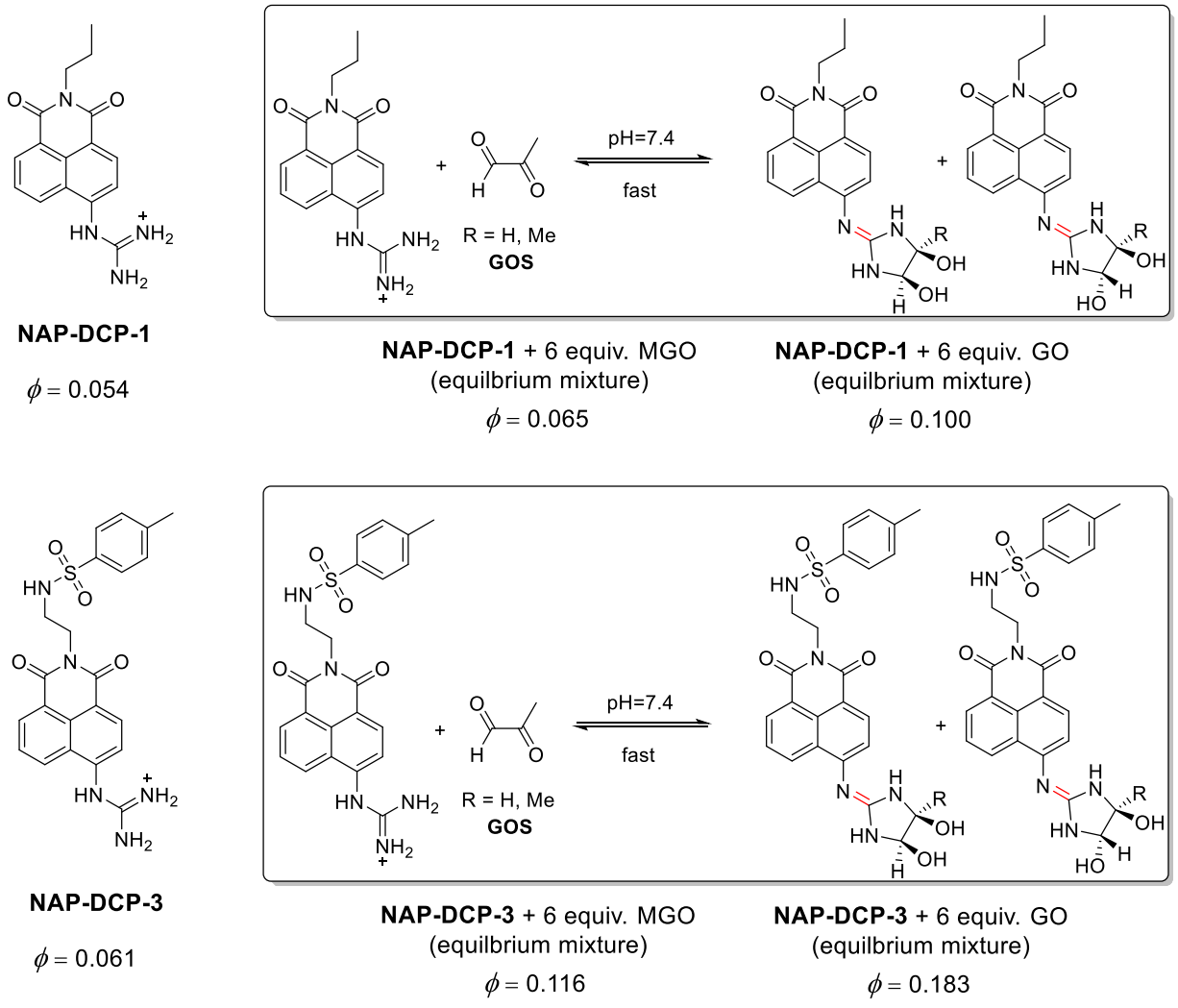

Figure S21 Fluorescence quantum yields of **NAP-DCP-1** and **NAP-DCP-3** and their equilibrium mixture with MGO or GO.

3.19 Measurement of two-photon absorption cross-section (δ) of the NAP-DCP-1 and NAP-DCP-3 towards GOS.

1 mM probe solutions for measurement of two-photon absorption cross-section were prepared from dilution of 300 μL 10 mM probe stock solution in DMSO with 2700 μL PBS buffer (10 mM, pH 7.4). An equilibrium solution of 1 mM probe and 100 mM MGO or GO for measurement of two-photon absorption cross-section were prepared from dilution of 300 μL 10 mM probe stock solution in DMSO with 2400 μL PBS buffer (10 mM, pH 7.4) followed by addition of 300 μL 1 M MGO or GO in water.

Two-photon excitation fluorescence (TPEF) spectra were determined using femtosecond laser pulse and Ti: sapphire system (680~1080 nm, 80 MHz, 140 fs, Chameleon II) as the light source. All measurements were carried out at room temperature. Two-photon absorption cross-sections were tested using two-photon-induced fluorescence measurement technique and thus the cross-sections can be calculated by way of the following equation (S1)[23]:

$$\delta = \delta_{ref} \frac{\Phi_{ref}}{\Phi} \frac{C_{ref}}{C} \frac{n_{ref}}{n} \frac{F}{F_{ref}} \qquad \text{(S1)}$$

Here, the subscripts *ref* stands for the reference molecule. δ is the two-photon absorption cross-sections value, *c* is the concentration of solution, *n* is the refractive index of the solution, *F* is the TPEF integral intensities of the solution emitted at the exciting wavelength, and Φ is the fluorescence quantum yield. The Φ_{ref} value of reference ($\Phi_{fluorescein}$ = 0.97) was taken from the literature[24]. The two-photon absorption cross-sections were tested with **NAP-DCP-1/-3** in the absence and presence of MGO/GO. The δ_{ref} value of fluorescein was taken from the literature[25], and the relative error of δ value in the experiment is about ±15%.

After measurement of two-photon absorption cross-section, 30 μL of aliquot of each sample were diluted to 3 mL with PBS buffer (10 mM, pH 7.4) and their UV-Vis spectra were measured (Figure S22).

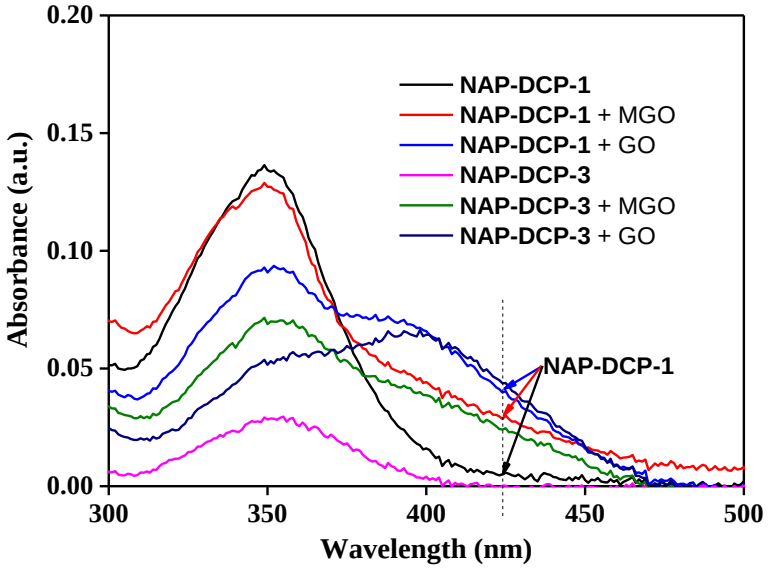

Figure S22 UV-Vis absorption spectra of 100-fold diluted samples in two-photon absorption cross-section measurements. (Note: the lower absorbance of **NAP-DCP-3** was caused by low solubility of **NAP-DCP-3**)

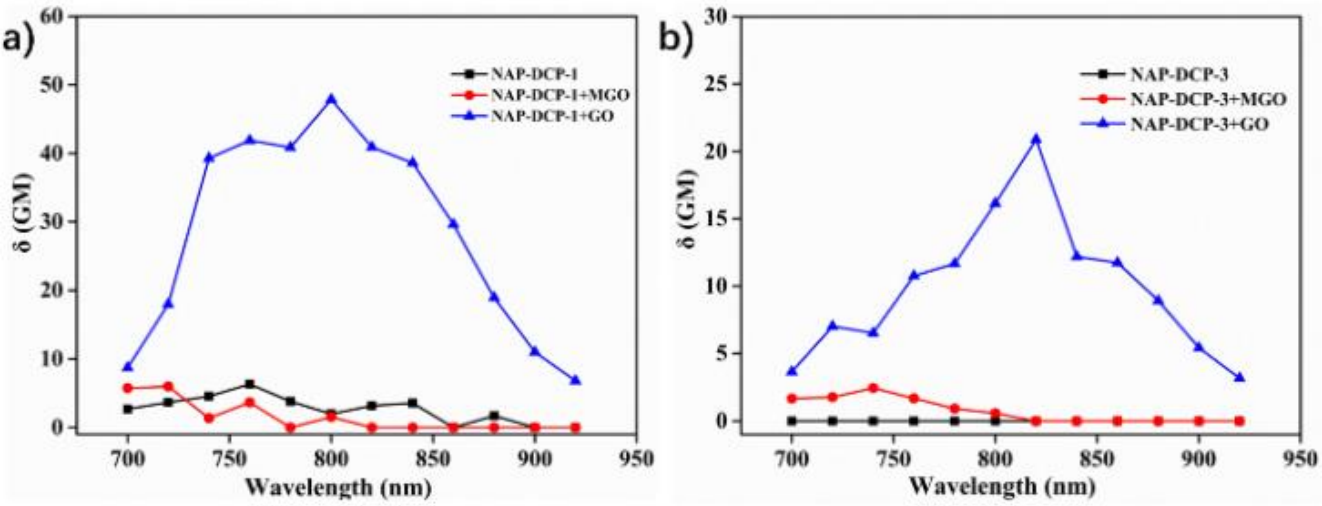

Figure S23 Two-photon absorption cross-section (δ) of 1 mM **NAP-DCP-1** (a) and 1 mM **NAP-DCP-3** (b) with or without 100 equiv. of MGO or GO in 10 mM PBS buffer : DMSO = 9:1 (v/v) (incubation time = 30 min).

Part IV: Mass Spectrum Studies

4.1 HRMS studies of a reaction mixture of the probe NAP-DCP-1 and MGO in acetonitrile.

To a suspended solution of **NAP-DCP-1** (6 mg, 0.02 mmol) in 1.5 mL acetonitrile was added 7.5 equiv. MGO (40% MGO in H_2O, 23 μL)，a clear solution was formed. The solution was taken for HRMS analysis. The peak m/z = 369.1564 was assigned to the $(M+H)^+$ peak of the dihydroxyimidazolidine adducts **5b**; while the peak m/z 297.1358 was assigned to the $(M+H)^+$ peak of **NAP-DCP-1**. The calculated values were 369.1557 and 297.1346, respectively (**Scheme S6**).

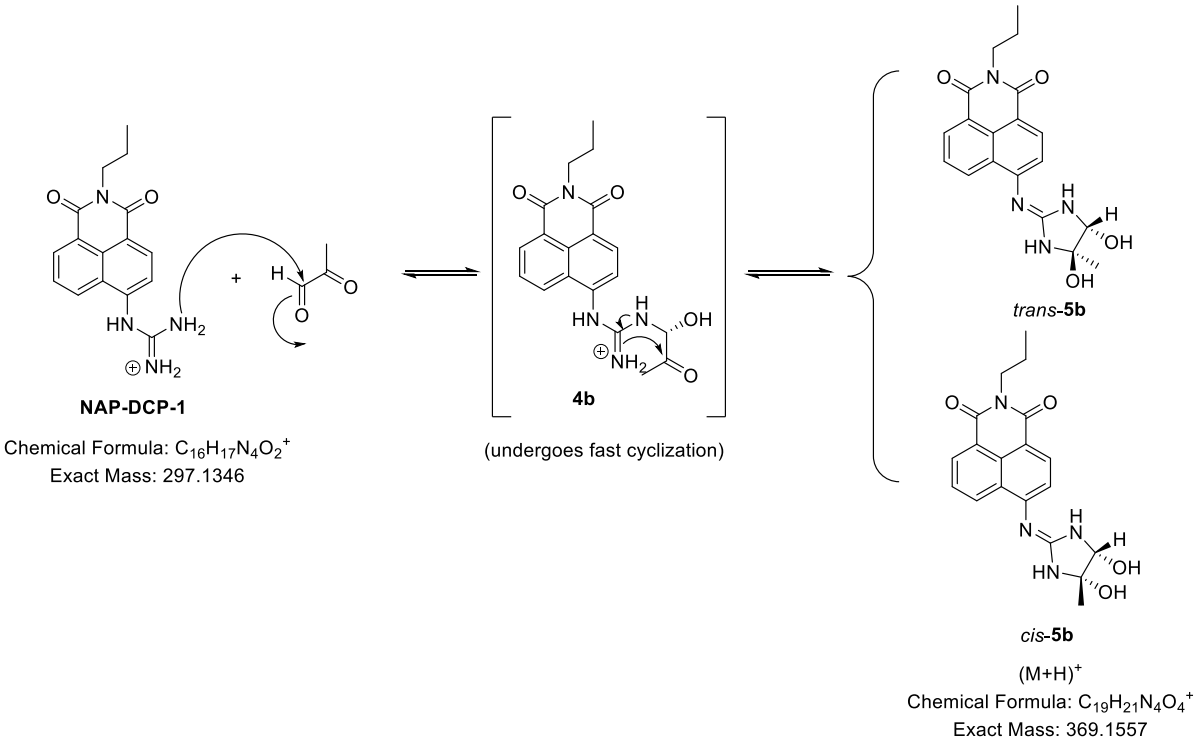

Scheme S6

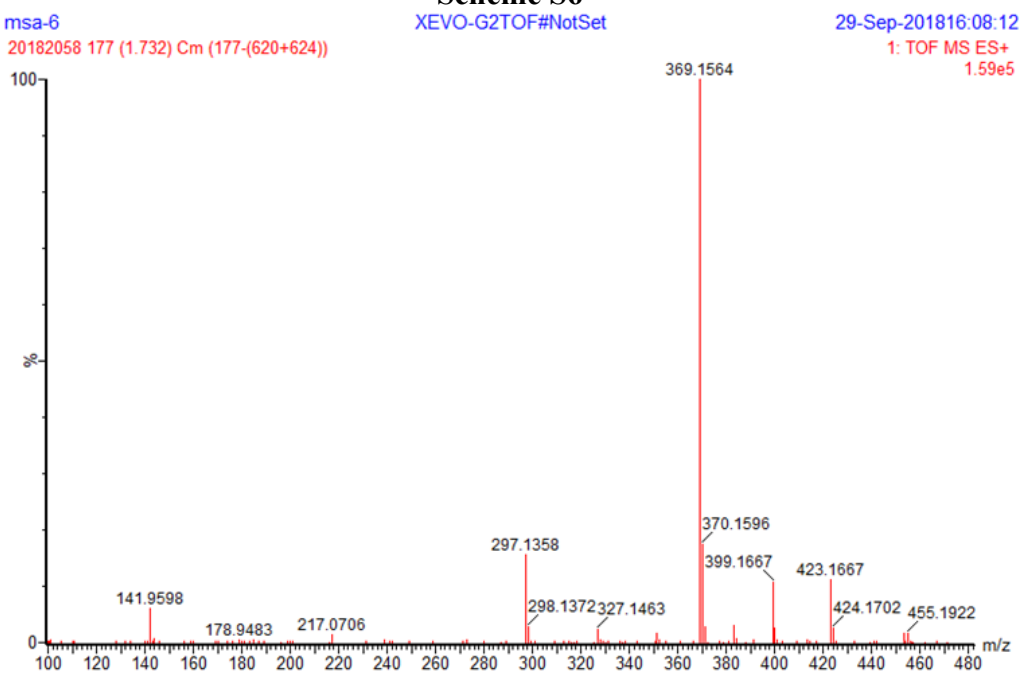

Figure S24 ESI-HRMS spectrum of the reaction mixture of **NAP-DCP-1** and **MGO**.

4.2 HRMS studies of a reaction mixture of the probe NAP-DCP-1 and GO in acetonitrile..

To a suspended solution of **NAP-DCP-1** (6 mg, 0.02 mmol) in 1.0 mL acetonitrile was added 10 equiv. GO (8.8 M in H_2O, 23 μL), a clear solution was formed. The solution was taken for HRMS analysis. The peak m/z = 355.1407 was assigned to the $(M+H)^+$ peak of the dihydroxyimidazolidine adducts **5a** with the calculated value of 355.1401 (**Scheme S7**).

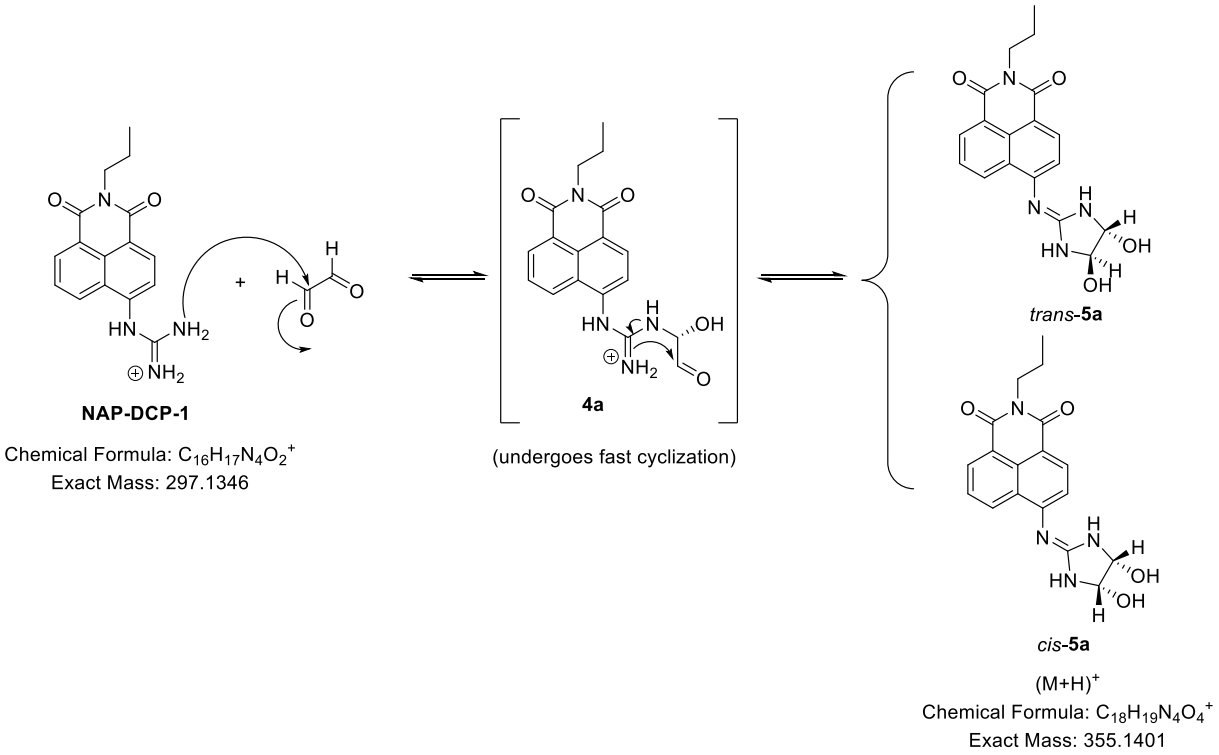

Scheme S7

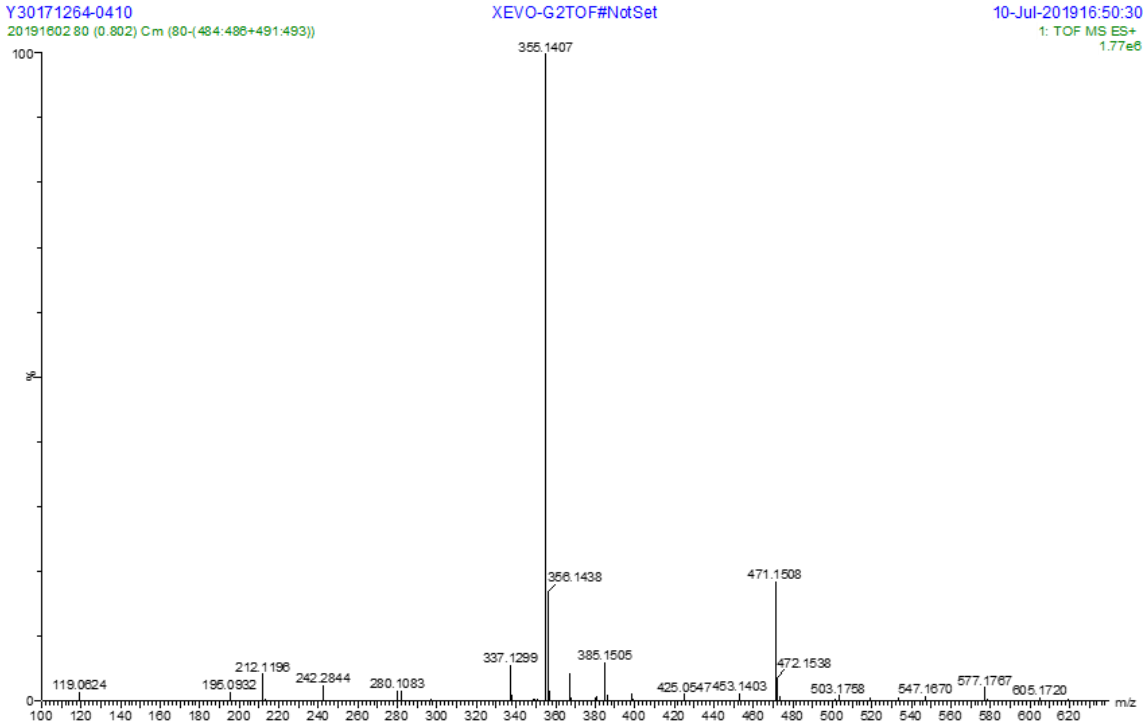

Figure S25 ESI-HRMS spectrum of the reaction mixture of **NAP-DCP-1** and **GO**.

4.3 UPLC-MS Studies of Model Reaction of NAP-FAP-1 with MGO

UPLC-MS analysis was performed on Thermo Scientific UltiMate 3000 with Q-Exactive™ plus MS/MS Mass Spectrometry equipped with Hypersil Gold C18 (Thermo Scientific) 3 μm, 100 mm×2.1 mm column. All the samples were eluted using a gradient mixture from 30:70 to 90:10 and back to 30:70 MeOH: H_2O containing 0.1 % formic acid at a flow rate of 0.3 mL/min in 8 min. LC peaks were monitored by UV absorptions at 349 and 388 nm, and MS was detected in ESI positive mode.

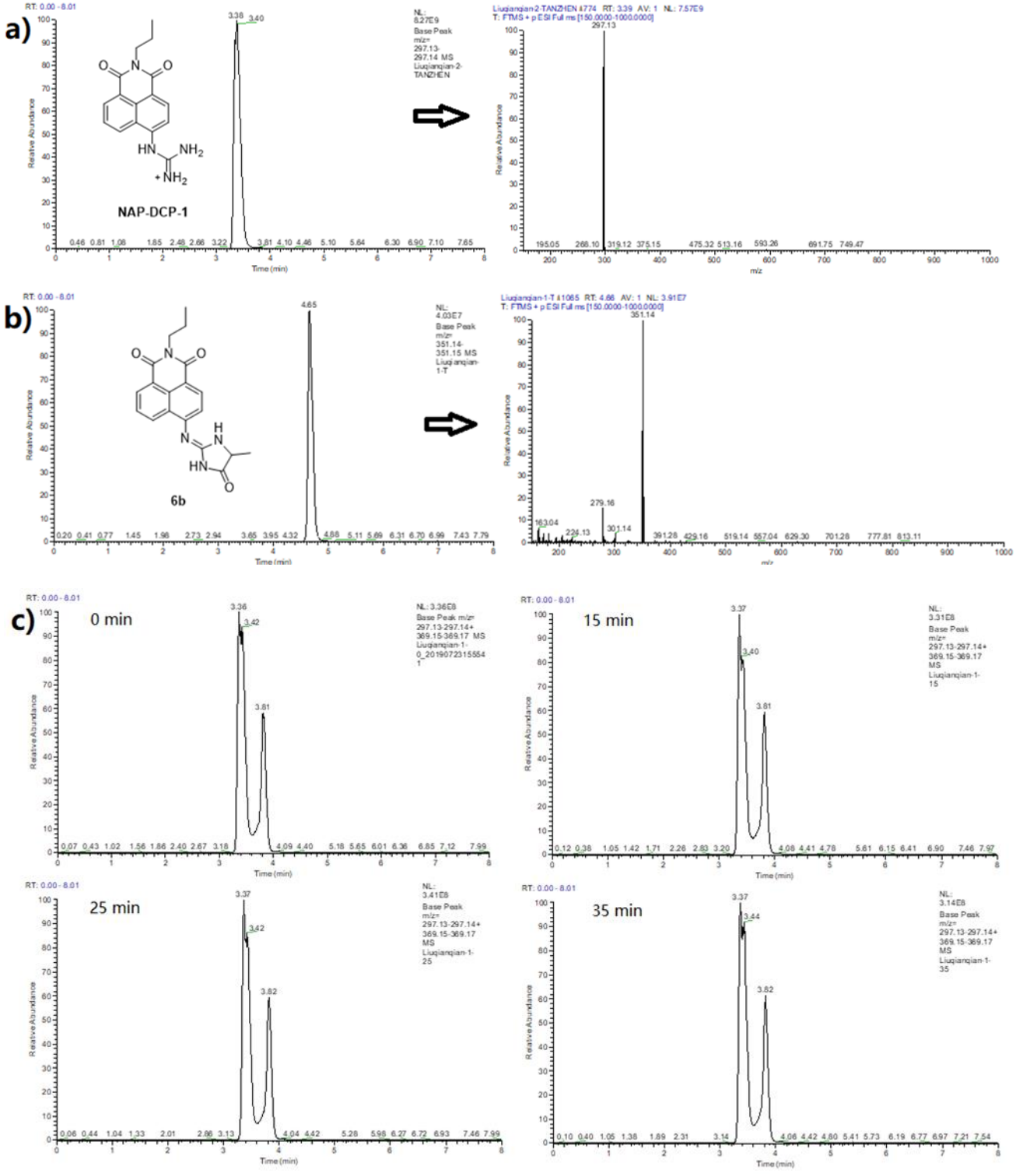

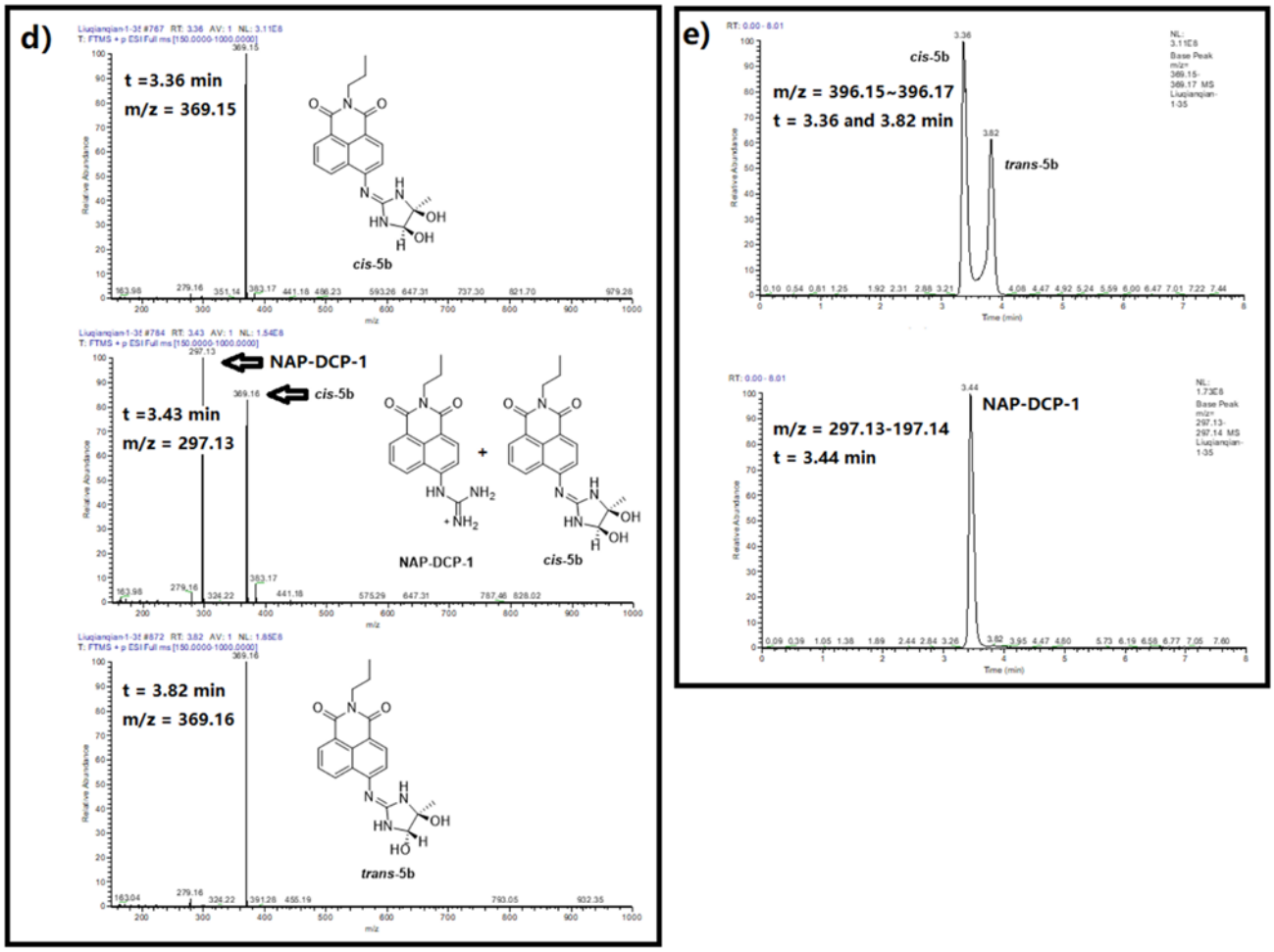

Figure S26 UPLC-MS analysis of **NAP-DCP-1** and **MGO**: a) UPLC analysis of the standard sample of **NAP-DCP-1** and the corresponding MS spectrum; b) UPLC analysis of the standard hydroimidazolone **6b** and the corresponding MS spectrum; c) UPLC spectra of the reaction mixture at various time points (0, 15, 25, and 35 min, reaction seemed to reach equilibrium immediately); d) MS spectra at various peak retention times (3.36, 3.43, and 3.82 min), the probe **NAP-DCP-1** peak at 3.43 min and ***cis*-5a** peak at 3.36 min was only partially resolved; e) Ion extraction UPLC peaks of the hydroimidazolone **5a** and the probe **NAP-DCP-1**. (Reaction mixture was prepared by first mixing 3 µL of 100 mM stock solution of **NAP-DCP-1** in DMSO and 97 µL PBS buffer (10 mM, pH = 7.4) together, and then 2.4 µL 1M MGO in water was added. The reaction mixture was stirred at room temperature. At each time-point, an aliquot of 10 µL of the reaction mixture was diluted with 1 mL PBS buffer (10 mM, pH = 7.4), filtered through a 0.2 µm micro-syringe filter (13 mm) , and then subjected to UPLC-MS analysis.)

4.4 MS Studies of Reaction of NAP-FAP-1 with FA in Acetonitrile.

To a suspended solution of **NAP-DCP-1** (6 mg, 0.02 mmol) in 1.0 mL acetonitrile was added 10 equiv. FA (37% FA in H_2O, 15.3 μL)，a clear solution was formed. The reaction solution was taken for MS analysis. The peak m/z = 327.1 was assigned to the $(M+H)^+$ peak of the aminol adduct **11**; while the peak m/z 297.1 was assigned to the $(M+H)^+$ peak of **NAP-DCP-1**. The calculated values were 327.15 and 297.13, respectively (**Scheme S8**).

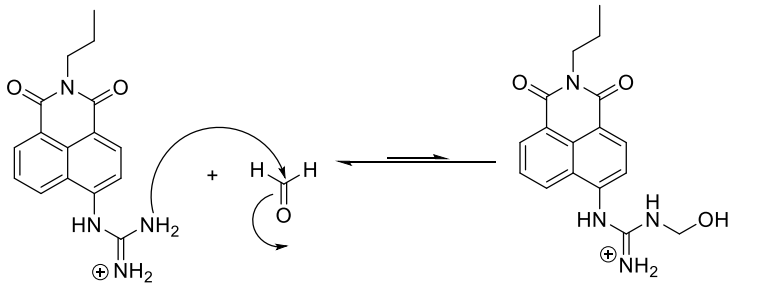

NAP-DCP-1

Chemical Formula: $C_{16}H_{17}N_4O_2^+$
Exact Mass: 297.13

11

Chemical Formula: $C_{17}H_{19}N_4O_3^+$
Exact Mass: 327.15

Scheme S8

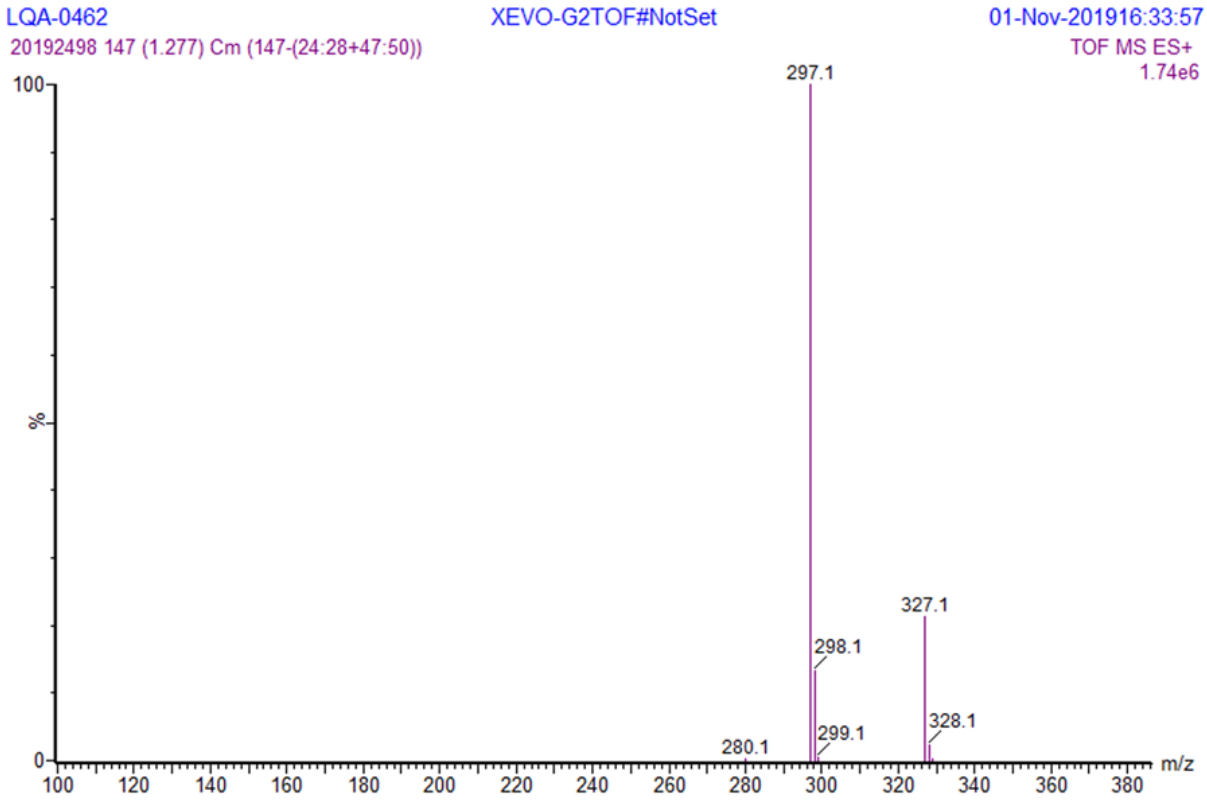

Figure S27 ESI-MS spectrum of the reaction mixture of **NAP-DCP-1** and **FA**

4.5 MS studies of a reaction mixture of the probe NAP-DCP-1 and NOC-18 in acetonitrile.

To a suspended solution of **NAP-DCP-1** (3 mg, 0.010 mmol) in a mixtured solvent of 1.0 mL acetonitrile and 0.5 mL water was added 3 equiv. NOC-18 (5 mg, 0.031 mmol), a clear solution was formed. The solution was taken for MS analysis. No adduct was identified from the mixuture.

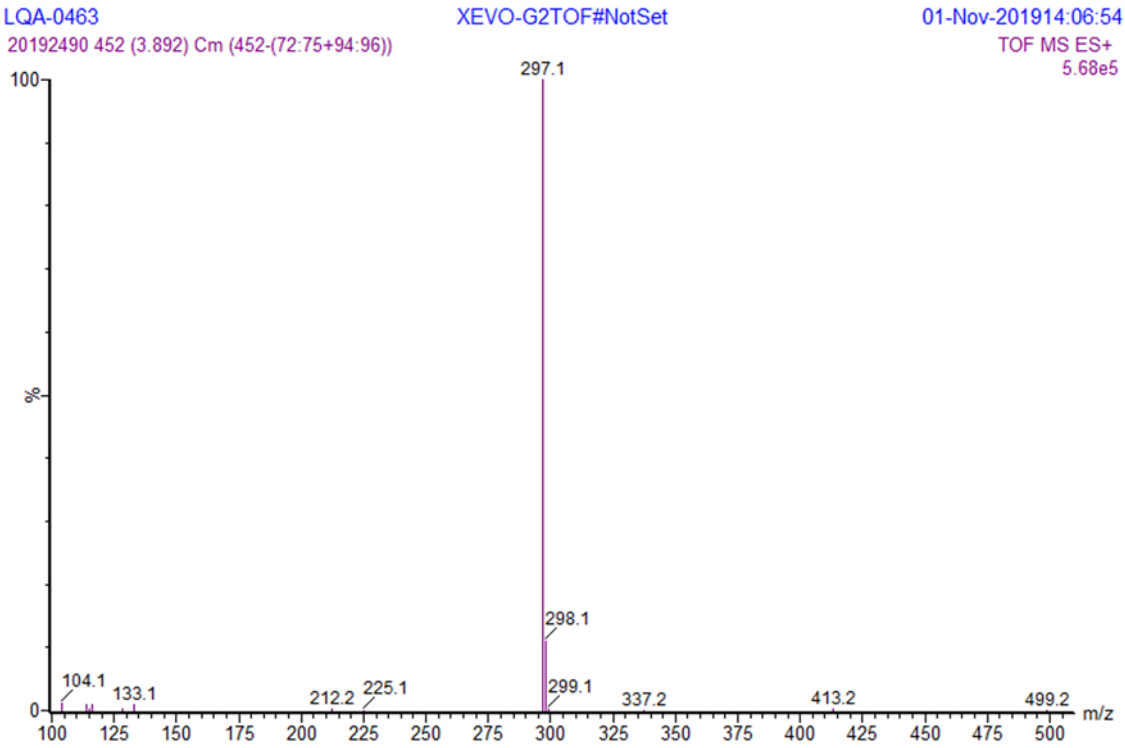

Figure S28 ESI-MS spectrum of mixture of **NAP-DCP-1** and **NOC-18**.

4.6 UPLC-MS Studies of Model Reaction of NAP-FAP-1 with 1:1 MGO and GO

UPLC-MS analysis was performed on Thermo Scientific UltiMate 3000 with Q-Exactive™ plus MS/MS Mass Spectrometry equipped with Hypersil Gold C18 (Thermo Scientific) 3 µm, 100 mm×2.1 mm column. All the samples were eluted using a gradient mixture from 30:70 to 90:10 and back to 30:70 MeOH: H_2O containing 0.1 % formic acid at a flow rate of 0.3 mL/min in 8 min. LC peaks were monitored by UV absorptions at 349 and 388 nm, and MS was detected in ESI positive mode.

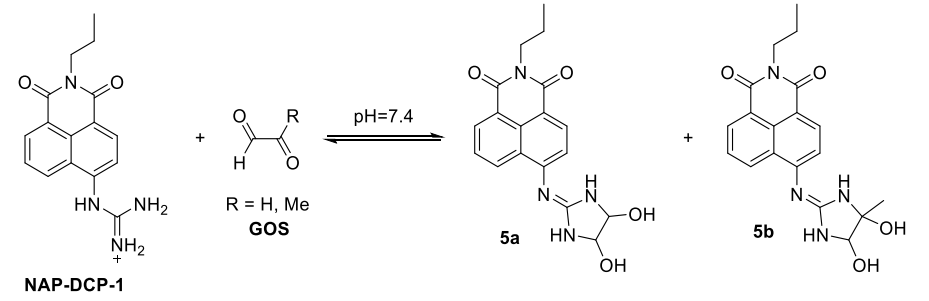

Scheme S9

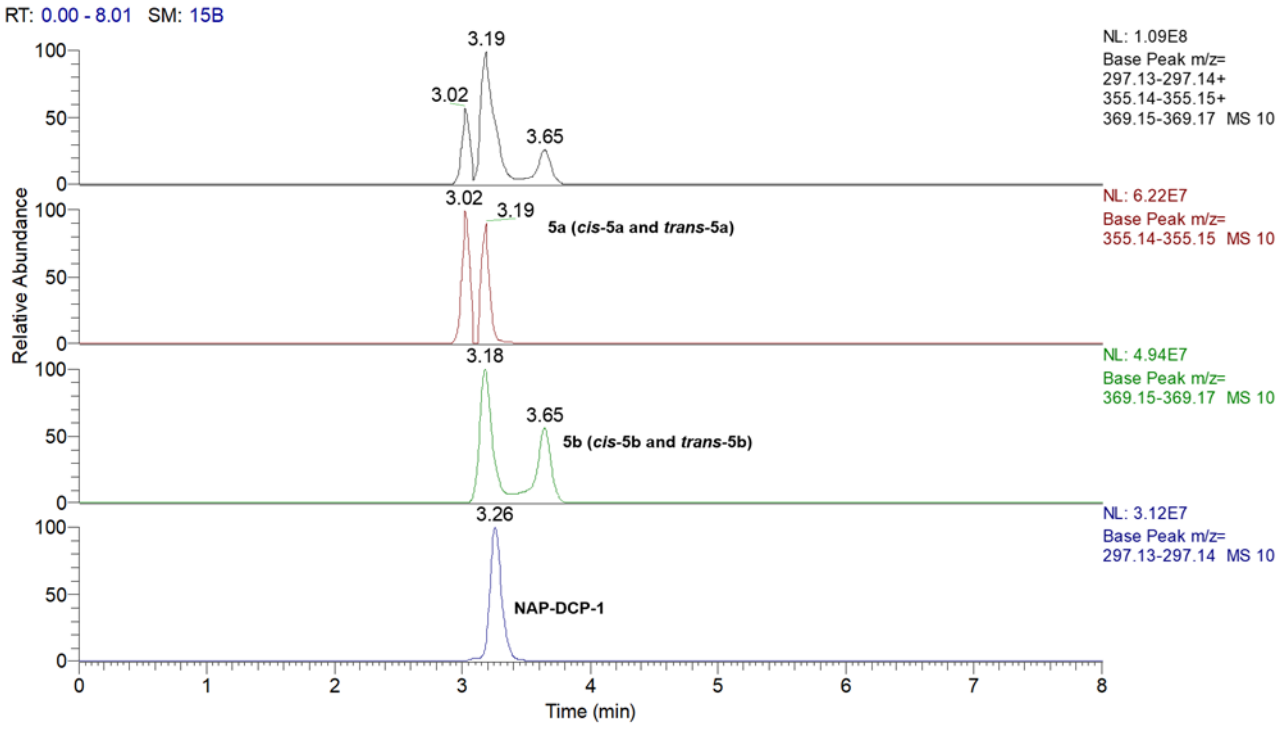

Figure S29 UPLC-MS analysis of reaction mixture of **NAP-DCP-1** with 1:1 MGO and GO at time point of 55 min. (Reaction mixture was prepared by first mixing 3 µL of 100 mM stock solution of **NAP-DCP-1** in DMSO and 97 µL PBS buffer (10 mM, pH = 7.4) together, and then 1.2 µL 1M MGO and 1.2 µL 1M GO in water was added. The reaction mixture was stirred at room temperature. At each time-point, an aliquot of 10 µL of the reaction mixture was diluted with 1 mL PBS buffer (10 mM, pH = 7.4), filtered through a 0.2 µm micro-syringe filter (13 mm), and then subjected to UPLC-MS analysis.)

Part V: Theoretical Calculations

5.1 Computational details

All the quantum chemistry calculations were conducted in SMD water solution with Gaussian 16 software.[26] The ground and excited state molecular geometries were calculated at the B3LYP/Def2-SVP and TD-CAM-B3LYP/Def2-SVP levels of theory, respectively. The frequencies were calculated at the same levels of theory for confirming the local minima on the energy potential surfaces and counting for the thermal corrections to Gibbs free energy. The ground and excited state electronic energies were obtained at the M062X/Def2-SVP level based on the B3LYP optimized geometries, and performed at the TD-CAM-B3LYP/Def2-SVP level using the corrected linear response (cLR) formalism[27], respectively. The Gibbs free energy of solute (ΔG_{solu}) is defined as:[28]

$$\Delta G_{solu} = (\Delta G_{gas} + \Delta G_{solv}) + \Delta G_{corr} + \Delta G_{phase} \quad \text{Equation (1)}$$

where ΔG_{gas} is the electronic energy in the gas phase; ΔG_{solv} denotes the solvation free energy calculated using SMD solvent model; ΔG_{corr} stands for the thermal correction to Gibbs free energy; and ΔG_{phase} (0.082 eV) is the change of Gibbs free energy from the gas phase (1 atm) to solution (1 M). The absolute hydration free energy of the proton is (-262.4 kcal/mol) adapted from Ref [29].

The natural transition orbitals (NTO)[30] and charge-transfer distance (d_{CT}) were performed with Multiwfn 3.4.0 software.[31] NTOs and d_{CT} can provide more information of the nature of excited states than the conventional molecular orbitals.[32, 33]

For the convenience of the calculation, the *N*-propyl side chain of the probe **NAP-DCP-1** was simplified to the *N*-methyl group and only the *trans*-diol isomer of the dihydroxyimidazoline products was calculated (**Figure S30**).

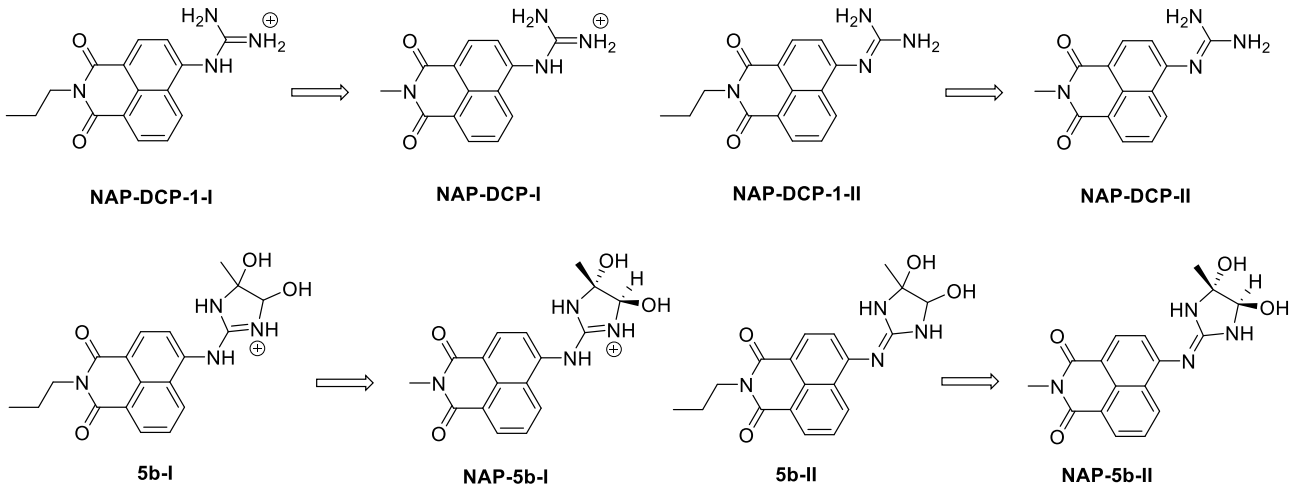

Figure S30 Structures used in the theoretical calculations.

5.2 Calculated Gibbs free energy differences between endocyclic and exocyclic dihydroxylimidazolines.

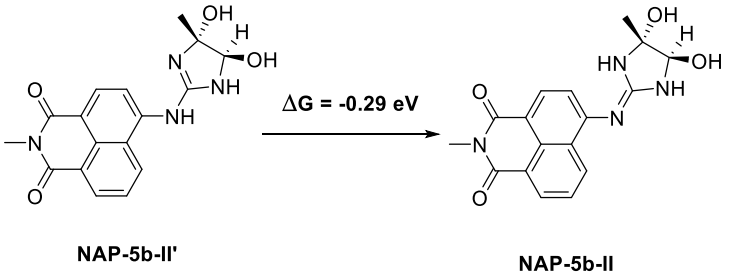

Figure S31 The Gibbs free energy differences between endocyclic dihydroxylimidazoline **NAP-5b-II'** and exocyclic dihydroxylimidazoline **NAP-5b-II**.

5.3 Calculated absorption and emission spectra of related species

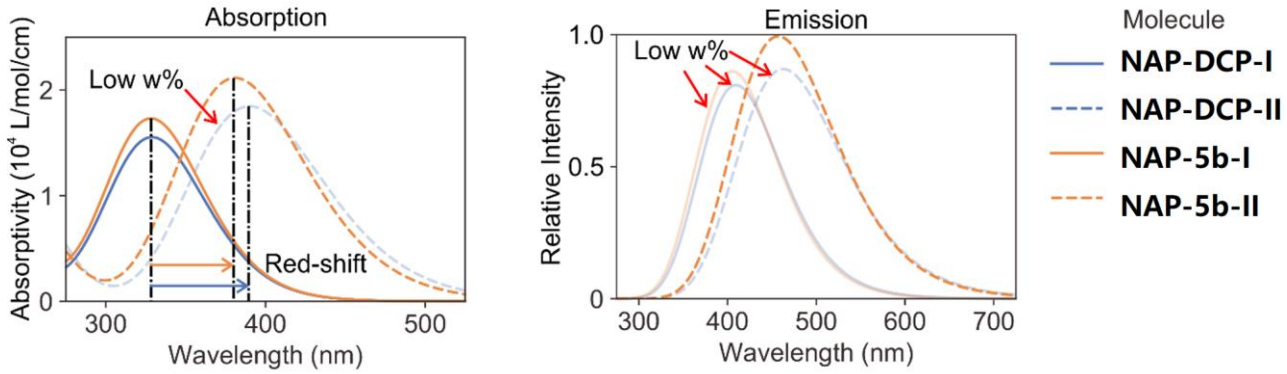

Figure S32 The corresponding absorption and emission spectra calculated at the CAM-B3LYP/Def2-SVP level in water solution for the model probe **NAP-DCP** and its MGO *trans*-adduct **NAP-5b**. Transparent curves suggest that the compounds are of low concentration (Low w%) due to the ESPT and controlled pH value (~7.4).

5.4 Computed molecular geometries, the oscillator strength and charge-transfer distance

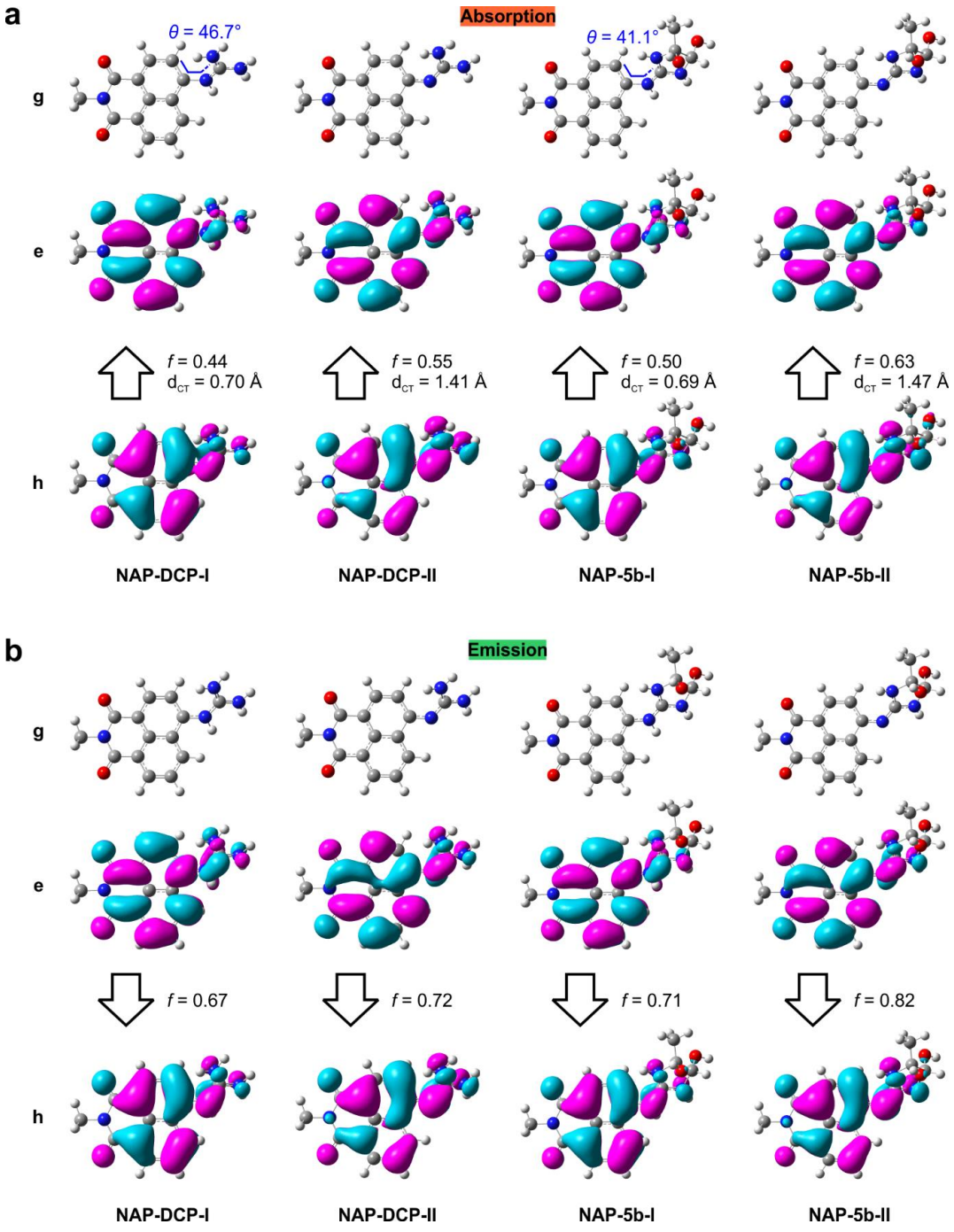

Figure S33 a) The molecular geometries (g), the distribution of electron (e) and hole (h) NTOs of compounds in their Frank-Condon (Absorption) state calculated at the CAM-B3LYP/Def2-SVP level in water; b) The molecular geometries (g), the distribution of electron (e) and hole (h) NTOs of compounds in their locally-excited (Emission) state calculated at the CAM-B3LYP/Def2-SVP level in water. The rotation angle (θ), oscillator strength (f), and charge-transfer distance (d_{CT}) are labelled in the inset.

5.5 Calculated HOMO and LUMO energy differences of related species

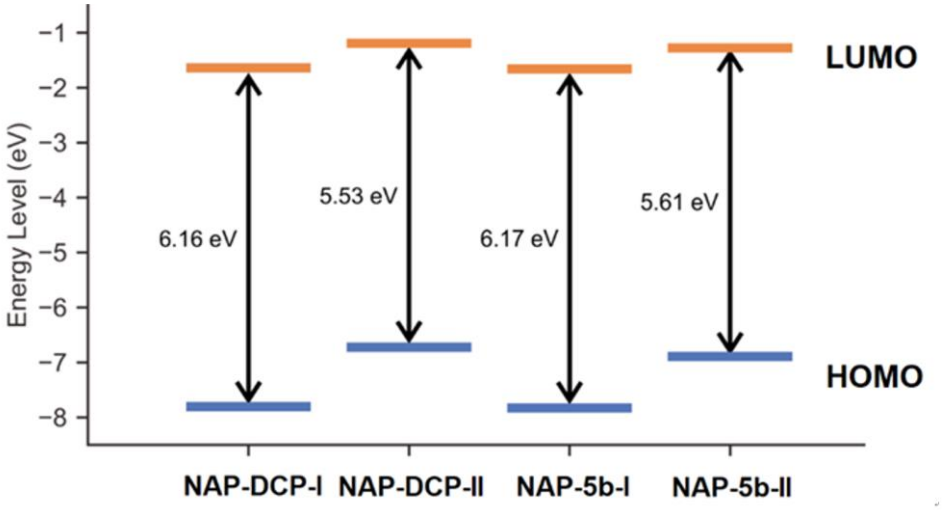

Figure S34 Energy level of HOMO and LUMO of cationic and neutral **NAP-DCP** and **NAP-5b** calculated at the CAM-B3LYP/Def2-SVP in water.

5.6 Calculated Gibb's free energy changes of ESPT

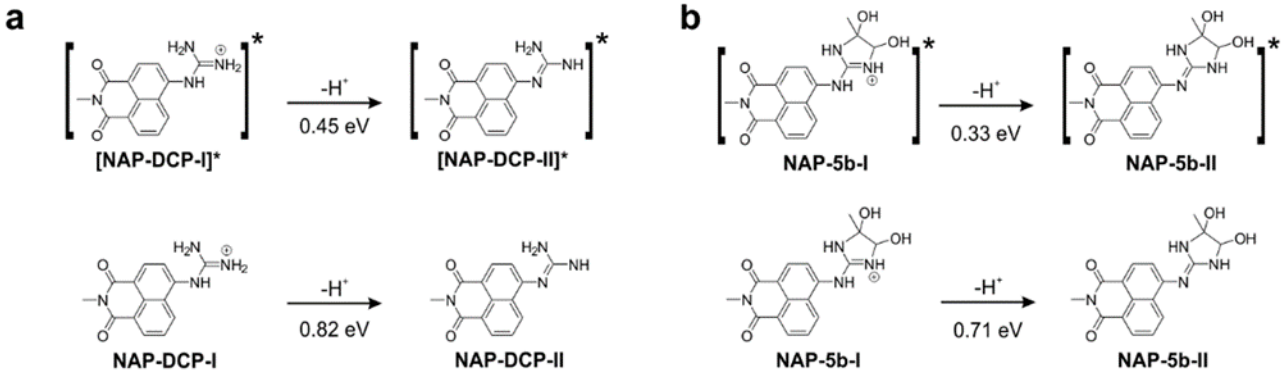

Figure S35 Comparison of the Gibbs free energy changes of ESPT of the protonated excited state (a) **[NAP-DCP-I]*** and (b) **[NAP-5b-I]*** with their respective specie in the ground state.

Part VI: Detection of Glyoxals in Live Cells

Cell culture: The HeLa human cervix cell line was obtained from the Stem Cell Bank, Chinese Academy of Sciences. HeLa cells were maintained in DMEM medium (Gibco) supplied with 10% Fetal Bovine Serum (FBS, Gibco) and 1% Glutamine (Gibco) at 37 °C in a humidified atmosphere containing 95% air and 5% CO_2.

6.1 Cytotoxicity assay of the NAP-DCP-1 and NAP-DCP-3

Cell survival was evaluated by the MTS assay (Promega CellTiter 96 AQueous One Solution Reagent, Cat No. G3582), based on the conversion of a tetrazolium compound, 3-(4,5-dimethylthiazol-2-yl)-5-(3-carboxymethoxy-phenyl)-2-(4-sulfophenyl)-2H tetrazolium (MTS), to a colored formazan product by living cells.[34] Absorbance was read by a microplate reader (Molecular Devices SpectraMax I3x) at 490 nm. The quantity of formazan product, as measured by the amount of absorbance, was directly proportional to the metabolic activity of viable cells in the culture.

Cell viability (% of control) = $(OD_{EG}-OD_{ZG})/(OD_{CG}-OD_{ZG})*100\%$

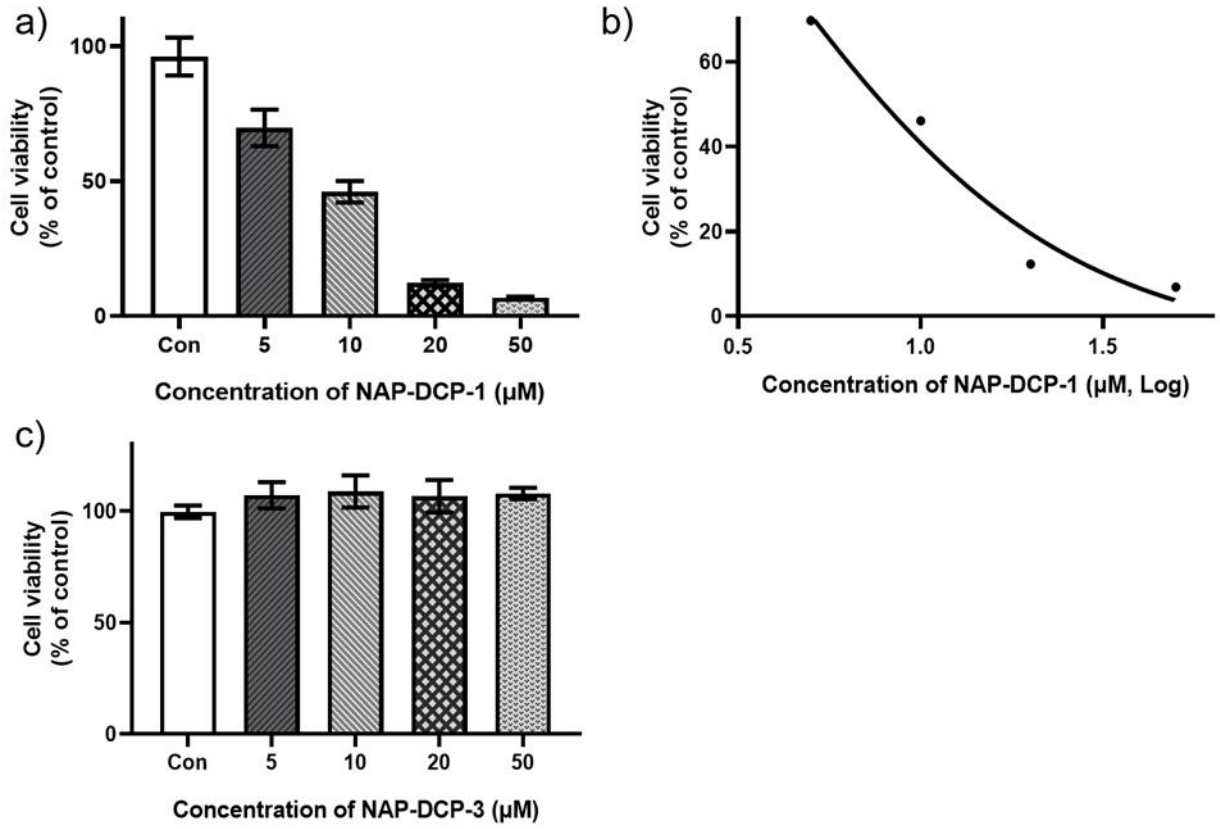

Figure S36 a) Cell viabilities of **NAP-DCP-1** at various concentrations for HeLa cells after 24 h incubation; b) Cell viability fitting curve for calculation of IC_{50} (the value = 10.4 μM, R^2=0.96); c) Cell viabilities of **NAP-DCP-3** at various concentrations for HeLa cells after 24 h incubation.

6.2 Exploration of DNA Damage from NAP-DCP-1 and NAP-DCP-3

HeLa cells were seeded in a T-25 cell culture flask in DMEM medium (with phenol red, Gibco) with 10% Fetal Bovine Serum and 1% Glutamine at 37 ˚C for 48 h. One day before the experiment, cells were transferred to a Nunc 6-well plate (Thermo Scientific) to allow the cells to adhere.

a) Comet assay kit (KeyGEN BioTECH) was used to detect the DNA damage induced by **NAP-DCP-1** and **NAP-DCP-3** in Hela cells. The cells were treated with 20 μM **NAP-DCP-1** and **NAP-DCP-3** at 37 ˚C for 2 h. Cells were washed and immobilized in low melting point agarose (Macklin) on a agarose-treated glass slide. Cells were lysed with Lysis Buffer at 4 ˚C overnight and DNA was unwound with NaOH-EDTA buffer (PH > 13) for 30 min at room temperature. The slides were then electrophoresed in ice cold NaOH-EDTA buffer for 45 min at 21 V. Slides were washed with ddH_2O and dried. Ethidium Bromide (Thermo Fisher) was used to stain the cells and the image was captured on a Nikon Ti-S fluorescence microscope.

b) Western Blot assay was used for the detection of γH2AX, the marker for double strand DNA breaks. The cells were treated with 20 μM **NAP-DCP-1** and **NAP-DCP-3** at 37 ˚C for 2 h. Positive control was induced by 100 μM etoposide (Sigma-Aldrich) for 2 h. Cells were lysed with RIPA buffer (Beyotime) and loaded on a polyacrylamide gel (20 μg protein/well). After the SDS-PAGE electrophoresis in a Bio-Rad chamber, proteins were transferred onto a nitrocellulose membrane using a Bio-Rad semi-dry transferring system. The membrane was blocked with 5% skim milk in TBST and incubated with the γH2AX and GAPDH antibody in TBST. HRP-conjugated secondary antibody was then added to the membrane, followed by the ECL detection reagent. The image was captured with a ChemiDoc MP gel imager (Bio-Rad).

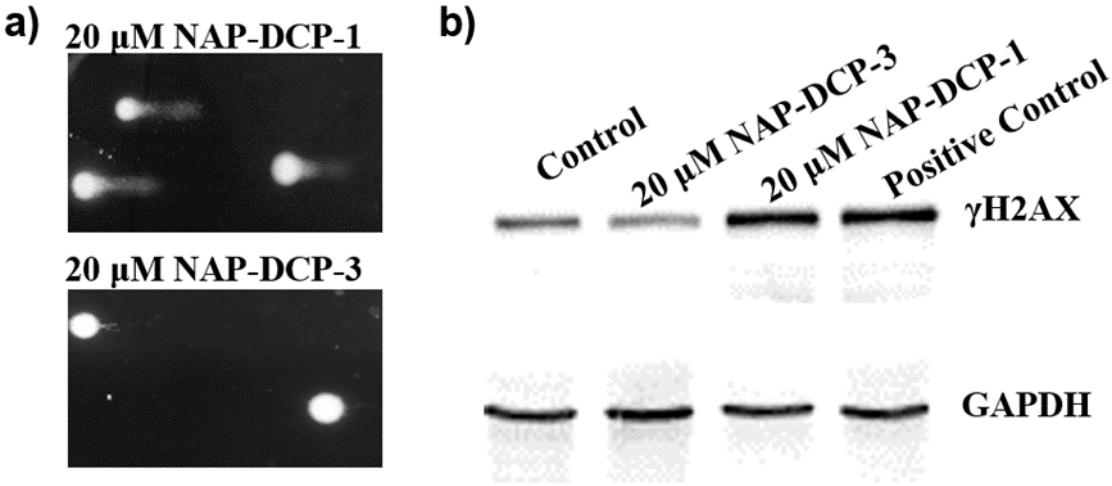

Figure S37 a) Single Cell Gel Electrophoresis (Comet) assay performed on HeLa cells treated with 20 μM **NAP-DCP-1** (up) or **NAP-DCP-3** (bottom) for 2 h. Longer tail movement indicates higher DNA damage. b) Western Blot assay of γH2AX performed on HeLa cells treated with 20 μM **NAP-DCP-1** or **NAP-DCP-3** for 2 h. Increased expression of γH2AX is a widely-used biomarker for DNA double strand breaks formation.

6.3 Confocal fluorescence microscope cell imaging experiments of the NAP-DCP-1 for GOS

HeLa cells were seeded in a T-25 cell culture flask in DMEM medium (with phenol red, Gibco) with 10% Fetal Bovine Serum and 1% Glutamine at 37 ˚C for 48 hours. One day before the experiment, cells were transferred to 3 Nunc 35 mm glass-bottom cell culture dishes (Thermo Scientific) to allow the cells to adhere. **NAP-DCP-1** was diluted in PBS buffer and added to the cell culture medium at a final concentration of 5 μM. After 1 h incubation at 37 ˚C in a cell culture incubator, the medium with **NAP-DCP-1** was removed. After two washes with PBS buffer, cell culture medium contained 20 μM MGO or GO were added to the MGO and GO dishes. The same amount of fresh medium was also added to the control (probe only dish). After a 30 min incubation at 37 ˚C in a cell culture incubator, cells were imaged on a Leica TCS SP8 equipped with 40× objective lens and PMT gain of 800 ($\lambda_{ex/em}$ = 405/530-590 nm). After the first imaging step, 5 mM NAC was added to the cell culture medium of the MGO and GO dishes. The cells were then incubated at 37 ˚C in a cell culture incubator for another 30 min. At the end of the incubation, the cell images were captured again on a Leica TCS SP8 equipped with 40× objective lens and PMT gain of 800 ($\lambda_{ex/em}$ = 405/530-590 nm). The results were shown in Figure S38.

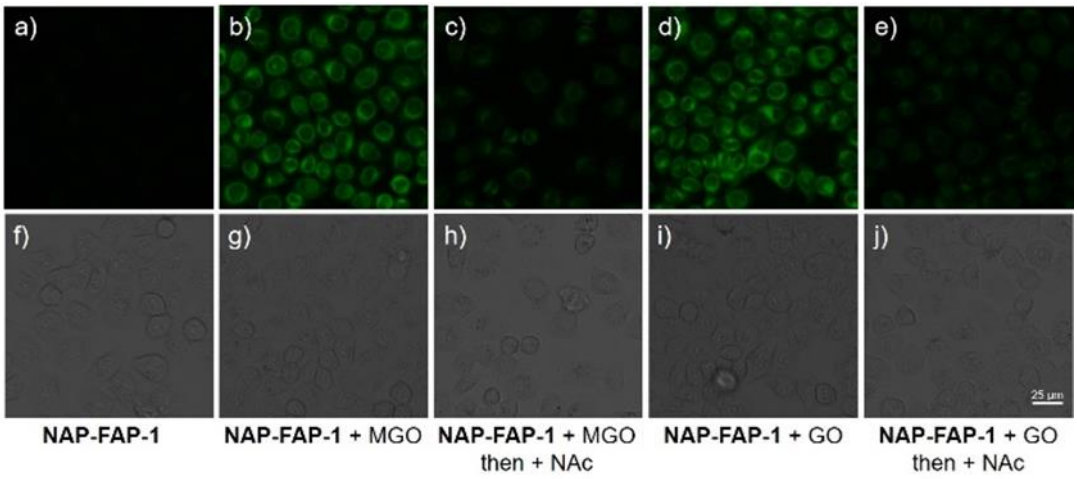

Figure S38 a-e) Confocal fluorescence images of HeLa cells: a) Cells were incubated in 5 μM **NAP-DCP-1** for 1 h, and then fresh media for 30 min; b, d) Cells were incubated in 5 μM **NAP-DCP-1** for 1 h, and then 20 μM MGO (b) or GO (d) for 30 min; c, e) Cells were imaged in (b) and (d) were further treated with 5 mM NAC for 30 min; f-j) Corresponding bright field images. Cell images were captured on a Leica TCS with $\lambda_{ex/em}$ = 405/530-590 nm (scale bar = 25 μM).

6.4 Time-dependent fluorescence tracking of GOS levels inside cells

HeLa cells were seeded in a T-25 cell culture flask in DMEM medium (with phenol red, Gibco) with 10% Fetal Bovine Serum and 1% Glutamine at 37 ˚C for 48 hours. One day before the experiment, cells were transferred to a Nunc 96-well microplate (Thermo Scientific) to allow the cells to adhere. **NAP-DCP-1** was diluted in PBS buffer and added to the cell culture medium at a final concentration of 5 μM. After 30 min incubation at 37 ˚C in a cell culture incubator, the medium with **NAP-DCP-1** was removed. After two washes with PBS buffer, cell culture medium contained 5 μM MGO or GO were added to the MGO wells. The same amount of fresh medium was also added to the control (media only) wells. The cells were incubated at 37 ˚C for 30 min, and then NAC was added to each wells to a final concentration of 5 mM. The cells were incubated at 37 ˚C for additional 30 min. Fluorescence intensity was recorded in every 5 min on a BioTek Synergy Lx microplate reader with the emission at 540 ± 25 nm (λ_{ex} = 440 nm). The results were shown in Figure S39.

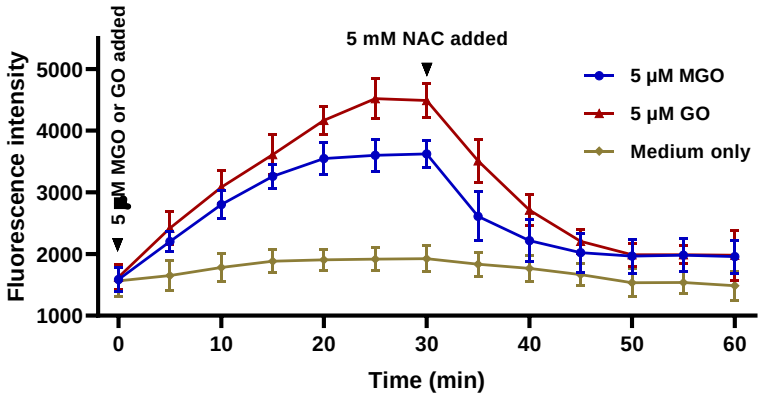

Figure S39. Time-dependent fluorescence intensity ($\lambda_{ex/em}$ = 440/515-565 nm) detected on a BioTek Synergy Lx microplate reader (mean ± SD) with of HeLa cells preincubated with 5 μM **NAP-DCP-1** upon addition of 5 μM MGO or GO and incubated for 30 min, and then addition of 5 mM NAC and incubated for another 30 min.

6.5 Detection of endogenous GOS levels inside of HeLa cells grown in high glucose media and monitoring GOS level drop upon addition of NAC

HeLa cells were seeded in a T-25 cell culture flask in DMEM medium (with phenol red, Gibco) with 10% Fetal Bovine Serum and 1% Glutamine at 37 ˚C for 48 hours. One day before the experiment, cells were transferred to a Nunc 96-well microplate (Thermo Scientific) to allow the cells to adhere. D-(+)-glucose (Sigma-Aldrich, Cat No. G8270) was diluted in DMEM medium and added to the cells in the high-glucose wells at a final concentration of 15 mM to achieve the final glucose concentration of 40 mM (25 mM in the original DMEM medium) in these wells. Same amount of medium without additional glucose was added to the wells of 25 mM glucose concentration. After 48 h of incubation at 37 ˚C, **NAP-DCP-1** was added to the cells at a final concentration of 5 μM. The cells were incubated at 37 ˚C for 30 min, and the fluorescence intensity was obtained on a BioTek Synergy Lx microplate reader with the emission at 540 ± 25 nm (λ_{ex} = 440 nm). After the detection of endogenous glyoxals, **NAC** was diluted in cell culture medium and added to the cells at a final concentration of 5 mM. The cells were incubated again at 37 ˚C for 30 min, and the fluorescence intensity was measured every 5 min on a BioTek Synergy Lx microplate reader with the emission at 540 ± 25 nm (λ_{ex} = 440 nm). The results were shown in Figure 2h.

6.6 Intracellular localization of NAP-DCP-3 and ER-Tracker Green in cells on a confocal fluorescence microscope

HeLa cells were seeded in a T-25 cell culture flask in DMEM medium (with phenol red, Gibco) with 10% Fetal Bovine Serum and 1% Glutamine at 37 ˚C for 48 hours. One day before the experiment, cells were transferred to Nunc 35 mm glass-bottom cell culture dishes (Thermo Scientific) to allow the cells to adhere. **NAP-DCP-3** and ER-Tracker Green (Ex/Em 504/511 nm) were diluted in PBS buffer and added to the cell culture medium at the final concentrations of 20 μM and 1 μM. After 1 h incubation at 37 ˚C in a cell culture incubator, the medium with both probes was removed from the dishes. After two washes with PBS buffer, cell culture medium contained 20 μM MGO or GO were added to the MGO and GO dishes. The same amount of fresh medium was also added to the control (probe only dish). After a 30 min incubation at 37 ˚C in a cell culture incubator, cells were imaged on a Leica TCS SP8 equipped with 40× objective lens and PMT gain of 800 ($\lambda_{ex/em}$ = 405/530-590 nm and $\lambda_{ex/em}$ = 488/480-540). Degrees of colocalization of the two probes were analyzed with Image-Pro Plus 6.0 (Media Cybernetics).

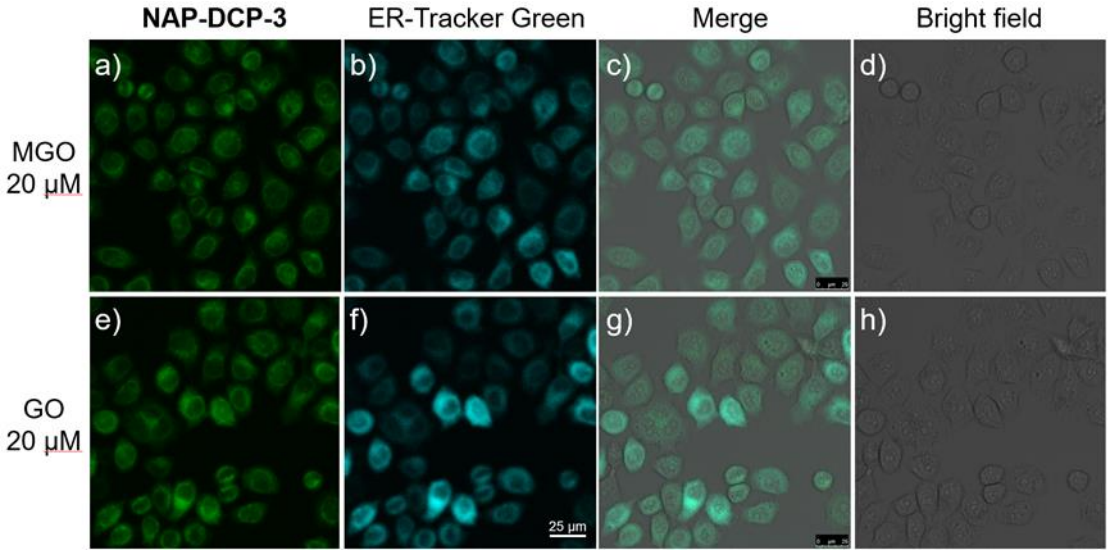

Figure S40 Confocal fluorescence images of HeLa cells in green channel (a&e, $\lambda_{ex/em}$ = 488/480-540 nm) and cyan channel (b&f, $\lambda_{ex/em}$ = 405/530-590 nm), and corresponding merge images (c&g) and bright field images (d&h): HeLa cells were preincubated with 20 μM **NAP-DCP-3** and 1 μM ER-Tracker Green for 1 h and then incubated with 20 μM MGO (a-d) or GO (e-h) for 30 min. Cell images were captured on a Leica TCS SP8 (scale bar = 25 μM).

6.7 Confocal fluorescence microscope cell imaging experiments of the NAP-DCP-3 for GOS detection

HeLa cells were seeded in a T-25 cell culture flask in DMEM medium (with phenol red, Gibco) with 10% Fetal Bovine Serum and 1% Glutamine at 37 ˚C for 48 hours. One day before the experiment, cells were transferred to 4 Nunc 35 mm glass-bottom cell culture dishes (Thermo Scientific) to allow the cells to adhere. **NAP-DCP-3** and ER-Tracker Green (Ex/Em 504/511 nm) were diluted in PBS buffer and added to the cell culture medium on all 4 dishes at the final concentrations of 20 μM and 1 μM. After 1 h incubation at 37 ˚C in a cell culture incubator, the medium with both probes was removed. After two washes with PBS buffer, cell culture medium contained 20 μM MGO or GO were added to the MGO and GO dishes. After a 30 min incubation at 37 ˚C in a cell culture incubator, cells were imaged on a Leica TCS SP8 equipped with 20× objective lens and PMT gain of 800 ($\lambda_{ex/em}$ = 405/530-590 nm and $\lambda_{ex/em}$ = 488/480-540 nm). After the first imaging step, 5 mM NAC was added to the cell culture medium of the MGO, GO and high glucose dishes. The cells were then incubated at 37 ˚C in a cell culture incubator for another 30 min. At the end of the incubation, the cell images were captured again on a Leica TCS SP8 equipped with 20× objective lens and PMT gain of 800 ($\lambda_{ex/em}$ = 405/530-590 nm and $\lambda_{ex/em}$ = 488/480-540 nm).

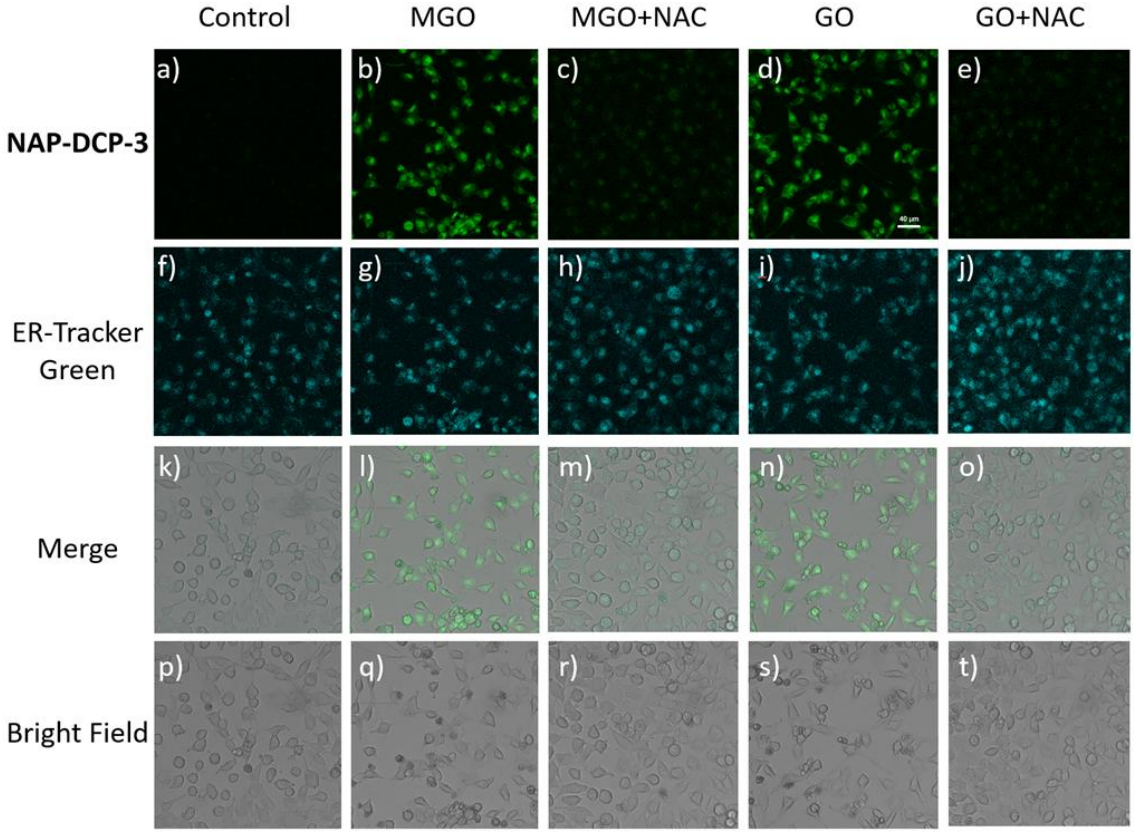

Figure S41 Confocal fluorescence images of HeLa cells in green channel (a-e, $\lambda_{ex/em}$ = 488/480-540 nm) and cyan channel (f-j, $\lambda_{ex/em}$ = 405/530-590 nm), and corresponding merge images (k-o) and bright field images (p-t): HeLa cells were incubated with 20 μM **NAP-DCP-3** and 1 μM ER-Tracker Green for 1 h and then incubated with blank media (a, f, k, p), 20 μM MGO (b, g, l, q), or 20 μM GO (d, i, n, s) for 30 min and images were taken, and then the HeLa cells treated with 20 μM MGO or GO were further incubated with 5 mM NAC for additional 30 min, and images were taken for MGO pretreated cells (c, h, m, r) or GO pretreated cells (e, j, o, t). Cell images were captured on a Leica TSP SP8 (scale bar = 40 μM).

6.8 Detection of ER GOS levels of HeLa cells grown in high glucose media and GOS level drop upon addition of NAC

HeLa cells were seeded in a T-25 cell culture flask in DMEM medium (with phenol red, Gibco) with 10% Fetal Bovine Serum and 1% Glutamine at 37 ˚C for 48 hours. One day before the experiment, cells were transferred to a Nunc 96-well microplate (Thermo Scientific) to allow the cells to adhere. D-(+)-glucose (Sigma-Aldrich, Cat No. G8270) was diluted in DMEM medium and added to the cells in the high-glucose wells at a final concentration of 15 mM to achieve the final glucose concentration of 40 mM (25 mM in the original DMEM medium) in these wells. Same amount of medium without additional glucose was added to the wells of 25 mM glucose concentration. After 48 h of incubation at 37 ˚C, **NAP-DCP-3** was added to the cells at a final concentration of 20 μM. The cells were incubated at 37 ˚C for 30 min. Cell images were captured on a Leica TCS SP8 with $\lambda_{ex/em}$ = 405/530-590 nm for green fluorescence channel from **NAP-DCP-3** and $\lambda_{ex/em}$ = 488/480-540 nm for cyan fluorescence channel from ER-Track Green (scale bar = 40 μM). After the detection of endogenous glyoxals, **NAC** was diluted in cell culture medium and added to the cells at a final concentration of 5 mM. The cells were incubated again at 37 ˚C for 30 min, and the fluorescence images were taken again. The results were shown in Figure 4.

6.9 Comparison of NAP-DCP-3 with an irreversible probe NP in monitoring endogenous GOS Levels

HeLa cells were seeded in a T-25 cell culture flask in DMEM medium (with phenol red, Gibco) with 10% Fetal Bovine Serum and 1% Glutamine at 37 ˚C for 48 hours. One day before the experiment, cells were transferred to a Nunc 96-well microplate (Thermo Scientific) to allow the cells to adhere. D-(+)-glucose (Sigma-Aldrich, Cat No. G8270) was diluted in DMEM medium and added to the cells in the high-glucose wells at a final concentration of 15 mM to achieve the final glucose concentration of 40 mM (25 mM in the original DMEM medium) in these wells. Same amount of medium without additional glucose was added to the wells of 25 mM glucose concentration. After 48 h of incubation at 37 ˚C, **NAP-DCP-3** and **NP** were added to the cells at a final concentration of 20 μM. The cells were incubated at 37 ˚C for 30 min, and the fluorescence intensity was obtained on a BioTek Synergy Lx microplate reader with the emission at 540 ± 25 nm (λ_{ex} = 440 nm). After the detection of endogenous glyoxals induced by high glucose, **NAC** was diluted in cell culture medium and added to the cells at a final concentration of 5 mM. The cells were further incubated at 37 ˚C for 30 min, and the fluorescence intensity was measured every 5 min on a BioTek Synergy Lx microplate reader with the emission at 540 ± 25 nm (λ_{ex} = 440 nm). The results were shown in Figure 5a.

6.10 Exploration of correlations between GOS and ROS levels by fluorescence microscope

HeLa cells were seeded in a T-25 cell culture flask in DMEM medium (with phenol red, Gibco) with 10% Fetal Bovine Serum and 1% Glutamine at 37 ˚C for 48 hours. One day before the experiment, cells were transferred to 5 Nunc 35 mm glass-bottom cell culture dishes (Thermo Scientific) to allow the cells to adhere. 20 μM MGO, 20 μM GO, 20 μM H_2O_2, and 50 μM Rosup (compound mixture to induce oxidative stress) were diluted with cell culture medium and added to the cells in respective dishes, the same amount of cell culture medium was also added to the control dish. After 2 h of incubation at 37 ˚C in a cell culture incubator, **NAP-DCP-3** and DCFH-DA (Ex/Em 504/529 nm) were diluted in PBS buffer and added to the cell culture medium on all 5 dishes at the final concentrations of 20 μM and 10 μM. After a 30 min incubation at 37 ˚C in a cell culture incubator, the medium in all

dishes was removed. After two washes with PBS buffer, fresh cell culture medium was added to the dishes. Cells were then imaged on a Leica TCS SP8 equipped with 20× objective lens and PMT gain of 800 ($\lambda_{ex/em}$ = 405/530-590 nm and $\lambda_{ex/em}$ = 488/490-550 nm). The imaging results were shown in Figure 7.

6.11 Exploration of perturbation of GOS Levels in ER from ROS, NO, or FA Exposure in Plate-reader based assays.

HeLa cells were seeded in a T-25 cell culture flask in DMEM medium (with phenol red, Gibco) with 10% Fetal Bovine Serum and 1% Glutamine at 37 ˚C for 48 h. One day before the experiment, cells were transferred to a Nunc 96-well microplate (Thermo Scientific) to allow the cells to adhere.

a) 20 μM H_2O_2, ROSup, and MAHMA NONOate (Sigma-Aldrich) were added to the cells diluted in cell culture medium at the final concentration of 20 μM. Same amount of medium was also added to the control wells. After 2 or 24 h of incubation at 37 ˚C, **NAP-DCP-3** was added to the cells at a final concentration of 20 μM. The cells were incubated at 37 ˚C for 30 min, and the fluorescence intensity was obtained on a BioTek Synergy Lx microplate reader with the emission at 540 ± 25 nm (λ_{ex} = 440 nm). The results were shown in Figure 8a.

b) FA was diluted in cell culture medium and added to the cells at the final concentrations of 10, 20, 50 and 100 μM. Cells were incubated at 37 ˚C for 2 or 24 h. After the incubation, **NAP-DCP-3** was added to the cells at a final concentration of 20 μM. The cells were incubated at 37 ˚C for 30 min, and the fluorescence intensity was obtained on a BioTek Synergy Lx microplate reader with the emission at 540 ± 25 nm (λ_{ex} = 440 nm). The results were shown in Figure 8b.

6.12 Imaging of GOS induction by FA using NAP-DCP-3

HeLa cells were seeded in a T-25 cell culture flask in DMEM medium (with phenol red, Gibco) with 10% Fetal Bovine Serum and 1% Glutamine at 37 ˚C for 48 h. One day before the experiment, cells were transferred to a Nunc 6-well plate (Thermo Scientific) to allow the cells to adhere. Cells were then treated with 0, 10, 50 and 100 μM FA for 24 h at 37 ˚C. After that, **NAP-DCP-3** was added to the cell culture media at a final concentration of 20 μM. After a 30 min incubation at 37 ˚C, the medium was removed and the cells were washed with PBS buffer twice. After the wash steps, fresh medium was added to the wells and the images were captured on a Nikon Eclipse Ti-S microscope (Ex 405) at 100 ms exposure time with 40× objective lens.

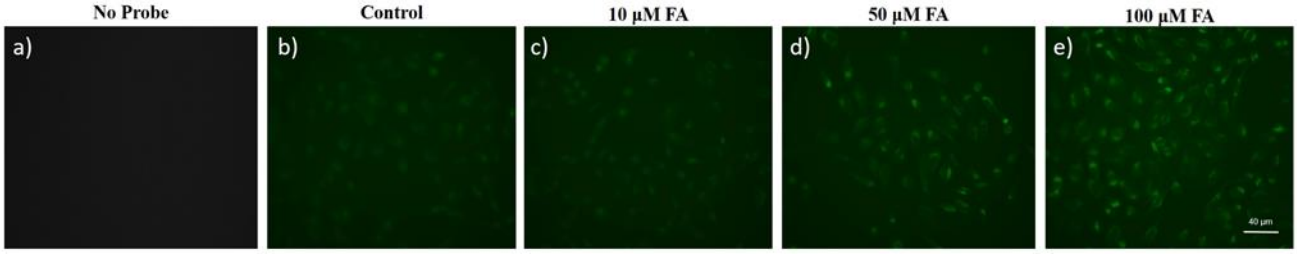

Figure S42 a) Background fluorescence image of HeLa cells without FA and NAP-DCP-3 treatment; b-e) Fluorescence images of HeLa cells preincubated with various concentration of FA for 24 h: blank media (b), 10 μM FA (c), 50 μM FA (d), 100 μM FA (e), and then incubated in 20 μM of **NAP-DCP-3** for 30 min for imaging of their respective GOS levels.

6.13 Exploration of GOS induction by endogenous FA from tetrahydrofolic acid using NAP-DCP-3.

HeLa cells were seeded in a T-25 cell culture flask in DMEM medium (with phenol red, Gibco) with 10% Fetal Bovine Serum and 1% Glutamine at 37 ˚C for 48 h. One day before the experiment, cells were transferred to a Nunc 96-well microplate (Thermo Scientific) to allow the cells to adhere. To explore the intracellular GOS levels induced by endogenous FA, THFA (Sigma-Aldrich) was diluted in cell culture medium and added to the cells at the final concentrations of 10, 20, 50 and 100 μM. Cells were incubated at 37 ˚C for 2 or 24 h. After the incubation, **NAP-DCP-3** was added to the cells at a final concentration of 20 μM. The cells were incubated at 37 ˚C for 30 min, and the fluorescence intensity was obtained on a BioTek Synergy Lx microplate reader with the emission at 540 ± 25 nm (λ_{ex} = 440 nm). The fluorescence intensity at the time point of 2 h and 24 h were shown in Figure 8c.

After fluorescence intensity were measured at the time point of 24 h, **NAC** was diluted in cell culture medium and added to the cells at a final concentration of 5 mM. The cells were further incubated at 37 ˚C for 30 min, and the fluorescence intensity was measured every 5 min on a BioTek Synergy Lx microplate reader with the emission at 540 ± 25 nm (λ_{ex} = 440 nm). The results were shown in Figure S43.

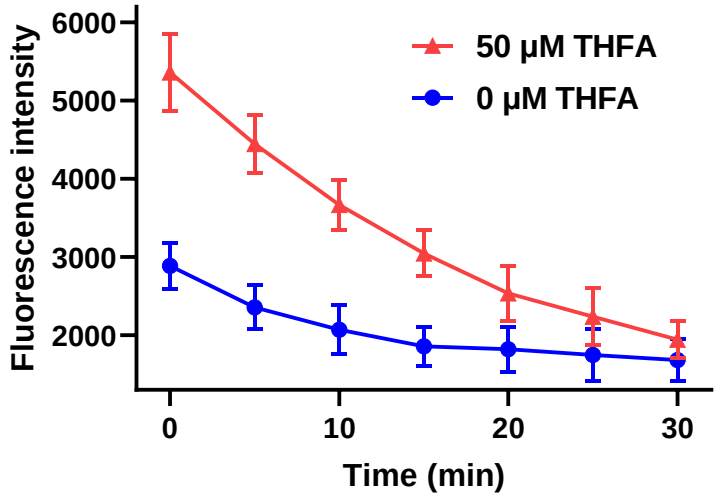

Figure S43 Time-dependent fluorescence intensity ($\lambda_{ex/em}$ = 440/515-565 nm) detected on a BioTek Synergy Lx microplate reader (mean ± SD) with of HeLa cells preincubated with 0 or 50 μM THFA for 24 h upon addition of 5 mM NAC.

Part VII: Detection of Glyoxals in Animal and Human Serum Samples

7.1 Generation of diabetic mouse models using Streptozotocin (STZ).[35-37]

Three-week old male Institute of Cancer Research (ICR) mice were purchased from JSJ Lab Animal (Shanghai, China) and acclimated in our animal facility for one week. The mouse experiments were performed in accordance with protocols approved by the Institutional Animal Use and Care Committee of East China University of Science and Technology (ECUST). 8 mice were randomly selected and grouped into the diabetic group (4 mice per cage in 2 cages). After the one week acclimation, the blood glucose concentrations of the mice in the diabetic group were monitored with Yuwell 580 blood glucose meter (Zhenjiang, Jiangsu, China) and the Yuwell blood glucose test strips (Lot: 590324, exp date: Mach 25, 2021) for continuous 3 weeks (Week 4-6) via tail vein bleeding to ensure that the mouse glucose levels were within the normal range. In order to induce the hyperglycemic status, the diabetic group of mice were given D12492 60kcal% high-fat chow (Research Diets) instead of the standard chow (Xietong Pharmaceutical) during the whole study period. At the end of the 3rd week, STZ (Macklin, Cat No. S6089) were dissolved in citric acid buffer (pH 4.5) and 130 mg/kg STZ were intraperitoneally injected into the mice to destroy their pancreatic β cells following an eight-hour fasting period. Blood glucose concentrations, body weights and water consumptions were monitored in the 3 weeks (Week 7-9) after the STZ injection to confirm that the mice were in diabetic conditions. Blood samples were collected from the diabetic and another non-diabetic group (n = 8) of mice at the end of each week in the 3-week period after a four-hour fasting and serum MGO and GO levels were measured by **NAP-DCP-1**.

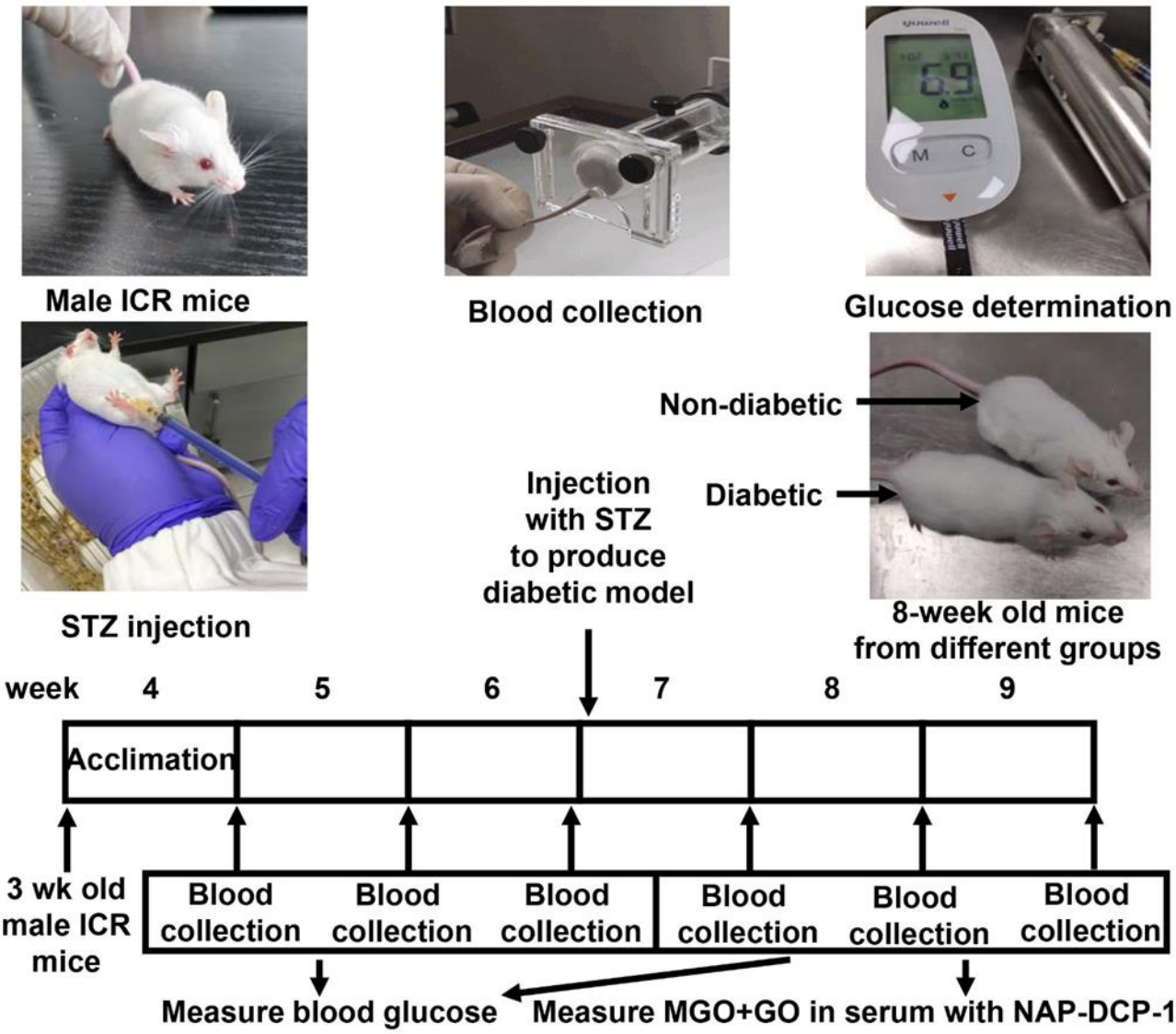

Figure S44 Experimental design of the diabetic mouse model. Male ICR mice were purchased and transferred to our animal facility at 3 week of age. After one week of acclimation, the blood glucose levels in the mice were measured at the end of each week in the 6-week experiment period to ensure if the mice were in diabetic condition. At the end of the 3rd week, mice were injected with 130 mg/kg STZ to generate the diabetic models. MGO and GO in the serum of the diabetic mice was measured with 10 μM **NAP-DCP-1**.

7.2 Detection of glyoxals in the serum of diabetic mouse models using NAP-DCP-1.

The diabetic mice models were generated by STZ injection (n = 8) as described above. 8 male ICR mice without STZ injection were also selected randomly and grouped as the non-diabetic group. Blood samples from both diabetic and non-diabetic groups were collected from the tail veins into 1.5 mL microcentrifuge tubes and 100 µl serum from each mouse was transferred onto a PE OptiPlate Black 96-well microplate after centrifugation. **NAP-DCP-1** was added to the serum at 10 µM concentration. After a 30 min incubation at r. t. in dark, the fluorescence intensity was measured on a SpectraMax i3x microplate reader (Molecular Devices) at excitation wavelength of 425 nm and the emission wavelength of 564 nm. The linear regression model was applied to fit the correlation between the blood glucose concentrations and the fluorescence intensity generated by adding **10 µM NAP-DCP-1.** The square of the sample correlation coefficient, R^2, was used to evaluate the degree of relevance.

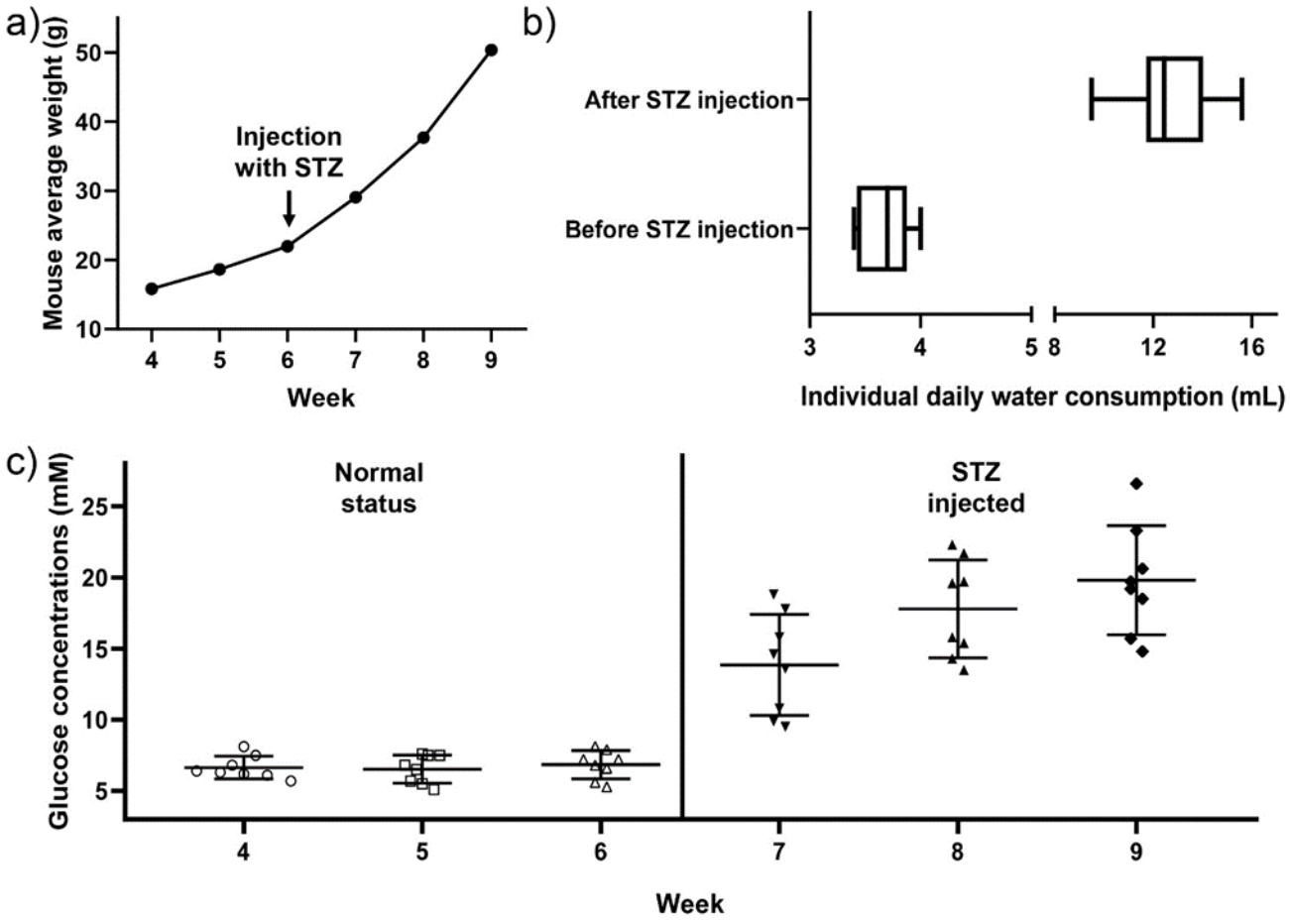

Figure S45 Characterization of the diabetic mouse model. a) Mouse average body weight was measured with a HC HTP312 electronic scale (Shanghai, China) and the average weight of the group (n = 8) was plotted. b) Daily water consumption by each mouse before and after the STZ injection calculated by weighing the water bottles. c) The blood glucose concentrations of the 8 mice measured at the end of each week during the 6 weeks of experiments. The values are mean ± SD.

7.3 Patient recruitment and sample collection.

All patient samples (both diabetic and non-diabetic) were collected at the Medical laboratory Department of Hua Shan Hospital North affiliated with Fudan University with written informed consent obtained from the patients. The study protocol was approved by the Institutional Review Board of Hua Shan Hospital North, and the identities (except the individual age and gender) of the patients were kept confidential to the researchers at East China University of Science and Technology (ECUST). Totally, 77 serum samples were collected from 57 patients with definite diagnosis of diabetes by physicians and 20 non-diabetic patients. All participated patients were aged between 35 to 75, without serious illness. The blood samples were extracted from a vein located on the inside of the elbow with a BD Preset 0.7 × 25 mm needle into a BD Vacutainer SST^{TM} II Advance tube. After clotting, the tubes were centrifuged at 1000 ×*g* for 10 min at 4 ˚C, and 300 μl serum samples were transferred to 1.5 mL microcentrifuge tubes. The samples were then frozen at -80 ˚C and transported to ECUST on dry ice. The samples were thawed and assayed immediately upon receiving at ECUST.

7.4 Examination of the glucose levels in the patients

The examinations of the patient glucose levels were conducted following the SOP of the Medical laboratory Department of Hua Shan Hospital North affiliated with Fudan University (ISO15189 certified). Basically, the glucose levels of patients were measured by the hexokinase catalysis method on a Roche Cobas C automated biochemistry analyzer. The hexokinase catalyzes the phosphorylation of glucose to glucose-6phosphate (G-6-P) by ATP, and G-6-P can be oxidized by dehydrogenase in the presence of NADP. The detection method measured the concentration of glucose by monitoring the rate of NADPH formation. The patient blood samples were collected from a vein located on the inside of the elbow with a BD Preset 0.7 × 25 mm needle into a BD Vacutainer tube with 5 mg sodium fluoride and 4mg potassium oxalate. After a brief centrifugation at 300 ×*g* for 3 min, the tubes were loaded on a Cobas C analyzer to measure the glucose levels in the patient blood samples.

Table S3 Genders, ages and blood glucose levels of 77 patients (57 diabetic and 20 non-diabetic) in the study

Disease status	Gender	Number	Age mean[1]	Age range[2]	Glucose[3]
Diabetic	Male	30	56 ± 13.5	35-73	11.9 ± 3.8
	Female	27	61 ± 12.4	38-75	10.6 ± 2.9
	Total	57	58 ± 13.3	35-75	11.4 ± 3.6
Non-diabetic	Male	10	54 ± 14.8	37-72	4.9 ± 1.8
	Female	10	50 ± 13.3	36-70	4.6 ± 1.4
	Total	20	52 ± 13.9	36-72	4.8 ± 1.6

1. Mean ± SD of the group.

2. All patients in the study were aged between 35 to 75.

3. Glucose levels (mM) were measured through the hexokinase method on a Roche Cobas C automated biochemistry analyzer. Mean ± SD of the group.

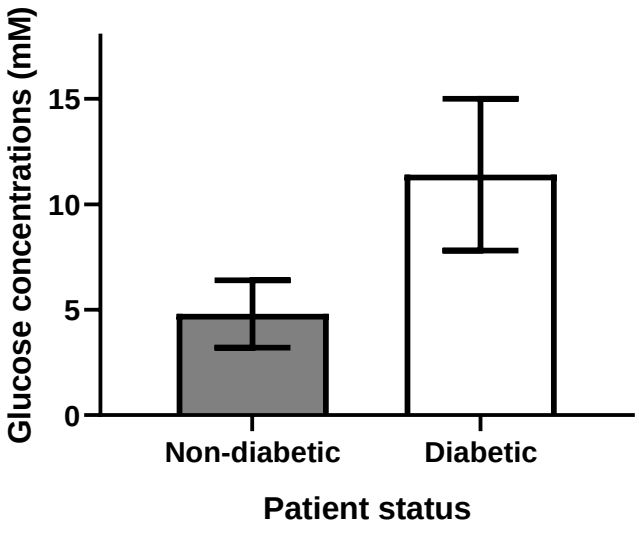

Figure S46 Glucose concentrations in the blood samples collected from the non-diabetic and diabetic patients. The glucose concentrations were measured on a Roche Cobas C automated biochemistry analyzer. The values are mean ± SD.

7.5 Detection of glyoxals in the human serum using NAP-DCP-1.

Human serum samples transported to ECUST were thawed and assayed immediately upon arrival. After a brief centrifugation at 1000 ×*g* for 5 min at 4 ˚C, 300 μL serum from each sample were transferred into 3 wells on a PE OptiPlate Black 96-well microplate (100 μL in each well). **NAP-DCP-1** was diluted in PBS buffer and added to the serum samples on the microplate at a final concentration of 10 μM. The plate was incubated at r.t. in dark for 30 min, and the fluorescence intensity was measured on a Synergy Lx microplate reader (BioTek) using the filters of 440 ± 15 nm (440/30x) excitation wavelength and 560 ± 20 nm (560/40m) emission wavelength. The average fluorescence intensity value of the 3 wells for each patient was used in the statistical calculation. The linear regression model was applied to fit the correlation between the blood glucose concentrations and the fluorescence intensity generated by adding 10 μM **NAP-DCP-1**. The square of the sample correlation coefficient, R^2, was used to evaluate the degree of relevance.

Part VIII: NMR and HRMS Data

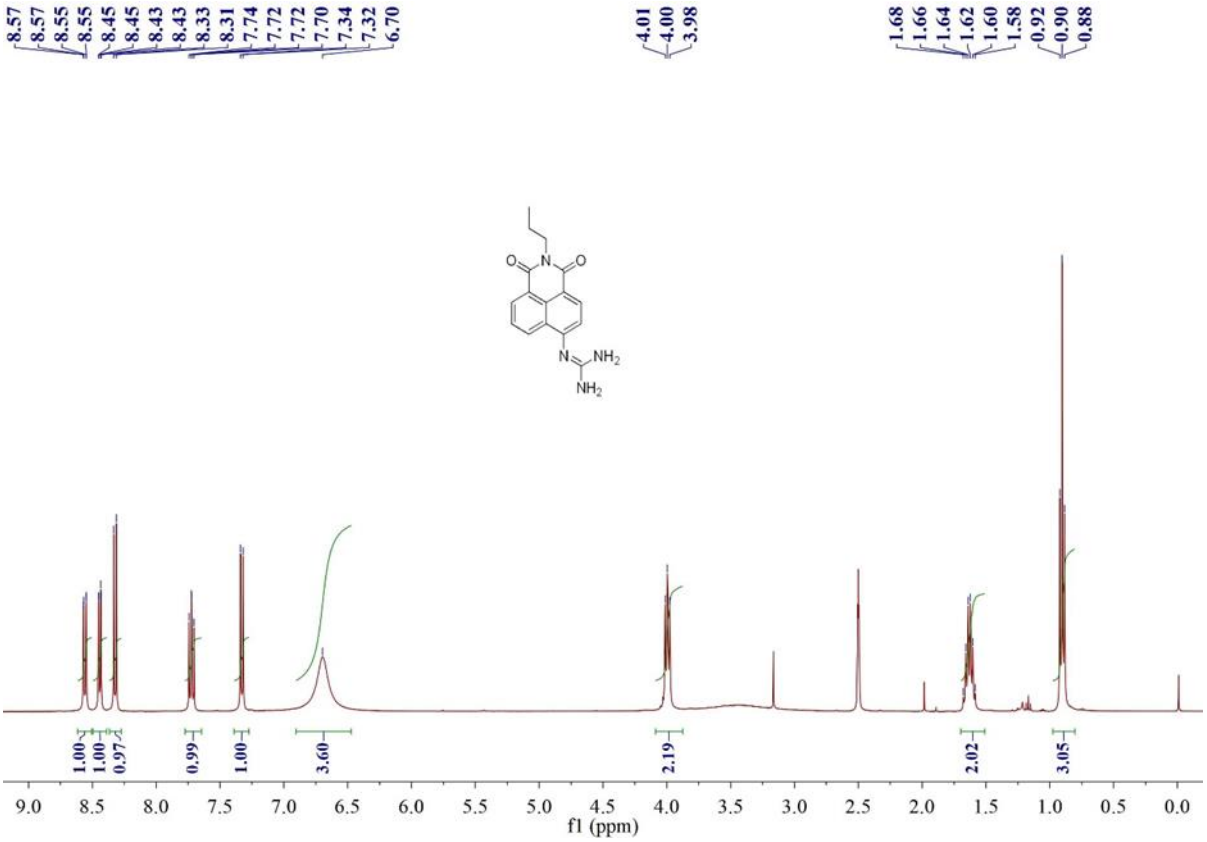

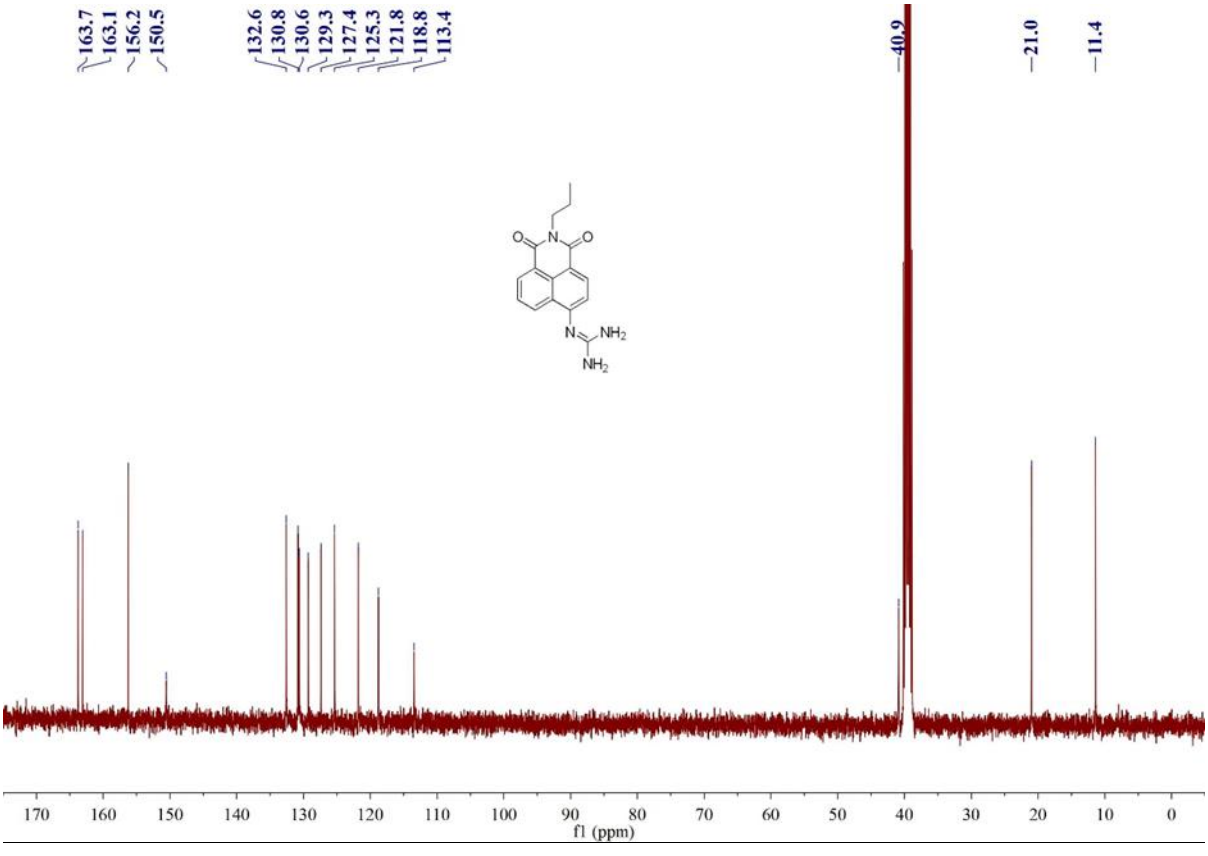

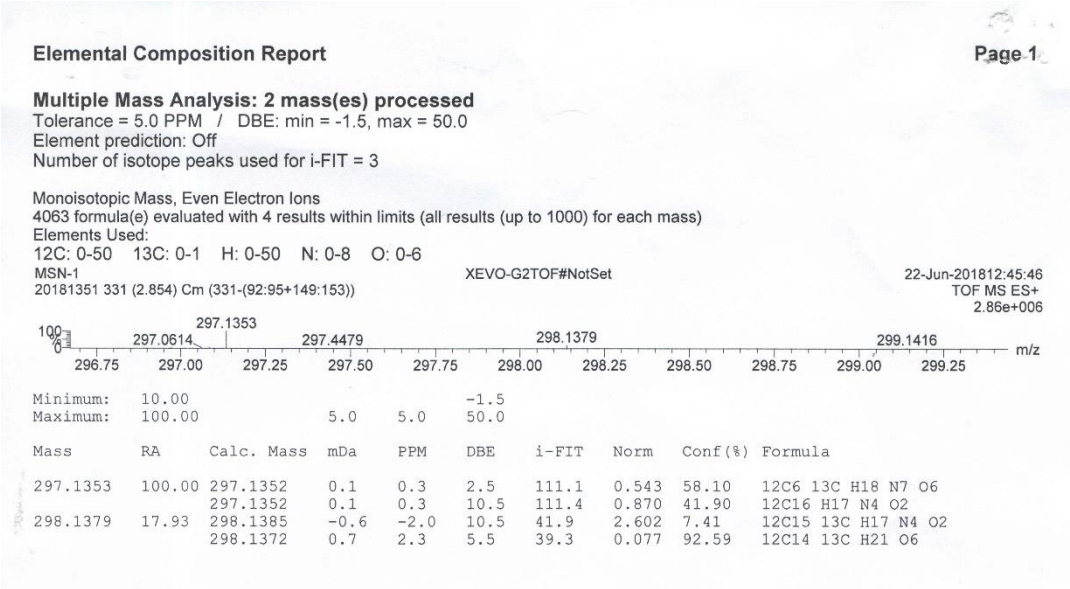

Elemental Composition Report Page 1

Multiple Mass Analysis: 2 mass(es) processed
Tolerance = 5.0 PPM / DBE: min = -1.5, max = 50.0
Element prediction: Off
Number of isotope peaks used for i-FIT = 3

Monoisotopic Mass, Even Electron Ions
4063 formula(e) evaluated with 4 results within limits (all results (up to 1000) for each mass)
Elements Used:
12C: 0-50 13C: 0-1 H: 0-50 N: 0-8 O: 0-6

MSN-1 XEVO-G2TOF#NotSet 22-Jun-201812:45:46
20181351 331 (2.854) Cm (331-(92:95+149:153)) TOF MS ES+
2.86e+006

Minimum:	10.00				-1.5				
Maximum:	100.00		5.0	5.0	50.0				
Mass	RA	Calc. Mass	mDa	PPM	DBE	i-FIT	Norm	Conf(%)	Formula
297.1353	100.00	297.1352	0.1	0.3	2.5	111.1	0.543	58.10	12C6 13C H18 N7 O6
		297.1352	0.1	0.3	10.5	111.4	0.870	41.90	12C16 H17 N4 O2
298.1379	17.93	298.1385	-0.6	-2.0	10.5	41.9	2.602	7.41	12C15 13C H17 N4 O2
		298.1372	0.7	2.3	5.5	39.3	0.077	92.59	12C14 13C H21 O6

Figure S47 ^{1}H NMR, ^{13}C NMR, and HRMS of **NAP-DCP-1**.

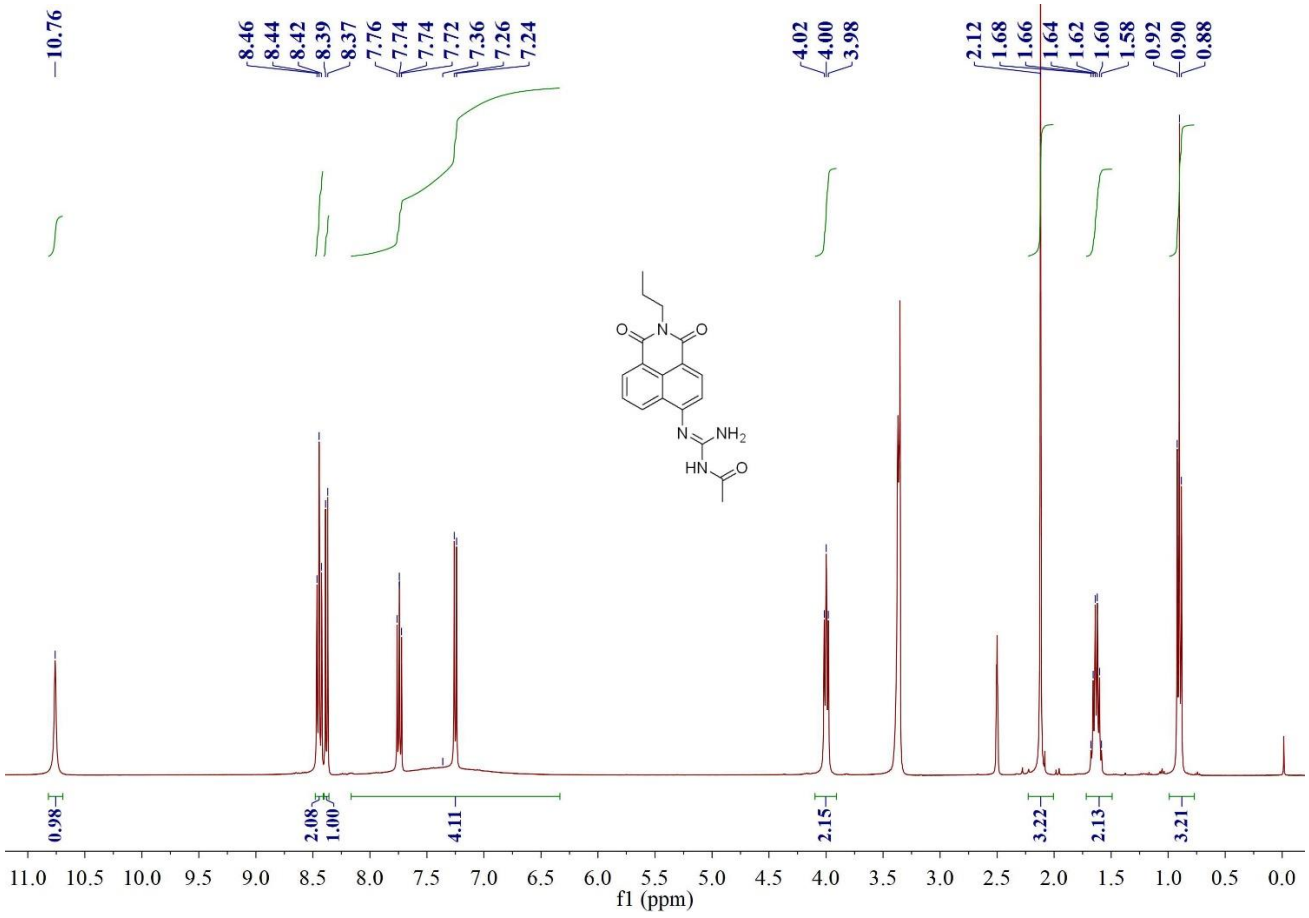

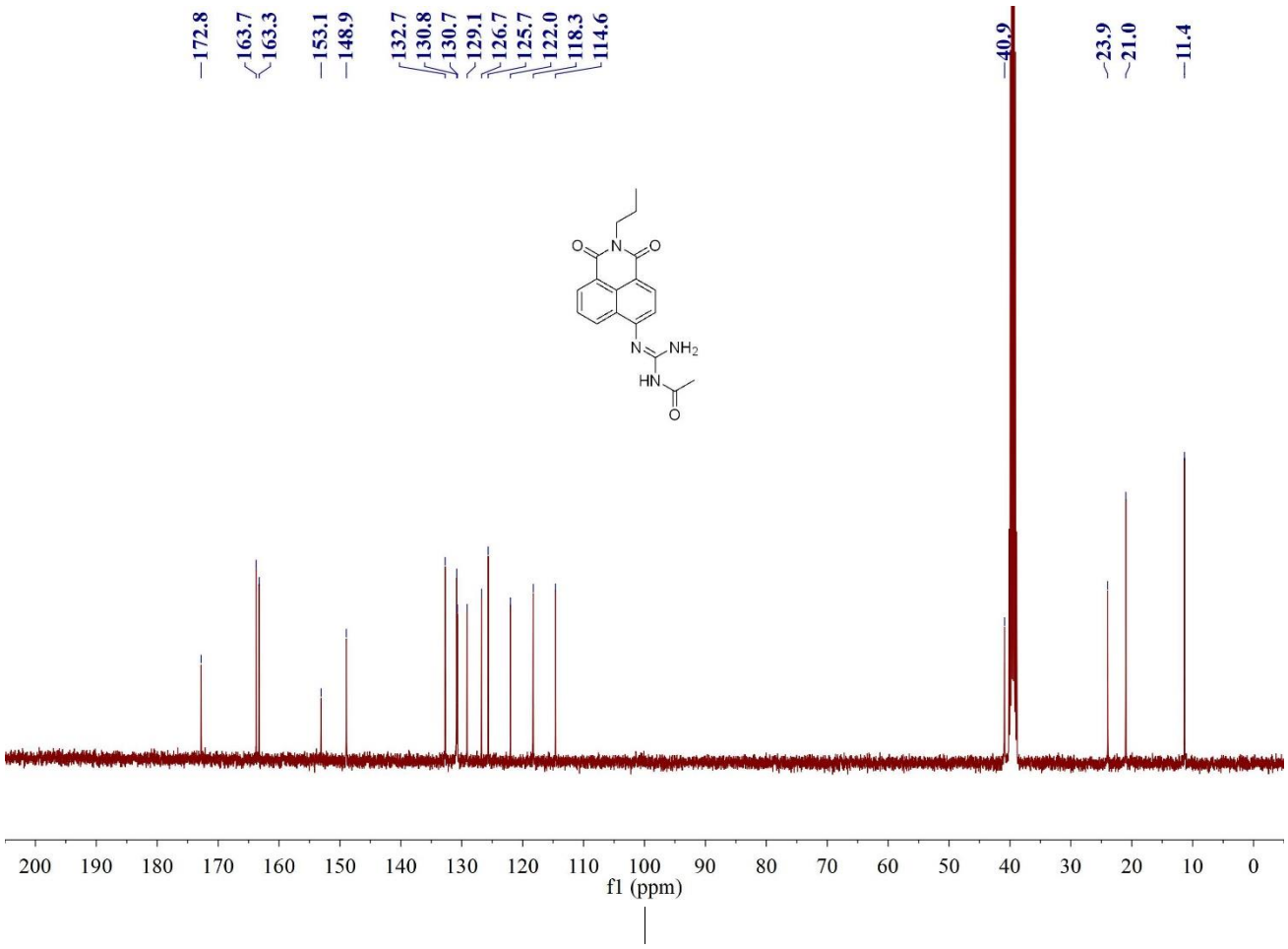

Elemental Composition Report Page 1

Multiple Mass Analysis: 2 mass(es) processed
Tolerance = 5.0 PPM / DBE: min = -1.5, max = 50.0
Element prediction: Off
Number of isotope peaks used for i-FIT = 3

Monoisotopic Mass, Even Electron Ions
7613 formula(e) evaluated with 6 results within limits (all results (up to 1000) for each mass)
Elements Used:
12C: 0-50 13C: 0-1 H: 0-50 N: 0-10 O: 0-10

MSA-189
20190272 126 (1.236) Cm (126-(514+518))

XEVO-G2TOF#NotSet

25-Feb-201915:41:02
1: TOF MS ES+
4.18e+005

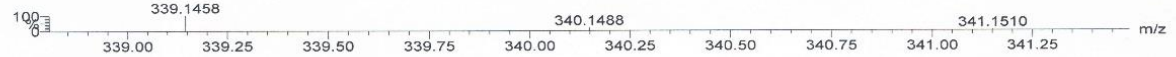

Minimum:	10.00				-1.5				
Maximum:	100.00		5.0	5.0	50.0				
Mass	RA	Calc. Mass	mDa	PPM	DBE	i-FIT	Norm	Conf(%)	Formula
339.1458	100.00	339.1458	0.0	0.0	3.5	34.6	1.472	22.94	12C8 13C H20 N7 O7
		339.1457	0.1	0.3	11.5	34.8	1.696	18.34	12C18 H19 N4 O3
		339.1444	1.4	4.1	6.5	33.6	0.532	58.72	12C17 H23 O7
340.1488	15.60	340.1491	-0.3	-0.9	11.5	34.1	0.614	54.13	12C17 13C H19 N4 O3
		340.1482	0.6	1.8	7.5	35.3	1.830	16.04	12C11 H18 N9 O4
		340.1477	1.1	3.2	6.5	34.7	1.210	29.83	12C16 13C H23 O7

Figure S48 ^{1}H NMR, ^{13}C NMR, and HRMS of the reference compound **2**.

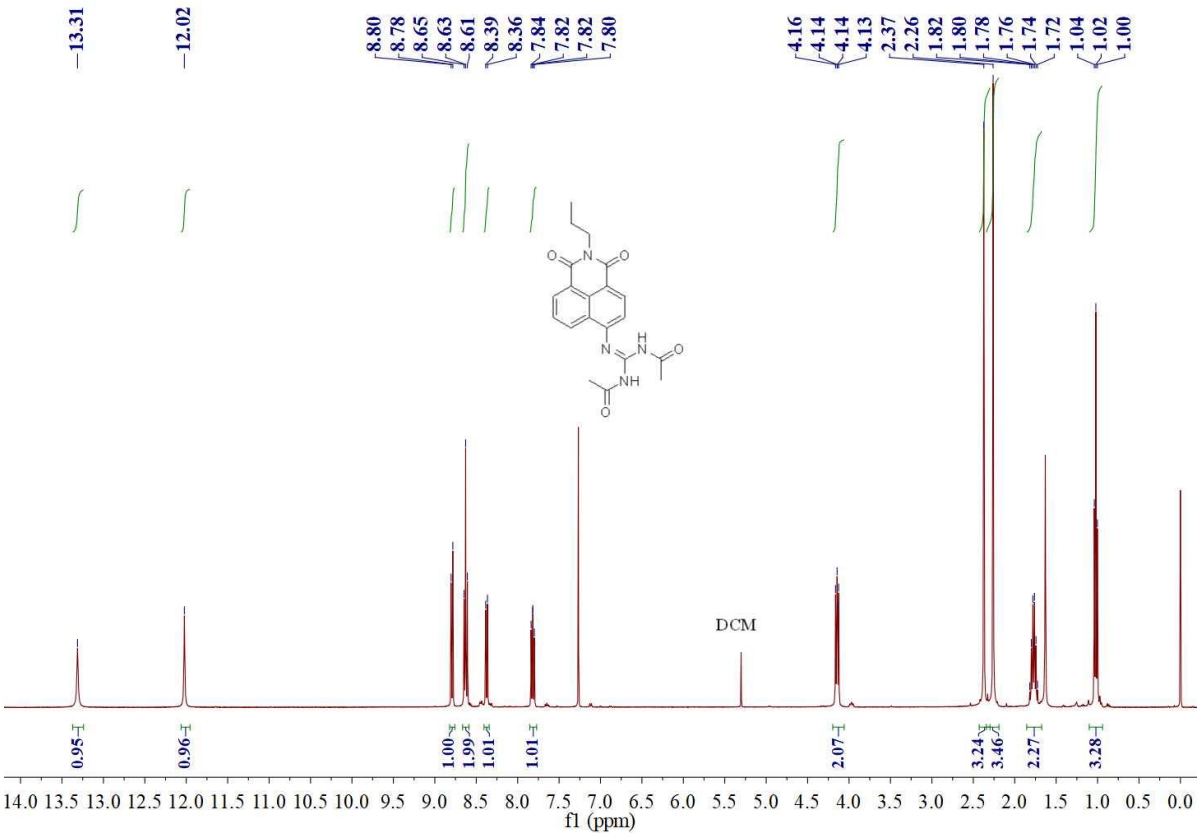
13.31
12.02
8.80
8.78
8.65
8.63
8.61
8.39
8.36
7.84
7.82
7.82
7.80
4.16
4.14
4.14
4.13
2.37
2.26
1.82
1.80
1.78
1.76
1.74
1.72
1.04
1.02
1.00
DCM
0.95
0.96
1.00
1.99
1.01
1.01
2.07
3.24
3.46
2.27
3.28
f1 (ppm)

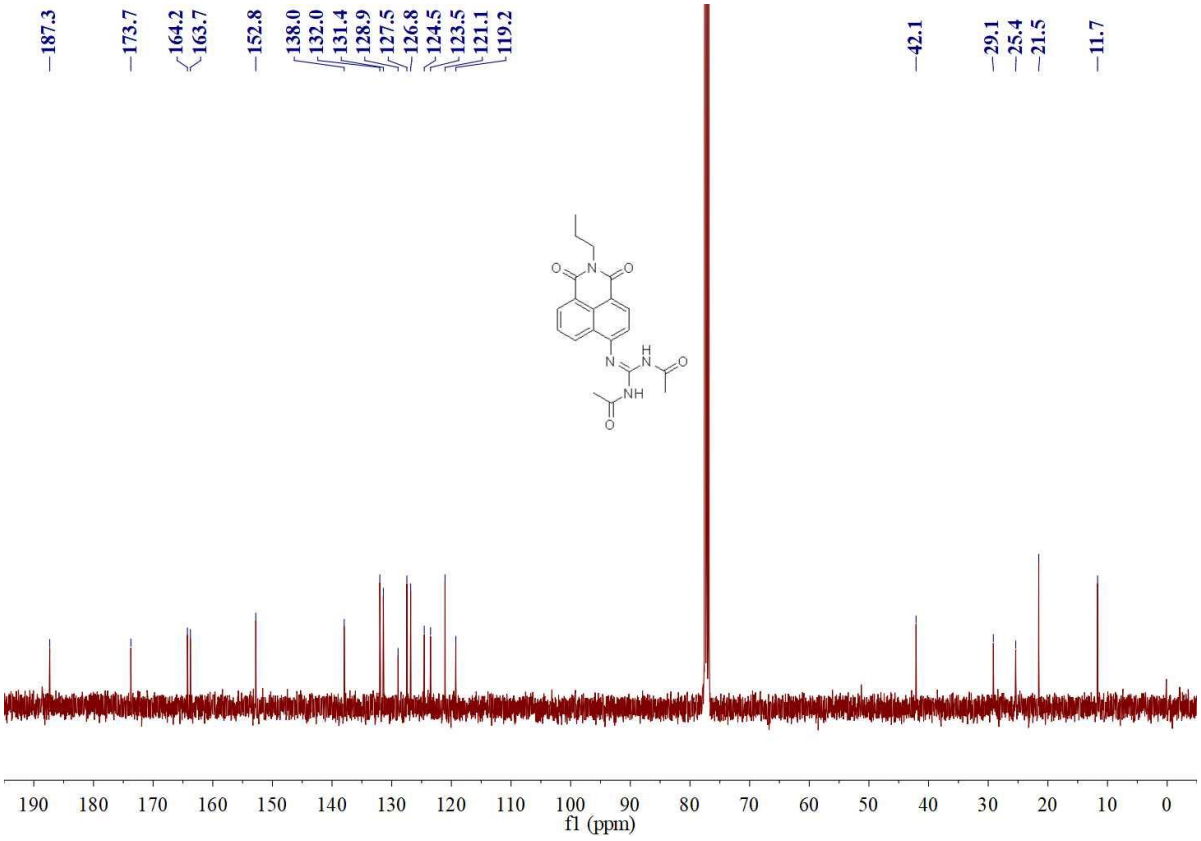
187.3
173.7
164.2
163.7
152.8
138.0
132.0
131.4
128.9
127.5
126.8
124.5
123.5
121.1
119.2
42.1
29.1
25.4
21.5
11.7
f1 (ppm)

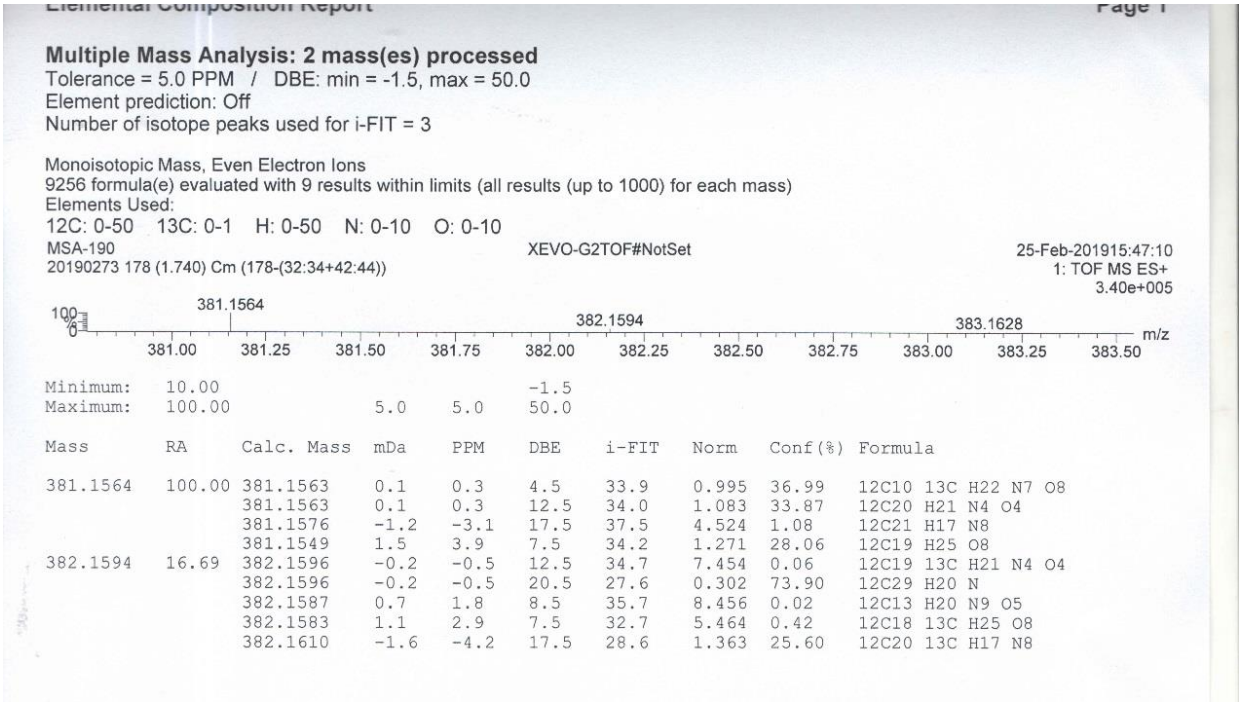

Multiple Mass Analysis: 2 mass(es) processed
Tolerance = 5.0 PPM / DBE: min = -1.5, max = 50.0
Element prediction: Off
Number of isotope peaks used for i-FIT = 3

Monoisotopic Mass, Even Electron Ions
9256 formula(e) evaluated with 9 results within limits (all results (up to 1000) for each mass)
Elements Used:
12C: 0-50 13C: 0-1 H: 0-50 N: 0-10 O: 0-10

MSA-190 XEVO-G2TOF#NotSet 25-Feb-201915:47:10
20190273 178 (1.740) Cm (178-(32:34+42:44)) 1: TOF MS ES+
3.40e+005

Minimum:	10.00				-1.5				
Maximum:	100.00		5.0	5.0	50.0				
Mass	RA	Calc. Mass	mDa	PPM	DBE	i-FIT	Norm	Conf(%)	Formula
381.1564	100.00	381.1563	0.1	0.3	4.5	33.9	0.995	36.99	12C10 13C H22 N7 O8
		381.1563	0.1	0.3	12.5	34.0	1.083	33.87	12C20 H21 N4 O4
		381.1576	-1.2	-3.1	17.5	37.5	4.524	1.08	12C21 H17 N8
		381.1549	1.5	3.9	7.5	34.2	1.271	28.06	12C19 H25 O8
382.1594	16.69	382.1596	-0.2	-0.5	12.5	34.7	7.454	0.06	12C19 13C H21 N4 O4
		382.1596	-0.2	-0.5	20.5	27.6	0.302	73.90	12C29 H20 N
		382.1587	0.7	1.8	8.5	35.7	8.456	0.02	12C13 H20 N9 O5
		382.1583	1.1	2.9	7.5	32.7	5.464	0.42	12C18 13C H25 O8
		382.1610	-1.6	-4.2	17.5	28.6	1.363	25.60	12C20 13C H17 N8

Figure S49 ^{1}H NMR, ^{13}C NMR, and HRMS of the reference compound **3**.

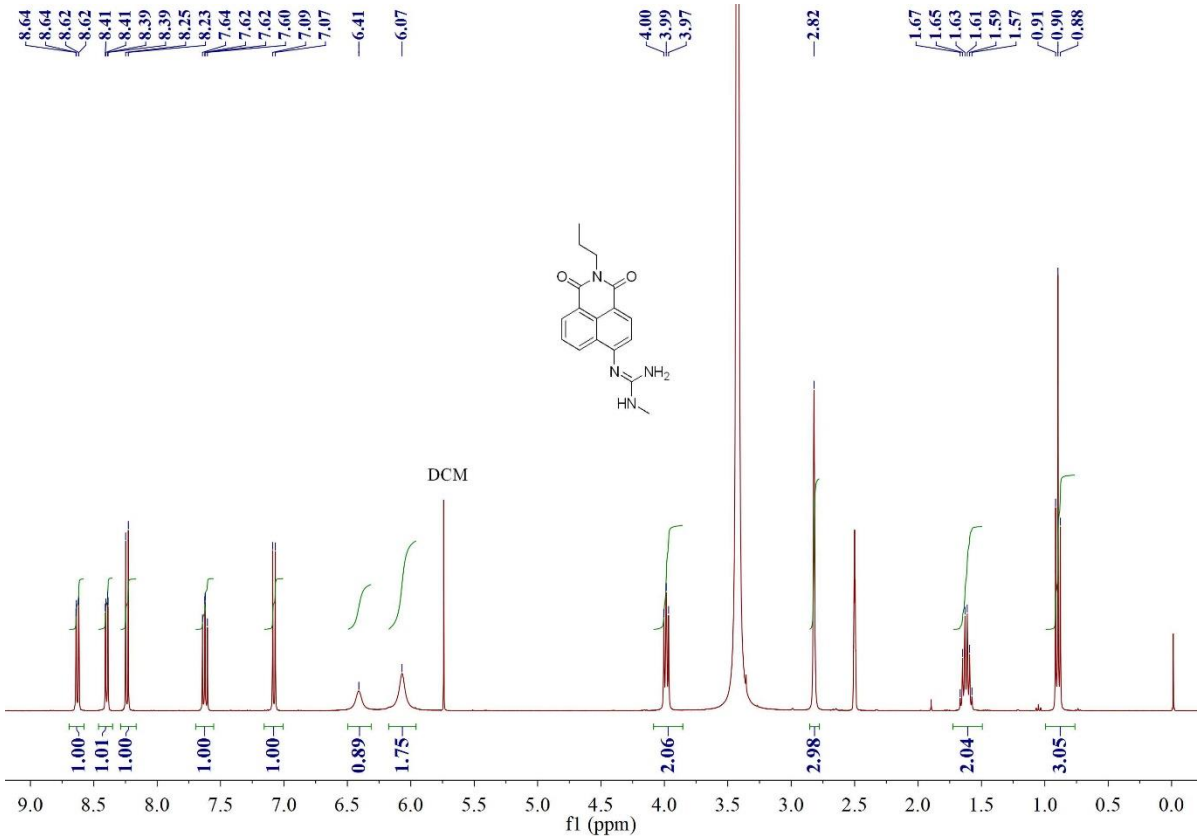

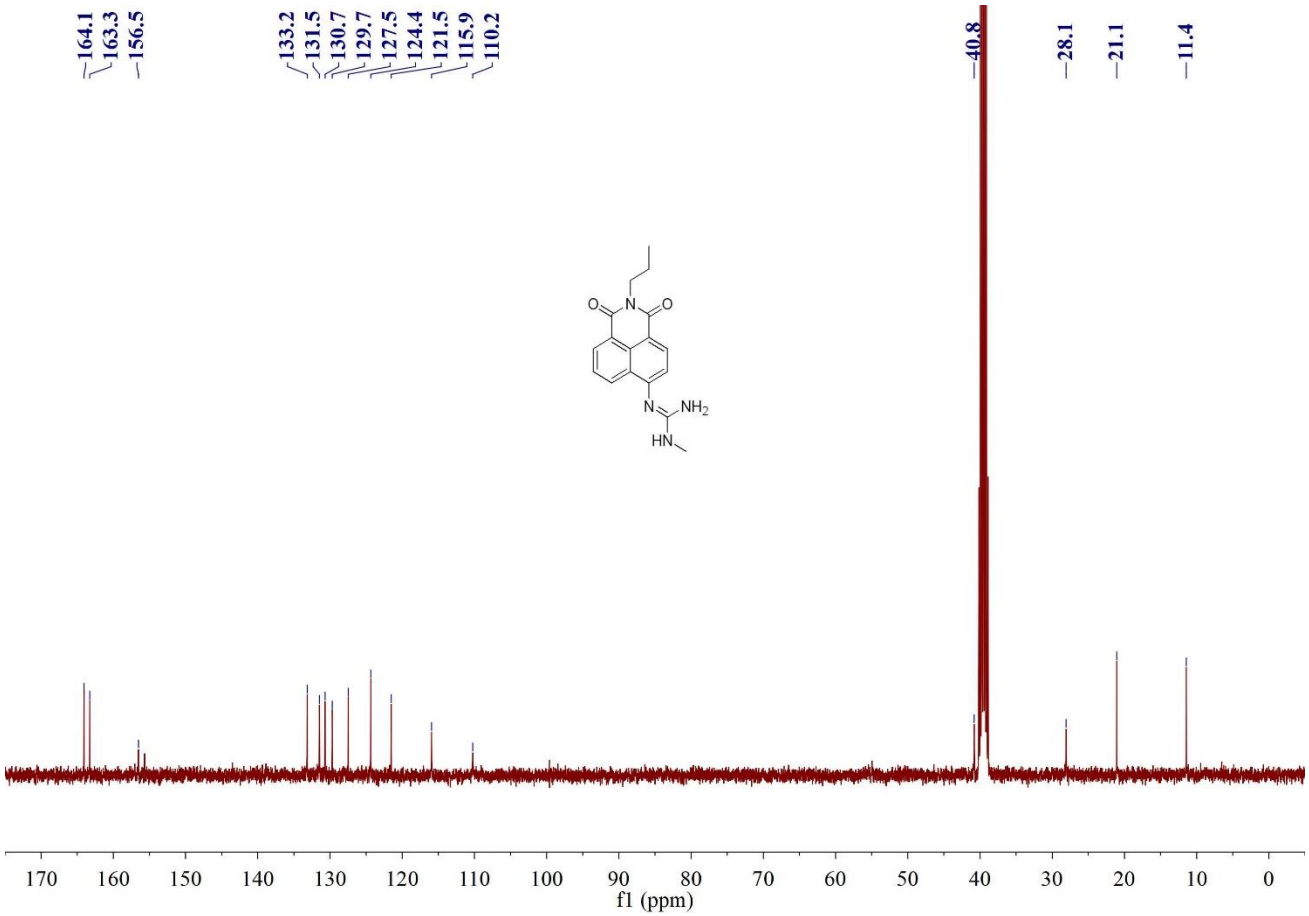

Elemental Composition Report

Page 1

Multiple Mass Analysis: 2 mass(es) processed
Tolerance = 5.0 PPM / DBE: min = -1.5, max = 50.0
Element prediction: Off
Number of isotope peaks used for i-FIT = 3

Monoisotopic Mass, Even Electron Ions
4964 formula(e) evaluated with 6 results within limits (all results (up to 1000) for each mass)
Elements Used:
12C: 0-50 13C: 0-1 H: 0-50 N: 0-10 O: 0-6

msn-2
20181329 817 (7.930) Cm (817-(1440+1446))

XEVO-G2TOF#NotSet

20-Jun-201813:56:09
1: TOF MS ES+
5.16e+005

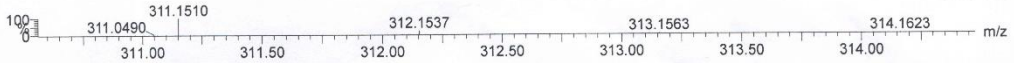

Minimum:	20.00				-1.5				
Maximum:	100.00		5.0	5.0	50.0				
Mass	RA	Calc. Mass	mDa	PPM	DBE	i-FIT	Norm	Conf(%)	Formula
311.1510	100.00	311.1509	0.1	0.3	2.5	93.6	1.160	31.35	12C7 13C H20 N7 O6
		311.1508	0.2	0.6	10.5	93.8	1.375	25.29	12C17 H19 N4 O2
		311.1495	1.5	4.8	5.5	93.3	0.835	43.37	12C16 H23 O6
312.1537	21.03	312.1533	0.4	1.3	6.5	42.9	0.767	46.43	12C10 H18 N9 O3
		312.1542	-0.5	-1.6	10.5	43.1	0.900	40.66	12C16 13C H19 N4 O2
		312.1528	0.9	2.9	5.5	44.2	2.048	12.90	12C15 13C H23 O6

Figure S50 ^{1}H NMR, ^{13}C NMR, and HRMS of **NAP-DCP-2**.

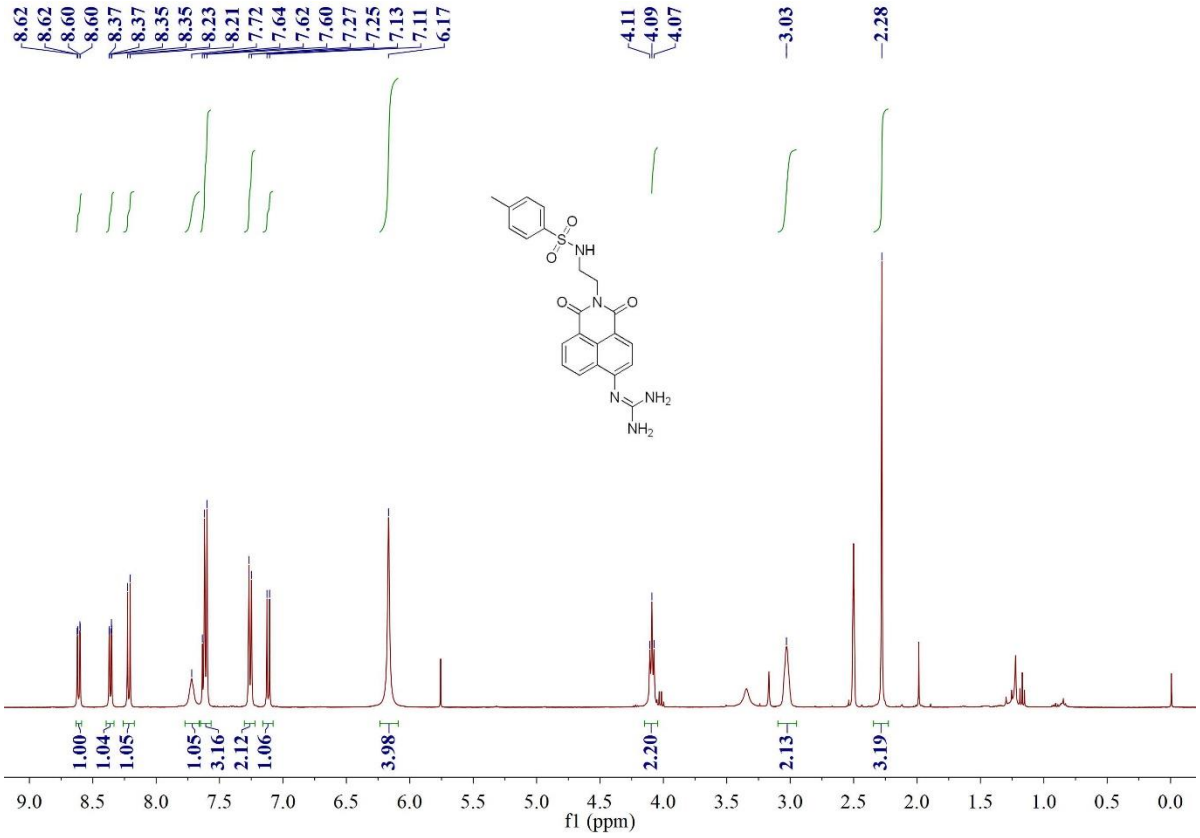
8.62
8.62
8.60
8.60
8.37
8.37
8.35
8.35
8.23
8.21
7.72
7.64
7.62
7.60
7.27
7.25
7.13
7.11
6.17
4.11
4.09
4.07
3.03
2.28
NH
NH2
NH2
1.00
1.04
1.05
1.05
3.16
2.12
1.06
3.98
2.20
2.13
3.19
f1 (ppm)

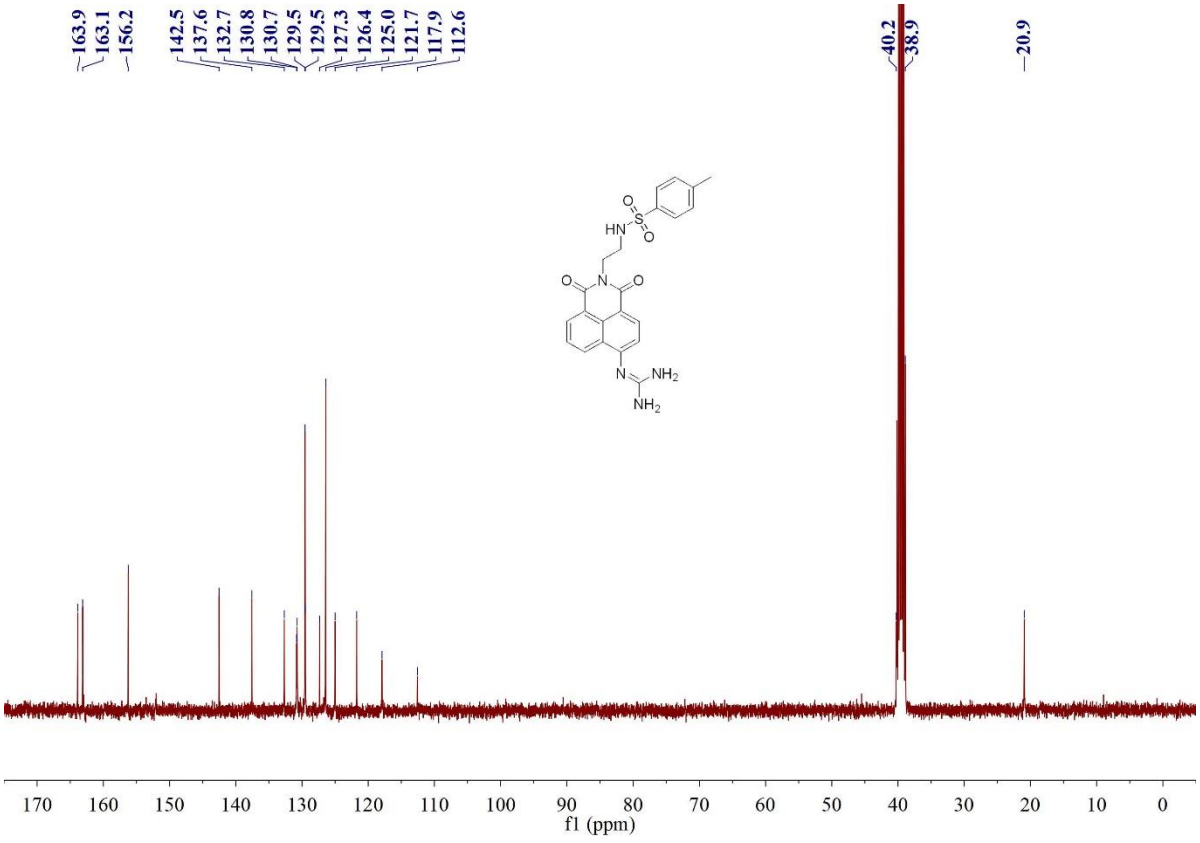
163.9
163.1
156.2
142.5
137.6
132.7
130.8
130.7
129.5
129.5
127.3
126.4
125.0
121.7
117.9
112.6
40.2
38.9
20.9
HN
NH2
NH2
f1 (ppm)

Elemental Composition Report Page 1

Multiple Mass Analysis: 2 mass(es) processed
Tolerance = 5.0 PPM / DBE: min = -1.5, max = 50.0
Element prediction: Off
Number of isotope peaks used for i-FIT = 3

Monoisotopic Mass, Even Electron Ions
10779 formula(e) evaluated with 13 results within limits (all results (up to 1000) for each mass)
Elements Used:
12C: 0-50 13C: 0-1 H: 0-50 N: 0-10 O: 0-10 S: 1-1
MSA-210 XEVO-G2TOF#NotSet 25-Feb-201915:52:55
20190274 101 (1.001) Cm (101-(9:12+26:28)) 1: TOF MS ES+
2.41e+005

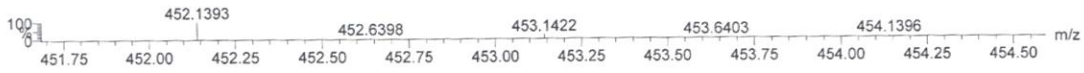

Minimum:	10.00				-1.5				
Maximum:	100.00		5.0	5.0	50.0				
Mass	RA	Calc. Mass	mDa	PPM	DBE	i-FIT	Norm	Conf(%)	Formula
452.1393	100.00	452.1393	0.0	0.0	6.5	66.1	1.995	13.60	12C12 13C H23 N8 O8 S
		452.1392	0.1	0.2	14.5	66.3	2.203	11.04	12C22 H22 N5 O4 S
		452.1401	-0.8	-1.8	18.5	65.5	1.396	24.76	12C28 13C H23 O3 S
		452.1406	-1.3	-2.9	19.5	66.7	2.605	7.39	12C23 H18 N9 S
		452.1379	1.4	3.1	9.5	65.1	0.945	38.85	12C21 H26 N O8 S
		452.1375	1.8	4.0	19.5	67.3	3.135	4.35	12C24 13C H19 N6 O S
453.1422	20.13	453.1425	-0.3	-0.7	22.5	48.3	3.011	4.93	12C31 H21 N2 S
		453.1426	-0.4	-0.9	14.5	47.5	2.230	10.75	12C21 13C H22 N5 O4 S
		453.1417	0.5	1.1	10.5	45.8	0.513	59.87	12C15 H21 N10 O5 S
		453.1413	0.9	2.0	9.5	50.1	4.800	0.82	12C20 13C H26 N O8 S
		453.1439	-1.7	-3.8	19.5	47.1	1.879	15.27	12C22 13C H18 N9 S
		453.1404	1.8	4.0	5.5	48.0	2.690	6.79	12C14 H25 N6 O9 S
		453.1444	-2.2	-4.9	9.5	49.4	4.153	1.57	12C19 H25 N4 O7 S

Figure S51 ^{1}H NMR, ^{13}C NMR, and HRMS of **NAP-FAP-3**.

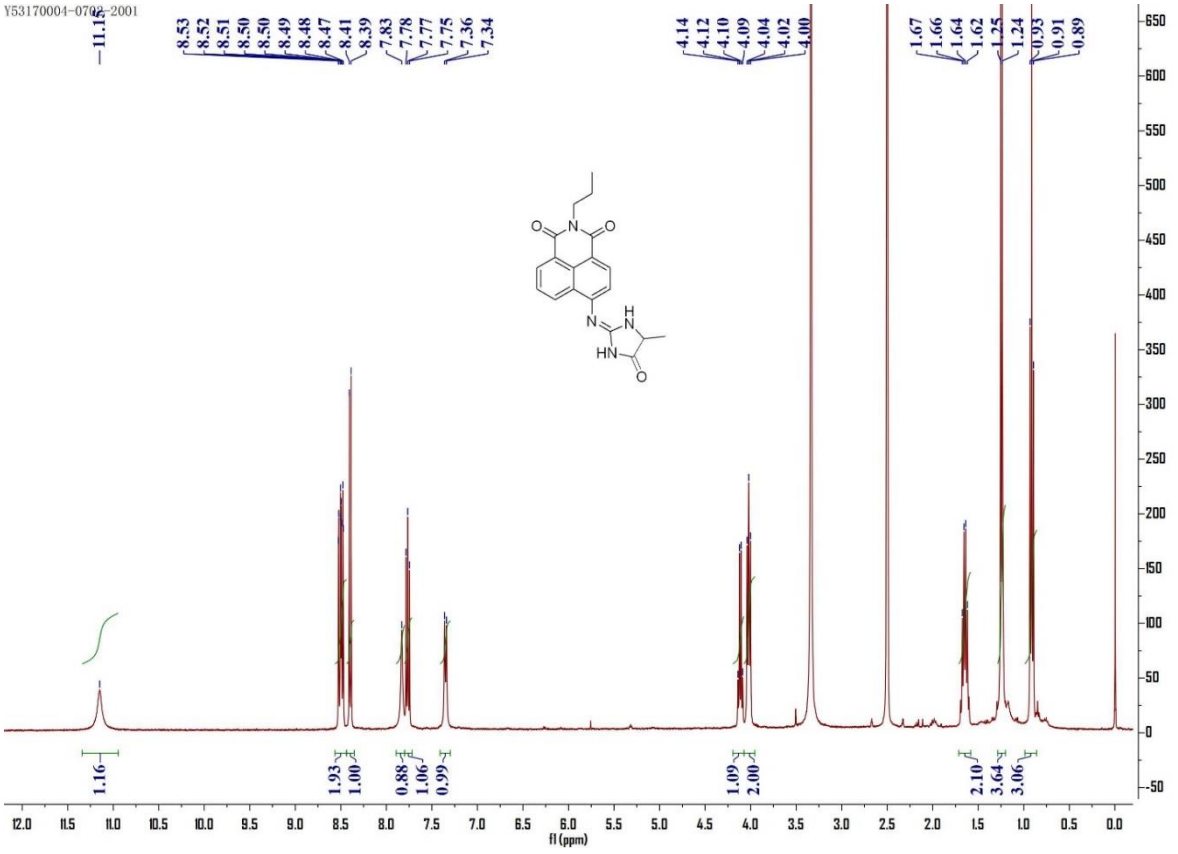

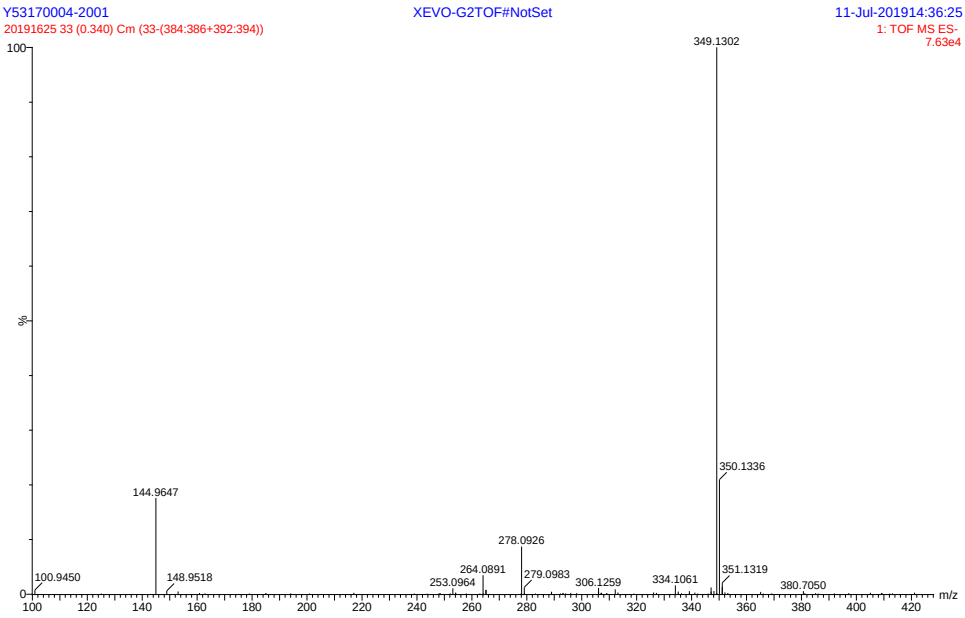

Figure S52 ^{1}H NMR and HRMS of **6b**.

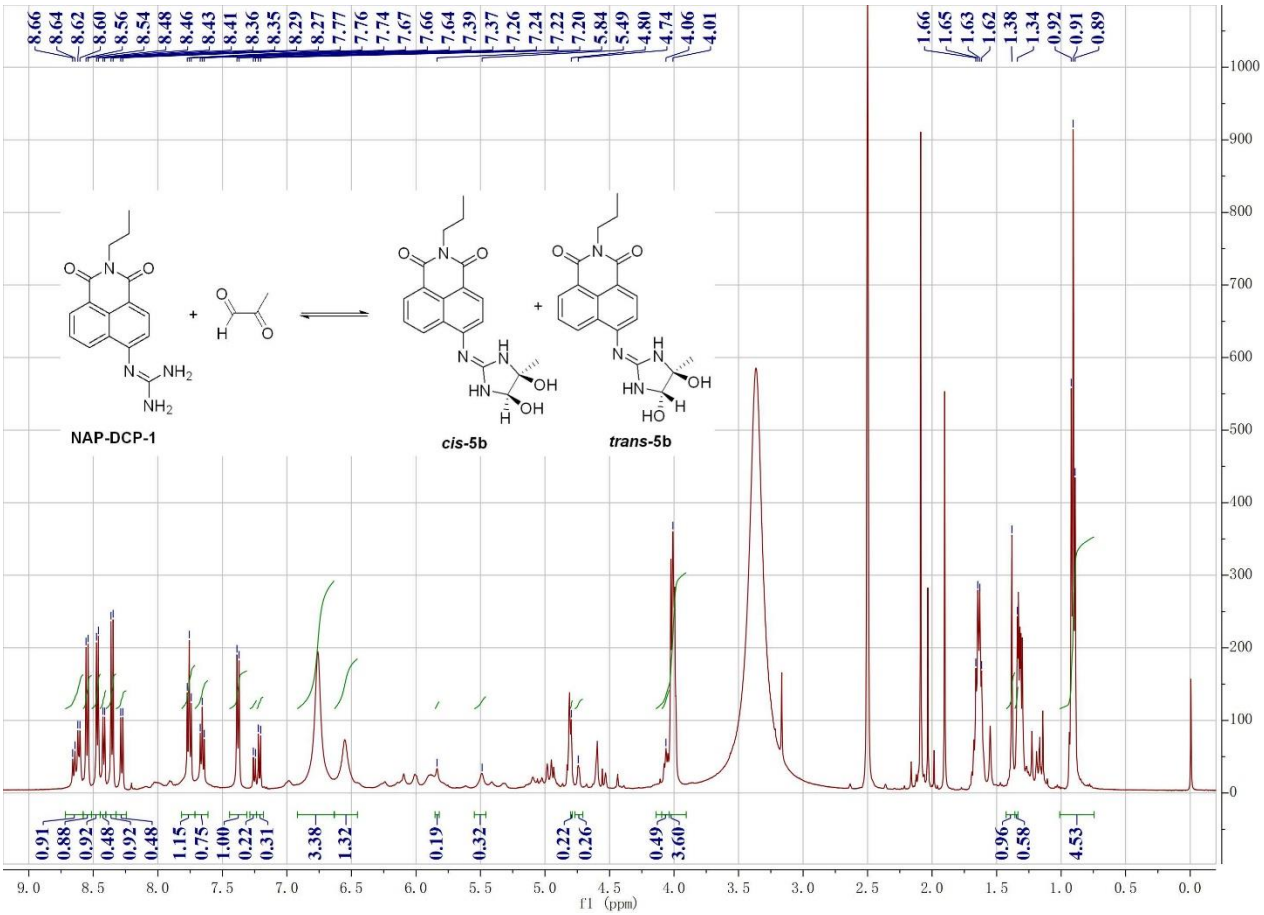

Figure S53 ^{1}H NMR of reaction mixture of **NAP-DCP-1** and 10 equiv. MGO in DMSO-d_6 at 30 min (also see **Figure S4**).

References

1. Wang, H.; Xu, Y.; Rao, L.; Yang, C.; Yuan, H.; Gao, T.; Chen, X.; Sun, H.; Xian, M.; Liu, C.; Liu, C., Ratiometric fluorescent probe for monitoring endogenous methylglyoxal in living cells and diabetic blood samples. *Anal. Chem.* **2019,** *91* (9), 5646-5653.

2. Yang, M.; Fan, J.; Zhang, J.; Du, J.; Peng, X., Visualization of methylglyoxal in living cells and diabetic mice model with a 1,8-naphthalimide-based two-photon fluorescent probe. *Chem. Sci.* **2018,** *9* (33), 6758-6764.

3. Gao, S.; Tang, Y.; Lin, W., Development of a highly selective two-photon probe for methylglyoxal and its applications in living cells, tissues, and zebrafish. *J. Fluoresc.* **2019,** *29* (1), 155-163.

4. Tang, T.; Zhou, Y.; Chen, Y.; Li, M.; Feng, Y.; Wang, C.; Wang, S.; Zhou, X., A two-photon fluorescent probe for selective methylglyoxal detection and application in living cells. *Anal. Methods* **2015,** *7* (6), 2386-2390.

5. Wang, T.; Douglass, E. F., Jr.; Fitzgerald, K. J.; Spiegel, D. A., A "turn-on" fluorescent sensor for methylglyoxal. *J. Am. Chem. Soc.* **2013,** *135* (33), 12429-12433.

6. Liu, C.; Jiao, X.; He, S.; Zhao, L.; Zeng, X., A reaction-based fluorescent probe for the selective detection of formaldehyde and methylglyoxal via distinct emission patterns. *Dyes Pigm.* **2017,** *138*, 23-29.

7. Shaheen, F.; Shmygol, A.; Rabbani, N.; Thornalley, P. J., A fluorogenic assay for methylglyoxal. *Biochem. Soc. Trans.* **2014,** *42* (2), 548-555.

8. Ding, C.; Wang, F.; Dang, Y.; Xu, Z.; Li, L.; Lai, Y.; Yu, H.; Luo, Y.; Huang, R.; Zhang, A.; Zhang, W., Imaging Tumorous Methylglyoxal by an Activatable Near-Infrared Fluorescent Probe for Monitoring Glyoxalase 1 Activity. *Anal. Chem.* **2019,** *91* (24), 15577-15584.

9. Dang, Y.; Wang, F.; Li, L.; Lai, Y.; Xu, Z.; Xiong, Z.; Zhang, A.; Tian, Y.; Ding, C.; Zhang, W., An activatable near-infrared fluorescent probe for methylglyoxal imaging in Alzheimer's disease mice. *Chem. Commun.* **2020,** *56* (5), 707-710.

10. Li, S.-J.; Zhou, D.-Y.; Li, Y.; Liu, H.-W.; Wu, P.; Ou-Yang, J.; Jiang, W.-L.; Li, C.-Y., Efficient two-photon fluorescent probe for imaging of nitric oxide during endoplasmic reticulum stress. *ACS Sens.* **2018,** *3* (11), 2311-2319.

11. Huang, C.-B.; Huang, J.; Xu, L., A highly selective fluorescent probe for fast detection of nitric oxide in aqueous solution. *RSC Adv.* **2015,** *5* (18), 13307-13310.

12. Yu, H.; Xiao, Y.; Jin, L., A Lysosome-Targetable and Two-Photon Fluorescent Probe for Monitoring Endogenous and Exogenous Nitric Oxide in Living Cells. *J. Am. Chem. Soc.* **2012,** *134* (42), 17486-17489.

13. Wang, M.; Xu, Z.; Wang, X.; Cui, J., A fluorescent and colorimetric chemosensor for nitric oxide based on 1,8-naphthalimide. *Dyes Pigm.* **2013,** *96* (2), 333-337.

14. Liu, L.; Zhang, F.; Xu, B.; Tian, W., Silica nanoparticles based on an AIE-active molecule for ratiometric detection of RNS in vitro. *J. Mater. Chem. B* **2017,** *5* (46), 9197-9203.

15. Huo, Y.; Miao, J.; Han, L.; Li, Y.; Li, Z.; Shi, Y.; Guo, W., Selective and sensitive visualization of endogenous nitric oxide in living cells and animals by a Sirhodamine deoxylactam-based near-infrared fluorescent probe. *Chem. Sci.* **2017,** *8* (10), 6857-6864.

16. Cao, T.; Gong, D.; Han, S.-C.; Iqbal, A.; Qian, J.; Liu, W.; Qin, W.; Guo, H., BODIPY-based fluorescent sensor for imaging of endogenous formaldehyde in living cells. *Talanta* **2018,** *189*, 274-280.

17. Zhang, X.; Kim, W. S.; Hatcher, N.; Potgieter, K.; Moroz, L. L.; Gillette, R.; Sweedler, J. V., Interfering with nitric oxide measurements - 4,5-Diaminofluorescein reacts with dehydroascorbic acid and ascorbic acid. *J. Biol. Chem.* **2002,** *277* (50), 48472-48478.

18. Zhou, X.; Zeng, Y.; Chen, L.; Wu, X.; Yoon, J., A Fluorescent Sensor for Dual-Channel Discrimination between Phosgene and a Nerve-Gas Mimic. *Angew. Chem. Int. Ed.* **2016,** *55* (15), 4729-4733.

19. Xia, H.-C.; Xu, X.-H.; Song, Q.-H., Fluorescent Chemosensor for Selective Detection of Phosgene in Solutions and in Gas Phase. *ACS Sens.* **2017,** *2* (1), 178-182.

20. Zhang, W.-Q.; Cheng, K.; Yang, X.; Li, Q.-Y.; Zhang, H.; Ma, Z.; Lu, H.; Wu, H.; Wang, X.-J., A benzothiadiazole-based fluorescent sensor for selective detection of oxalyl chloride and phosgene. *Org. Chem. Front.* **2017,** *4* (9), 1719-1725.

21. Tang, Y.; Kong, X.; Xu, A.; Dong, B.; Lin, W., Development of a two-photon fluorescent probe for imaging of endogenous formaldehyde in living tissues. *Angew. Chem. Int. Ed.* **2016,** *55* (10), 3356-3359.

22. Cui, L.; Zhong, Y.; Zhu, W.; Xu, Y.; Qian, X., Selective and sensitive detection and quantification of arylamine N-acetyltransferase 2 by a ratiometric fluorescence probe. *Chem. Commun.* **2010,** *46* (38), 7121-7123.

23. Xu, C.; Webb, W. W., Measurement of two-photon excitation cross sections of molecular fluorophores with data from 690 to 1050 nm. *J. Opt. Soc. Am. B* **1996,** *13* (3), 481-491.

24. Demas, J. N.; Crosby, G. A., The measurement of photoluminescence quantum yields. A review. *J. Phys. Chem.* **1971,** *75* (8), 991-1024.

25. Makarov, N. S.; Drobizhev, M.; Rebane, A., Two-photon absorption standards in the 550-1600 nm excitation wavelength range. *Optics Express* **2008,** *16* (6), 4029-4047.

26. Frisch, M. J.; Trucks, G. W.; Schlegel, H. B.; Scuseria, G. E.; Robb, M. A.; Cheeseman, J. R.; Scalmani, G.; Barone, V.; Petersson, G. A.; Nakatsuji, H.; Li, X.; Caricato, M.; Marenich, A. V.; Bloino, J.; Janesko, B. G.; Gomperts, R.; Mennucci, B.; Hratchian, H. P.; Ortiz, J. V.; Izmaylov, A. F.; Sonnenberg, J. L.; Williams; Ding, F.; Lipparini, F.; Egidi, F.; Goings, J.; Peng, B.; Petrone, A.; Henderson, T.; Ranasinghe, D.; Zakrzewski, V. G.; Gao, J.; Rega, N.; Zheng, G.; Liang, W.; Hada, M.; Ehara, M.; Toyota, K.; Fukuda, R.; Hasegawa, J.; Ishida, M.; Nakajima, T.; Honda, Y.; Kitao, O.; Nakai, H.; Vreven, T.; Throssell, K.; Montgomery Jr., J. A.; Peralta, J. E.; Ogliaro, F.; Bearpark, M. J.; Heyd, J. J.; Brothers, E. N.; Kudin, K. N.; Staroverov, V. N.; Keith, T. A.; Kobayashi, R.; Normand, J.; Raghavachari, K.; Rendell, A. P.; Burant, J. C.; Iyengar, S. S.; Tomasi, J.; Cossi, M.; Millam, J. M.; Klene, M.; Adamo, C.; Cammi, R.; Ochterski, J. W.; Martin, R. L.; Morokuma, K.; Farkas, O.; Foresman, J. B.; Fox, D. J. *Gaussian 16*, Wallingford, CT, 2016.

27. Caricato, M.; Mennucci, B.; Tomasi, J.; Ingrosso, F.; Cammi, R.; Corni, S.; Scalmani, G., Formation and relaxation of excited states in solution: a new time dependent polarizable continuum model based on time dependent density functional theory. *J. Chem. Phys.* **2006,** *124* (12), 124520.

28. Marenich, A. V.; Cramer, C. J.; Truhlar, D. G., Universal solvation model based on solute electron density and on a continuum model of the solvent defined by the bulk dielectric constant and atomic surface tensions. *J. Phys. Chem. B* **2009,** *113* (18), 6378-96.

29. Zhan, C.-G.; Dixon, D. A., Absolute Hydration Free Energy of the Proton from First-Principles Electronic Structure Calculations. *J. Phys. Chem. A* **2001,** *105* (51), 11534-11540.

30. Martin, R. L., Natural transition orbitals. *J. Chem. Phys.* **2003,** *118* (11), 4775-4777.

31. Lu, T.; Chen, F., Multiwfn: a multifunctional wavefunction analyzer. *J. Comput. Chem.* **2012,** *33* (5), 580-592.

32. Wang, C.; Deng, C.; Wang, D.; Zhang, Q. S., Prediction of Intramolecular Charge-Transfer Excitation for Thermally Activated Delayed Fluorescence Molecules from a Descriptor-Tuned Density Functional. *J. Phys. Chem. C* **2018,** *122* (14), 7816-7823.

33. Wang, C.; Zhang, Q., Understanding Solid-State Solvation-Enhanced Thermally Activated Delayed Fluorescence Using a Descriptor-Tuned Screened Range-Separated Functional. *J. Phys. Chem. C* **2018,** *123* (7), 4407-4416.

34. Cory, A. H.; Owen, T. C.; Barltrop, J. A.; Cory, J. G., Use of an aqueous soluble tetrazolium/formazan assay for cell growth assays in culture. *Cancer Commun.* **1991,** *3* (7), 207-12.

35. Goyal, S. N.; Reddy, N. M.; Patil, K. R.; Nakhate, K. T.; Ojha, S.; Patil, C. R.; Agrawal, Y. O., Challenges and issues with streptozotocin-induced diabetes - A clinically relevant animal model to understand the diabetes pathogenesis and evaluate therapeutics. *Chem. Biol. Interac.* **2016,** *244*, 49-63.

36. Radenkovic, M.; Stojanovic, M.; Prostran, M., Experimental diabetes induced by alloxan and streptozotocin: The

current state of the art. *J. Pharmacol. Toxicol. Methods* **2016,** *78*, 13-31.

37. Bourebaba, L.; Saci, S.; Touguit, D.; Gali, L.; Terkmane, S.; Oukil, N.; Bedjou, F., Evaluation of antidiabetic effect of total calystegines extracted from Hyoscyamus albus. *Biomed. Pharmacother.* **2016,** *82*, 337-344.